Automating Urban Parameter Calculations

Juan Hernández
Master's Thesis

Technische Hochschule Ostwestfalen-Lippe
Detmolder Schule für Gestaltung
Master of Engineering in Integrated Design
Specialization in Computational Design

Automating Urban Parameter Calculations: A Comparative Study of GIS Workflows and Spatial Query Methods for Large-Scale Urban Analysis.

Master's Thesis

Submitted by: Juan Camilo Hernández Leal
(15466021)

Supervisors: Prof. Dipl.-Ing. Jens-Uwe Schulz
Prof. Dr.-Ing. Jörg Rainer Noennig

Date: June 2025

Zusammenfassung

Diese Masterarbeit vergleicht zwei Arbeitsabläufe zur Berechnung der Grundflächenzahl (GRZ) unter Verwendung von Katasterdaten aus Hamburg. Sie evaluiert einen semi-automatisierten Ansatz mit QGIS sowie eine vollautomatisierte Methode auf Basis von SQL-Abfragen mit der PostGIS-Erweiterung, wobei der Fokus auf Skalierbarkeit und Reproduzierbarkeit für großmaßstäbliche Stadtanalysen liegt. Beide Arbeitsabläufe nutzen standardisierte Katasterdaten aus dem ALKIS-System und sind darauf ausgelegt, die GRZ auf Flurstücksebene zu berechnen, wobei zwischen Haupt- und Nebenanlagen gemäß deutschem Planungsrecht (§ 19 BauNVO) unterschieden wird.

Eingebettet in ein Forschungsprojekt an der HafenCity Universität Hamburg adressiert diese Arbeit praktische Bedürfnisse der öffentlichen Planung, indem sie eine transparente, rechtlich konforme und skalierbare Methode zur Bewertung urbaner Dichte und Landnutzungsmuster anbietet. Darüber hinaus reflektiert die Arbeit die weitreichenden Implikationen der Automatisierung urbaner Raumanalysen und beleuchtet Herausforderungen in Bezug auf Data Governance, algorithmische Transparenz sowie die normativen Dimensionen digitaler Planungstools. Die Erkenntnisse tragen zur Entwicklung reproduzierbarer Methodologien für flurstücksbezogene Stadtmetriken bei und bieten übertragbare Arbeitsabläufe für die Anwendung in ganz Deutschland.

Abstract

This thesis compares two workflows for calculating the Building Coverage Ratio (BCR), or Grundflächenzahl (GRZ), using cadastral data from Hamburg. It evaluates a semi-automated approach using QGIS and a fully automated method based on SQL queries with PostGIS extension, emphasizing scalability and reproducibility for large-scale urban analysis. Both workflows operate on standardised cadastral data from the ALKIS system and are designed to compute GRZ at the parcel level while distinguishing between main and ancillary building structures following the German planning law (§19 BauNVO).

Embedded within a research project at HafenCity Universität Hamburg, this work addresses practical needs in public planning by offering a transparent, legally aligned, and scalable method for assessing urban density and land use patterns. The thesis also reflects on the broader implications of automating urban spatial analysis, highlighting challenges related to data governance, algorithmic transparency, and the normative dimensions of digital planning tools. The findings contribute to reproducible methodologies for parcel-based urban metrics and provide transferable workflows for application across Germany.

Keywords: urban morphology, building coverage ratio (BCR), geospatial analysis, QGIS / PostGIS workflows, automated planning metrics.

Contents

1. Introduction **1**

1.1. Problem Statement 1
1.2. Research Objectives 2
1.3. Hamburg as Urban Research Context 2
1.4. Significance and Contribution 2
1.5. Structure of the Thesis 3

2. Literature Review **4**

2.1. Urban Parameters and Their Applications 4
2.2. The German Planning Framework 5
2.3. Automated Calculation Methods 6
2.4. Examination of Institutional Spatial Data 7
2.5. Summary of Literature Insights 8

3. Methodology **9**

3.1. Study Area 9
3.2. Data Sources 9
3.3. Dataset Review and Analytical Readiness 11
3.4. Dataset Linkage 19
3.5. Building Coverage Ratio Calculation Method 21
3.6. Comparative Analysis Setup 25
3.7. Data Visualisation and Interpretation 25
3.8. Methodological and Data Limitations 26

4. Results **27**

4.1. GRZ Results from GIS Workflows 27
4.2. GRZ Results from Spatial Query Methods 34
4.3. Workflow Comparison Results 38

5. Discussion **46**

5.1. Interpretation of Findings 46
5.2. Limitations of the Study 46
5.3. Urban Research Implications 47
5.4. Ethical and Societal Implications 48
5.5. Future Research Directions 49

6. Conclusion **52**

7. References **54**

8. Appendices **57**

8.1. Appendix A. Data & Dataset Documentation 57
8.2. Appendix B. SQL and Script Listings 64
8.3. Appendix C. Extended Results 69
8.4. Appendix D. Legal Context & References 72
8.5. Appendix E. Research Data Management Strategy 81
8.6. Appendix F. AI Tools and Assistance Disclosure 83

List of Figures

Fig 01. Diagram illustrating the BCR 1
Fig 02. Diagram representing the FAR 1
Fig 03. Orthophoto of the Campus Tower building 1
Fig 04. Diagram summarising the chapter structure 4
Fig 05. Extract showing urban surface parameters 7
Fig 06. Children's game 7
Fig 07. Location of the Altona district 9
Fig 08. QGIS Layer Panel displaying all layers 10
Fig 09. Visualisation of all spatial layers 11
Fig 10. Cadastral parcels in Hamburg at scale 1:250.000 12
Fig 11. Attribute filtering process for the ALKIS parcel dataset 13
Fig 12. Comparison between the original and pruned parcel datasets 14
Fig 13. Flowchart illustrates the process of validating and repairing geometries 14
Fig 14. Map showing the location of the six parcels with corrected geometries 15
Fig 15. Timeline of feature counts for parcels and buildings 15
Fig 16. Visualization of polygons 16
Fig 17. Visualization of polygons with the attribute AX_Bauteil 16
Fig 18. Visualization of polygons with the attribute AX_Gebaeude 17
Fig 19. Hierarchical classification of building features in the ALKIS dataset 17
Fig 20. Visualisation comparing features labelled as Main and Ancillary 18
Fig 21. Examples of minor geometry intersections 18
Fig 22. Intersection case 18
Fig 23. Orthophoto of parcel in the Wandsbek district 19
Fig 24. Visualisation of repeated building geometries 19
Fig 25. Multi-parcel building footprints 20
Fig 26. Map of Altona 20
Fig 27. Diagram for the dictionary-based workflow 21
Fig 28. Flowchart illustrating the complete GRZ calculation 22
Fig 29. Workflow diagram for GRZ_main and GRZ_aux 23
Fig 30. Parcels in Hamburg with calculated GRZ_main values 27
Fig 31. Parcels in Hamburg with GRZ_main values between 0 and 0,001 27
Fig 32. Parcels with GRZ_main>1,0 in the Hamburg Airport complex 28
Fig 33. GRZ_main values across Hamburg, classified into six intervals 28
Fig 34. Parcels in Hamburg with GRZ_main values greater than 0,8 29
Fig 35. Close-up view of parcels with GRZ_main>0,8 in Altona-Nord 30
Fig 36. Example of a cadastral layout 30
Fig 37. Parcels in Hamburg with GRZ_main between 0,05 and 0,2 31
Fig 38. Detailed GRZ_main distribution 32
Fig 39. Extract from Sasel 33
Fig 40. Distribution of GRZ_main values 34
Fig 41. Pie chart 35
Fig 42. Schematic overview of SQL-based workflow 36
Fig 43. SQL-based workflow 37
Fig 44. Stacked comparison of non-zero and zero values 38
Fig 45. Comparison of GRZ_main distribution 39
Fig 46. Scatter plot comparing the GRZ_main values 40
Fig 47. Area-based refinement of the GRZ_main comparison 41
Fig 48. Two examples where parcels intersect with building polygons 42
Fig 49. Bland–Altman plot 43
Fig 50. Comparison of GRZ workflow execution times 44
Fig 51. Processing time vs. dataset size 44
Fig 52. Map of building eligible land use categories in Hamburg 50

List of Tables

Table 1. Terminology Table V
Table 2. Overview of ALKIS dataset versions 10
Table 3. Comparison of the cadastral parcel datasets 12
Table 4. Overview of selected ALKIS parcel attributes 13
Table 5. Overview of selected ALKIS builidng attributes 16
Table 6. Attributes and corresponding values 17
Table 7. Summary of statistical metrics 25
Table 8. Overview of visualization types used 26
Table 9. Distribution of values for GRZ calculaiton 38
Table 10. Frequency distribution of GRZ_main 39
Table 11. Processing times for key steps in the Manual GIS Workflow 44
Table 12. Comparative overview of key workflow steps 45

Table 1. Terminology Table

Term / Acronym	Definition
Building Coverage Ratio BCR	A ratio expressing the proportion of a parcel that is covered by buildings. It is calculated by dividing the building footprint area by the parcel area. Also known as GRZ in the German context.
Grundflächenzahl GRZ	The German equivalent of BCR. Legally defined in §19 of the Baunutzungsverordnung (BauNVO). Indicates the maximum allowable coverage of a parcel by building footprints.
Floor Area Ratio FAR	Ratio between the gross floor area of a building and the total area of the parcel it sits on. It is used to indicate built density, especially vertically. In Germany, this is referred to as GFZ (Geschossflächenzahl).
Geschossflächenzahl GFZ	German planning term for Floor Area Ratio (FAR). Defined in §20 BauNVO. Represents total floor area divided by plot size.
ALKIS	Amtliches Liegenschaftskataster-Informationssystem. Germany's official cadastral database, combining geometric and attribute information onV land parcels and buildings. Maintained by state surveying authorities.
PostGIS	An open-source spatial database extension for PostgreSQL. It adds support for geographic objects, enabling location queries to be run in SQL.
QGIS	A free and open-source Geographic Information System (GIS) software used for spatial data visualization, processing, and analysis.
Hauptanlagen	"Main structures" as defined by §19(2) BauNVO. These are the principal buildings on a parcel that fully count toward the GRZ.
Nebenanlagen (im weiteren Sinne)	"Ancillary structures in the broader sense," defined by §19(4) BauNVO. Includes garages, garden houses, and other auxiliary structures. Their area may contribute partially to GRZ.
Gebäudefunktion GFK	Attribute in ALKIS that indicates a building's primary function or use (e.g., residential, commercial). Used to classify structures as main or ancillary.
XPlanung	A German standard for digital spatial planning data exchange. Used to represent legally binding development plans (e.g., Bebauungspläne).
OGC API	API standards defined by the Open Geospatial Consortium. Enables access to geospatial data via web services for dynamic and real-time analysis.
EPSG:25832	The coordinate reference system used in your study (ETRS89 / UTM zone 32N), suitable for spatial analysis in Germany.
Flurstück	A land parcel unit in the German cadastral system (ALKIS). Each has a unique identifier and recorded geometry.

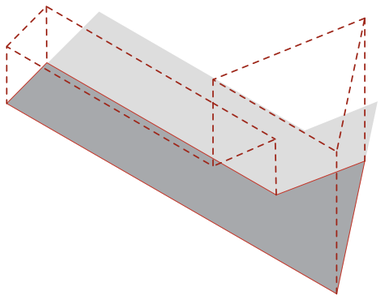

Figure 1. Diagram illustrating the BCR of the parcel occupied by the *Campus Tower* building in Hamburg. The darker shaded area represents the building footprint (author, 2025).

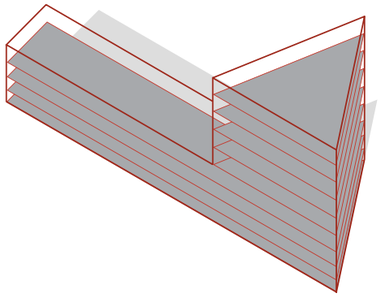

Figure 2. Diagram representing the FAR of the parcel occupied by the *Campus Tower* building. Stacked planes illustrate the total gross floor area (author, 2025).

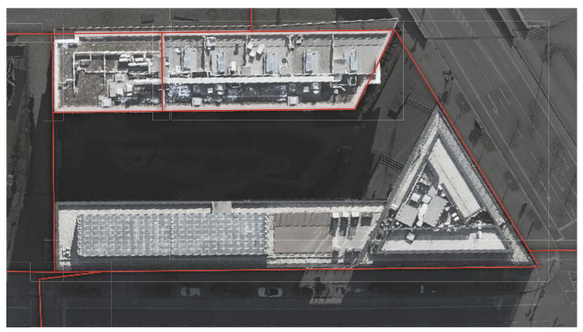

Figure 3. Orthophoto of the *Campus Tower* building in Hamburg. Parcel boundaries overlaid in red. (*Freie und Hansestadt Hamburg, Landesbetrieb Geoinformation und Vermessung (LGV), 2025).*

1. Introduction

1.1. Problem Statement

Urban morphological parameters such as the **Building Coverage Ratio** (BCR) and **Floor Area Ratio** (FAR) are fundamental tools in urban planning, design regulation, and spatial analysis. These metrics provide quantitative insight into the spatial structure of the built environment, supporting evaluations of density, land-use intensity, and environmental impact (Dovey and Pafka, 2016).

BCR is defined here as the ratio of the ground-level footprint area of a building to the total area of the parcel it occupies. As demonstrated in Figure 01, it reflects the extent to which land is physically covered by structures, offering a measure of openness versus built form on a given site.

FAR, by contrast, is calculated as the ratio of a building's total gross floor area (across all levels) to the total area of the parcel. It represents the overall volume or intensity of development on a site (illustrated in Figure 02). FAR is often used to regulate bulk, massing, and spatial capacity within zoning frameworks.

The precise definitions and variants of ground-level footprint area and total gross floor area (critical components of these calculations) will be examined in detail in the following chapter.

Together, BCR and FAR capture the horizontal and vertical dimensions of urban form. They are used to assess compliance with zoning laws, guide urban design decisions, and evaluate the spatial efficiency of land use. These metrics also play a role in environmental performance assessments, affecting factors such as impervious surface area, green space provision, and urban microclimates.

Traditional methods for calculating urban parameters computationally are often based on manually entering data into spreadsheets. This method is time-consuming, labour-intensive, and prone to errors, particularly when dealing with large urban datasets (Eicker et al., 2015). As cities' studies and self-awareness grow and evolve, the need to calculate these parameters efficiently and accurately becomes more important.

To address this challenge, the thesis compares two automation strategies: a GIS[1]-based workflow using QGIS and a database-driven workflow using PostGIS. The QGIS approach offers an interactive, user-friendly environment for geospatial analysis, whereas the PostGIS approach leverages SQL queries in a spatial database for scalable, fully automated processing. By using these tools to represent fundamentally different workflows, the research aims to develop a guided and reliable workflow for calculating urban ratios. In this way, it brings support to planners in efficiently analysing large-scale urban environments and data-driven development strategies.

1.2. Research Objectives

This research addresses critical limitations in traditional urban parameter calculations by developing and comparing automated methods for geospatial analysis. In this context, **automation** refers to the use of scripting and database queries to execute spatial operations and calculations with minimal manual intervention. This approach is increasingly essential in complex, data-rich urban environments (Yang et al., 2008).

The main goal of this thesis is to evaluate the agreement of results and efficiency of two contrasting workflows for calculating urban morphological parameters, with particular attention to how varying levels of process automation impact the precision of spatial analysis.

To guide the investigation, two key research questions are posed: First, *how do GIS Workflows compare with Spatial Query Methods in performing urban parameter calculations at scale?* Second, *what are the comparative advantages and limitations of these methodological approaches in terms of computational efficiency, and scalability?*

By addressing these questions, the presented thesis aims to provide a deeper understanding of how different process-oriented strategies, ranging from interactive spatial analysis to fully programmatic querying, perform under large-scale urban data conditions

1.3. Hamburg as Urban Research Context

Hamburg presents a compelling case study for investigating urban parameter calculation methodologies due to its complex urban landscape and ongoing challenges in urban development. As Germany's second-largest city, with a population of approximately 1.850.000 as of December 31, 2023[2], Hamburg offers a unique urban environment characterised by diverse architectural typologies and dynamic spatial transformations.

The selection of Hamburg is grounded in three key factors. The first, as already introduced, is its urban complexity and spatial diversity. Hamburg's urban fabric represents a blend of historical urban structures and contemporary development zones, particularly exemplified by the HafenCity district's large-scale urban regeneration project (Bruns-Berentelg, 2014). The city complexity provides an ideal testing ground for urban parameter calculation methodologies, allowing for comprehensive evaluation across varied urban morphologies.

The second factor relates to Hamburg's active engagement with digital urban planning tools and data-driven planning processes. The city has taken a leading role in experimenting with innovative planning methods, exemplified by its use of the CityScope platform. Developed in collaboration with HafenCity Hamburg GmbH, CityScope was applied during the planning process for the new Grasbrook district, where it enabled real-time, modular analysis of urban parameters such as noise propagation, stormwater runoff, and walkability. This interactive platform allowed both designers and decision-makers to test and refine proposals iteratively, making planning discussions more transparent and evidence-based (Baeza et al., 2021). These qualities position Hamburg as a forward-thinking and contextually rich case study for exploring the integration of automated urban analysis methods in contemporary planning practice.

The third factor relates to a larger research project context. This Master's thesis is part of a broader research initiative at HafenCity University (HCU). Its concrete focus is explained on Section 1.4.1. This institutional context significantly enhances the scope and depth of the study, allowing for practical relevance.

1.4. Significance and Contribution

From a practical perspective, this research builds on developments in urban informatics and addresses critical challenges related to computational efficiency and the management of large spatial datasets.

1. Geographic Information System

2. source: www.destatis.de, accessed May 2025

In terms of **efficiency**, automated geospatial methods significantly reduce manual effort and the potential for human error. Studies have shown that such automation can cut data processing times by up to 70% compared to traditional techniques (Casali et al., 2022), enabling planners to evaluate scenarios more quickly and make timely, data-informed decisions during planning processes.

Regarding the **management** of complex datasets, contemporary urban environments increasingly rely on detailed, high-volume spatial information. The methodology proposed in this thesis, demonstrates robust capabilities in handling large-scale cadastral datasets like ALKIS®. A more detailed discussion of this dataset is provided in Section 2.4.

To its contribution to urban planning and analysis, the thesis offers a structured comparative evaluation of two contrasting methodological approaches. This comparison provides urban planners with a clearer understanding of the relative strengths and limitations of visual GIS workflows versus spatial querying approaches.

The proposed method establishes a replicable framework for conducting urban spatial analysis in complex metropolitan contexts. While Hamburg serves as the case study, the use of a nationally standardised dataset allows for the findings and workflows to be transferable to other regions across Germany.

1.4.1. HCU–LIG Research Initiative

This thesis is embedded within a broader research initiative led by HCU in collaboration with the Landesbetrieb Immobilienmanagement und Grundvermögen (LIG), Hamburg's State Agency for Immovable Property and Real Estate Management. The initiative partly focuses on identifying urban growth potentials in Hamburg by analysing the current built environment against what is legally permissible under planning regulations.

A central objective of this project is the comparison between **ALKIS** (which documents the existing physical state of parcels) and **XPlanung** (which reflects planning permissions and future land use designations). Through this comparison, the project seeks to identify underutilised parcels-cases where actual land use falls short of the development potential according to zoning regulations.

This institutional framework not only guides the selection of data and methods but also positions the research within a real-world planning context. The collaboration with LIG provides access to comprehensive datasets and practical planning insights, ensuring the study's relevance to ongoing urban policy discussions in Hamburg. This background also shapes the methodological priorities of the thesis, particularly the emphasis on automation, transparency, and legal compliance in spatial analysis.

1.5. Structure of the Thesis

This thesis is structured into **eight main chapters**, each progressively contributing to a comprehensive understanding of automated methods for calculating urban morphological parameters, particularly the **BCR**, in the context of Hamburg.

After the Introduction, **Chapter 2** provides a review of relevant literature, covering urban morphological parameters, the German planning framework, and methods for automated spatial analysis. This includes a discussion of the BCR indicator as defined by national regulation, as well as a review of the ALKIS dataset as a key institutional data source.

Chapter 3 outlines the research methodology, detailing the study area, data sources, and data preparation steps. It introduces two automated workflows for calculating BCR values: one based on semi-automated GIS operations in QGIS, and the other using automated spatial queries within a PostgreSQL database. The chapter concludes with a description of the comparative analysis framework and a discussion of key methodological limitations.

Chapter 4 presents the results of the BCR calculations, comparing the outcomes of both workflows through spatial visualisations, statistical summaries, and performance metrics.

Chapter 5 discusses these results concerning the research questions, emphasising methodological insights and implications for urban research and planning practice. It also reflects on study limitations and proposes directions for future research.

Chapter 6 concludes the thesis, summarising the main findings and contributions. The final chapters include a complete list of references and appendices containing supporting materials such as dataset documentation, script excerpts, and supplementary tables.

Together, these chapters guide the reader through the process of designing, implementing, and evaluating automated workflows for urban parameter calculation, with a practical focus on real-world spatial datasets and planning applications.

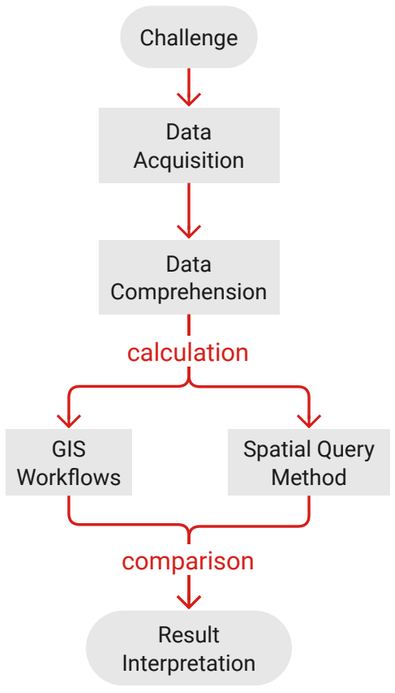

Figure 4. Diagram summarising the chapter structure of the thesis, tracing its logical progression (author, 2025).

2. Literature Review

2.1. Urban Parameters and Their Applications

Urban parameters, or ratios, are quantitative measures used to describe the relationships between different elements of the built environment, such as building size, land area, and open space. They are essential tools in urban planning, design, and environmental analysis, providing a way to understand and control the intensity of land use (Berghauser Pont and Haupt, 2021). These ratios offer a method for moving beyond purely qualitative assessments of urban space by providing numerical representations of urban form and density. Through the use of urban parameters, planners can evaluate the impact of design and development proposals in a structured and measurable way.

FAR, also sometimes called the Floor Space Index, is a fundamental element in defining the character and intensity of urban development and is often used in zoning regulations to control building heights and densities (Yin, 2008).

BCR, or building density, impacts the microclimate, pedestrian movement, and overall urban quality (Baeza et al.,2021). In the context of urban management, the maximum (or "legal") BCR and FAR limits are fundamental tools for district-scale zoning regulation. These limits are used to legally control the shape and volume of buildings, supporting more effective urban planning while also contributing to the quality of the urban landscape (Le et al., 2022).

It is worth noting that there is no universally fixed terminology for describing these spatial indicators. The spatial arrangement of urban elements may be defined through geometrical measures and relationships, which are referred to in the literature using varying terms, such as urban surface parameters (Lindberg et al., 2018), morphological parameters (Kent et al., 2019), or roughness parameters (Darmanto et al., 2017). Similarly, the naming conventions and calculation methods for urban ratios can differ depending on the application context or scale of analysis.

FAR and BCR are both key indicators in urban planning and are instrumental in determining whether a new development aligns with local planning frameworks. Although this thesis focuses on BCR, the workflows developed here provide a conceptual foundation for future studies aimed at calculating additional urban parameters.

On a practical level, urban parameters directly affect infrastructure and resource planning, influencing projected demands for water, energy, mobility, and social services. These ratios also shape housing typologies and guide how new developments integrate with long-term urban strategies. Importantly, they reflect the spatial organisation and morphology of the urban fabric. Higher BCR and FAR values typically indicate a more compact form, while lower values signal dispersed development patterns. While high-density areas can support more efficient public services, low-density neighbourhoods, often characterised by suburban expansion, tend to require more land, rely more on private transportation, and pose different challenges for social and environmental sustainability (Berghauser Pont and Haupt, 2021).

It is also important to clarify that "high density" does not necessarily imply "high-rise." For instance, low-rise developments can still achieve high population densities. A notable example is the *Eixample* district of Barcelona, designed by Ildefons Cerdà in the mid-19th century. Eixample features a compact, gridded layout with uniform building heights of six to eight stories, demonstrating that density can be achieved while maintaining a human-scale urban environment (Roberts, 2019).

2.2. The German Planning Framework

A critical challenge in comparative urban morphological analysis is the absence of internationally harmonised definitions for urban parameter calculations. Despite the widespread application of density metrics such as BCR, FAR, and related indicators across planning jurisdictions globally, no universally accepted computational framework exists within established international standards organisations.

This definitional fragmentation presents significant methodological challenges for cross-jurisdictional research and comparative urban studies. A systematic review of literature on urban density calculations reveals a notable absence of studies that explicitly reference standards for urban ratio computation, suggesting that current academic practice relies predominantly on jurisdiction-specific regulatory frameworks rather than internationally standardised methodologies.

Within the German planning context, the focus of this research, the *Grundflächenzahl* (GRZ) serves as the regulatory equivalent to the Building Coverage Ratio. Its definition and calculation methodology are prescribed through national legislation, specifically the Baunutzungsverordnung (BauNVO), with GRZ codified in § 19. The original BauNVO text and its English translation are provided as Entry 01 and Entry 02 in Appendix D.

To understand the practical application of these regulatory provisions, this study draws primarily on the book *Flächenmanagement in der Immobilienwirtschaft: Grundlagen und konkrete Anwendung* (Zeitner et al., 2019), which offers detailed explanations of GRZ and other urban planning parameters, including practical distinctions between **main structures** (*Hauptanlagen*) and **ancillary structures** (*Nebenanlagen im weiteren Sinne*). An English translation of key content from this source is provided in Entry 03 of Appendix D.

According to the regulatory framework outlined in this source, § 19(4) of the BauNVO defines **ancillary structures** to include: garages and parking spaces (carports and driveways), outbuildings and technical structures (sheds and greenhouses), and underground structures. The specific classification criteria used to distinguish between these structure types will be defined in Section 3.3.2 (Buildings Dataset).

The treatment of underground structures presents particular complexity for GRZ calculations. Underground structures count toward GRZ if they seal the ground surface. However, structures covered by more than one metre of topsoil may be excluded from GRZ calculations, subject to official approval. This thesis adopts a conservative approach, counting all underground structures toward GRZ unless clear evidence supports their exclusion.

Beyond GRZ, the BauNVO outlines a comprehensive set of legal parameters that govern the Maß der baulichen Nutzung (extent of building use). These include the **permitted types of land use** (§ 17), the **number of full storeys** (Vollgeschosse) and **FAR** (Geschossflächenzahl, GFZ) as specified in § 20. **Buildable area of a plot** (überbaubare Grundstücksfläche), which is regulated by **building lines** (Baulinien), **boundaries** (Baugrenzen), or **building depths** (Bebauungstiefen) according to § 23. Together, these parameters provide a legal framework for shaping urban form and density (Zeitner et al., 2019).

To apply these regulatory parameters, accurate area measurements are important. Although standards like DIN EN 15221-6[3] exist for measuring areas in Facility Management, this thesis uses the area values already provided in the ALKIS dataset. These include the Amtliche Fläche (official

3. Facility Management - Part 6: Area and Space Measurement in Facility Management; German version.

parcel area) and the Grundfläche (building footprint area). These values are not recalculated but taken as given. This approach is explained further in Section 3.3.

Moving forward, this research employs both **BCR** and **GRZ** terminology to reflect international and German planning context.

2.3. Automated Calculation Methods

Automated methods using GIS tools and spatial databases provide an efficient alternative to traditional approaches. This section outlines key tools, specifically QGIS and PostGIS, used to perform spatial operations relevant to urban parameter analysis.

QGIS and PostGIS are two powerful tools that play a central role in automating urban ratio calculations. QGIS is a free and open-source GIS platform that runs on Windows, macOS, and Linux, offering a user-friendly platform for viewing, analysing, and editing spatial data (Mwanja, 2023). It supports a wide range of data formats, including raster, vector, and point cloud layers, and provides key spatial analysis tools such as line length calculations, nearest neighbour analysis, heatmaps, and multi-criteria overlay analysis. QGIS also includes a robust processing framework for batch processing and automation through its graphical modeller. Moreover, its functionality can be extended using a broad set of plugins tailored to specific planning and analysis needs (Chen et al., 2024).

PostgreSQL, an open-source relational database system, becomes significantly more powerful with the addition of the PostGIS extension, which enables support for geographic objects and spatial queries. PostGIS allows for advanced spatial operations using SQL, including spatial joins, distance calculations, and area measurements. Its ability to efficiently store, retrieve, and manipulate large spatial datasets makes it particularly suitable for managing complex urban data. This makes it highly relevant for planning workflows that rely on automated spatial data integration and analysis (Ostadabbas et al., 2020).

In practice, **QGIS** provides a more accessible interface, ideal for users without advanced technical backgrounds. Its graphical tools and scripting support make it suitable for interactive and semi-automated spatial analysis. However, when working with very large datasets, performance may become a limiting factor (Majic and Pafka, 2019).

PostGIS, by contrast, excels in handling large spatial datasets and running fully automated workflows using SQL queries (Obe, 2015). Despite these strengths, it lacks a graphical interface and requires a steeper learning curve, making it less approachable for users unfamiliar with database environments.

Aside from vector-based approaches, raster grid methods are also widely used in urban research. These involve overlaying regular grid cells (100 m, 500 m, or 1 km) across a study area to calculate urban parameters. While useful for summarising large-scale spatial patterns, they lack the precision required for parcel-level analysis and legal or cadastral applications.

This raster methodology is especially common in environmental and climate research, such as urban heat island studies or climate adaptation planning (Ferreira et al., 2021; Esposito et al., 2023). In these contexts, grid-based urban ratios serve as model inputs for simulations. However, research that explores urban parameters at the cadastral level, where legal ownership and planning regulations intersect, is more limited.

Automation, while beneficial, introduces certain trade-offs. It often requires significant technical preparation, such as data cleaning, script development, and geometry checks. Errors in any part of the workflow can propagate and affect results. Automation can obscure the logic behind spatial operations, reducing transparency for non-technical stakeholders (Sanchez and Ye, 2025). These challenges underline the need for clear documentation and methodological transparency when designing automated workflows.

In addition to QGIS and PostGIS, other tools further expand the automation landscape. **FME** (Feature Manipulation Engine) is known for transforming and integrating spatial datasets across formats and systems, including urban ratio calculations (Zahid, 2023). **ArcGIS** offers robust spatial tools, though its proprietary nature and licensing costs can be limiting. Python-based tools such as **GeoPandas** and **PyQGIS** offer scriptable alternatives, combining data handling and spatial analysis capabilities (Nguyen and Quarg, 2024). Together, this ecosystem provides planners and researchers with a flexible toolkit for automating urban parameter analysis at multiple scales.

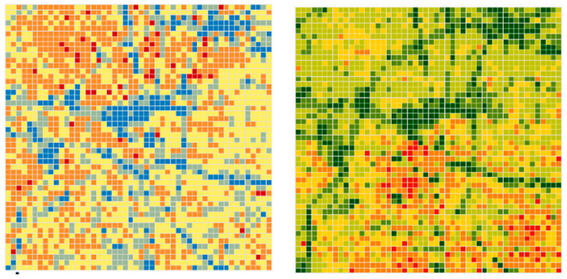

Figure 5. Extract showing urban surface parameters calculated using a 100 m resolution square grid (Ferreira et al., 2021)

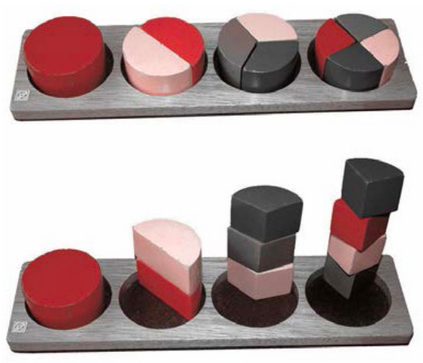

Figure 6. Children's game, illustrating the relation between BCR and FAR (Berghauser Pont and Haupt, 2021).

2.3.1. Existing Work on GRZ Calculation

Despite growing interest in automated spatial analysis, relatively few studies focus specifically on the calculation of the GRZ at the parcel level using cadastral datasets. This gap is particularly relevant in contexts like Germany, where the GRZ is a key legal metric.

Most existing urban morphological studies employ raster-based approaches, which are better suited for analysing urban form at the district or city scale. While these methods are useful for general pattern recognition, they often lack the spatial resolution required for planning or legal compliance. For instance, Esposito et al. (2023) and Ferreira et al. (2021) describe raster grid techniques in environmental modelling but do not link building coverage to individual parcel boundaries.

A recent trend in urban morphology research applies deep learning (DL) techniques to extract building footprints from aerial imagery, enabling automated GRZ estimation in areas where official spatial data may be unavailable. This method allows for GRZ values extraction using drone or satellite imagery, particularly valuable in rapidly urbanising regions.

In a case study of the *Sihwa* industrial district in South Korea, DL-based methods were used to extract building footprints from unmanned aerial vehicle imagery and compute the GRZ at both the block and parcel levels. By using cadastral data for parcel areas and validating results against a ground-truth dataset, the DL approach achieved an average accuracy of 86,6 % at the block scale and 85,2 % at the parcel scale, with median accuracy exceeding 94 % (Le et al., 2022).

Recent contributions from German technical universities (e.g. Zahid, 2023) indicate growing interest in utilising official datasets such as ALKIS and XPlanung for automated compliance monitoring. However, implementation details are often under-documented. The lack of open-source workflows or published code examples further hampers reproducibility in this domain.

2.4. Examination of Institutional Spatial Data

Having reviewed available tools for automation, we now turn to the key dataset used in this study. Urban planners use spatial data sources, which offer insights into the built and natural environments. These sources can be broadly categorised based on origin, including **official data**, **volunteered geographic information**, and **remote sensing products**. One of the most important sources for detailed urban analysis in Germany is

the ALKIS (*Amtliches Liegenschaftskatasterinformationssystem*), or Authoritative Real Estate Cadastre Information System, which provides institutional spatial data on parcel boundaries, land use, and building geometry (Arbeitsgemeinschaft der Vermessungsverwaltungen - AdV-Online, consulted March 2025).

Established in all German federal states by 2015, ALKIS represents a major step toward unified and redundancy-free data management by combining the former cadastral map and property registry systems into a single, integrated database. For the first time, spatial and non-spatial property-related information were stored together in a systematic and standards-compliant way (Ostadabbas et al., 2020). ALKIS was developed by the Surveying Authorities of the States of the Federal Republic of Germany (AdV), which designed a functional and unified data model using the UML standard (AdV, 2009; Seifert, 2005).

This integrated approach results in a comprehensive data structure that serves multiple analytical purposes. The comprehensive structure of ALKIS includes both **graphical data** (e.g. geometries of parcels and buildings) and **attribute data** (e.g. land use classifications, administrative identifiers, usage types), making it an essential resource for urban planning and property management. The data is structured into feature classes that represent points, lines, and polygons, which are updated and maintained by state-level land surveying authorities. This regular maintenance ensures high reliability and up-to-date spatial representations of urban form (Ostadabbas et al., 2020). The reliability of ALKIS data stems from its adherence to fundamental principles of spatial data management: quality, consistency, and interoperability of spatial data are essential for effective urban planning and analysis. Data **quality** refers to the accuracy, completeness, and reliability of information; **consistency** ensures coherence across time and datasets; and **interoperability** enables data from different systems to be combined and used effectively. (Berghauser Pont and Haupt, 2021).

From a technical implementation perspective, QGIS allows direct import of ALKIS data provided in formats such as Shapefiles or GML, enabling access through its graphical interface. PostGIS, when used with a PostgreSQL database, can load ALKIS data by importing these formats into spatial database tables. Both tools support standard geospatial formats, making them compatible with the ALKIS data structure. The data integration steps for each tool are described in more detail in Chapter 3 (Methodology).

2.4.1. Data Uncertainty

Despite its strengths as a comprehensive and authoritative dataset, ALKIS is not free from uncertainty. Minor geometric inaccuracies, outdated attributes, or incomplete records can affect data reliability, particularly when used for automated spatial analysis at scale. For example, inconsistencies in parcel boundaries or missing building classifications may introduce small but significant deviations in calculated planning metrics. The complexity of ALKIS's data model can create semantic ambiguities, especially when interpreting building use types or distinguishing between main and ancillary structures.

These sources of uncertainty do not undermine the value of ALKIS but highlight the importance of critical data assessment and preprocessing. Addressing these issues is essential for ensuring analytical accuracy and is further discussed in Section 3.3 (Dataset Review and Analytical Readiness).

2.5. Summary of Literature Insights

While automation in urban analysis is gaining momentum (Majic and Pafka, 2019; Casali, Aydin and Comes, 2022), few studies directly compare GRZ calculation methods across platforms. Most existing work focuses on raster-based generalisations (Ferreira et al., 2021; Esposito et al., 2023).

Crucial aspects such as spatial accuracy, processing efficiency, and legal interpretability, particularly the distinction between Hauptanlagen and Nebenanlagen per §19 BauNVO, remain insufficiently addressed. This gap is significant, as GRZ calculations must reconcile technical precision with regulatory definitions.

These limitations reveal a clear research need: the development and systematic comparison of automated GRZ calculation workflows that can handle the complexities of German planning law while maintaining computational efficiency and spatial accuracy. This gap shapes the methodological approach of this thesis, which develops two complementary automated workflows. Chapter 3 presents the design, implementation, and comparative framework for these workflows.

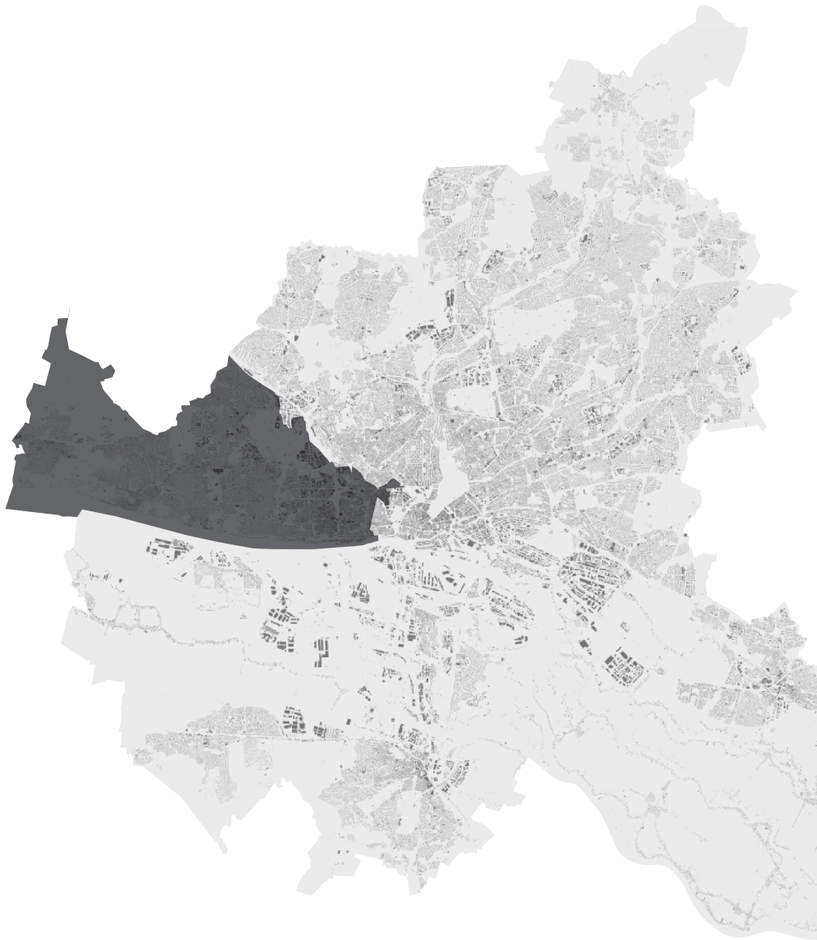

Figure 7. Location of the Altona district within the city of Hamburg (author, 2025).

3. Methodology

3.1. Study Area

Within Hamburg's broader context as established above, the district (Bezirk) of Altona was selected as a focused test area to support the development and refinement of the spatial calculation methods. Given the high processing demands of city-wide analysis, Altona offered a more computationally manageable setting for iterative testing.

As one of Hamburg's seven Bezirke (highlighted in Figure 7), Altona provides a representative mix of building densities and urban typologies, making it well-suited for evaluating the algorithm's performance across varied spatial conditions. Compared to denser districts like Eimsbüttel and Hamburg-Nord, its built environment is more varied, shaped in part by post-war reconstruction guided by the principles of a *gegliederte und aufgelockerte Stadt* (structured and loosened city) (petersen pörksen partner, 2012). This diversity makes Altona an ideal setting for evaluating smaller tests, while maintaining the flexibility to scale the approach to the entire city dataset when needed.

3.2. Data Sources

The study's analyses are based on Hamburg's official cadastral data, which provides the necessary parcel and building information. The ALKIS dataset (cadastral data) for Hamburg can be accessed via GeoPortal Hamburg (https://geoportal-hamburg.de/), a specialised web platform for searching and retrieving digital geographic information. The dataset is available for download in 3 km × 3 km tiles, requiring 275 files to cover the entire city. For the purposes of this thesis, the complete ALKIS dataset for Hamburg was provided as a single vector Geodatabase[4] (.gdb) file by LIG, as part of the research collaboration with HCU.

Table 2 summarises the collection of ALKIS datasets accessed for the study, providing details such as access dates, data sources, dataset names, formats, file sizes, and corresponding data timestamps. The datasets were obtained in various formats, including XML[5] and Geodatabase (GDB)

4. GDB is a proprietary spatial data format developed by Esri. Supports the storage of multiple spatial layers and attribute tables within a single file-based database

5. In geospatial contexts, XML is often used in formats like GML (Geography Markup Language)

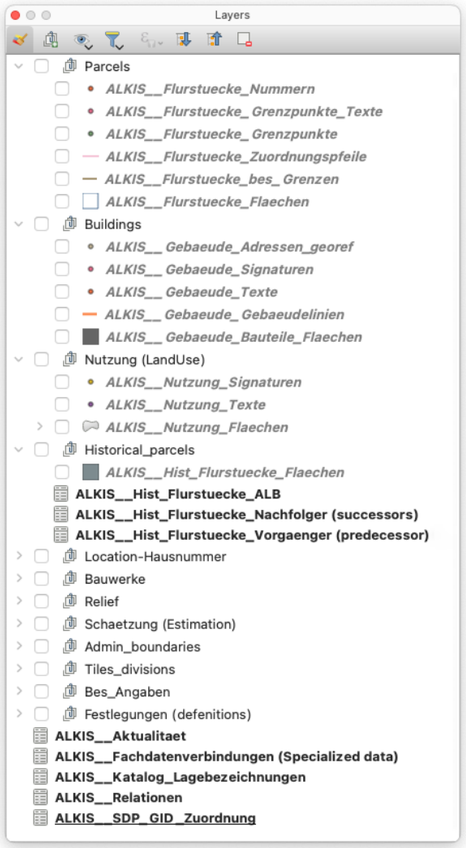

Figure 8. QGIS Layer Panel displaying all layers from the file `ALKIS_SDP_2023.gdb`. Datasets are grouped by content, such as parcels, buildings, land use, and other relevant categories.

files. Additional notes offer context regarding the scope of each dataset, indicating whether they provide full city coverage or focus on specific themes such as parcels and buildings.

Table 2. Overview of ALKIS dataset versions and sources used in this research.

Access Date	Source	Dataset Name	Format	Size (MB)	Data Timestamp	Notes
20.03.24	GeoPortal	ALKIS_ HH_0001-0249	XML	12 886	31.01.24	275 files to cover whole HH
27.03.24	LIG	ALKIS_ SDP_2023	GDB	2 355	30.12.23	Geodatabase single file
05.11.24	LIG	Aktive_ Flurstuecke_ Hamburg	GDB	91.0	28.10.24	Parcel data only
05.11.24	LIG	Gebaude_ Flurstuecke	GDB	92.4	28.10.24	Building data only
29.04.24	LIG	SDP_2024	GBD	1 849	31.12.24	Geodatabase single file

The file `ALKIS_SDP_2023.gdb` contains 60 layers, 52 of which include spatial geometry (point, line, or polygon). Figure 8 presents a thematic grouping of these layers based on their content. Using this thematic and geometric classification, specific layers were selected for analysis. Among those containing parcel information, the `ALKIS__Flurstuecke_Flaechen` layer was chosen for the calculations in this study. This polygon-based layer includes all relevant metadata, and its contents were cross-checked with related layers (`ALKIS__Flurstuecke_Grenzpunkte`) to ensure completeness and consistency.

A similar selection process was applied to the building-related data. Among several options, the `ALKIS__Gebaeude_Bauteile_Flaechen` layer was chosen for its suitability in capturing building footprints for area-based analysis.

In addition to these core parcel and building layers, the ALKIS dataset provides extensive contextual and administrative information. The `ALKIS__Aktualitaet` layer provides metadata on data update frequency and reliability, while historical layers such as `ALKIS__Hist_Flurstuecke_ALB`, track parcel lineage, enabling longitudinal analysis for land use change studies. Additional layers include information on land use (`ALKIS__Nutzung_Flaechen`),

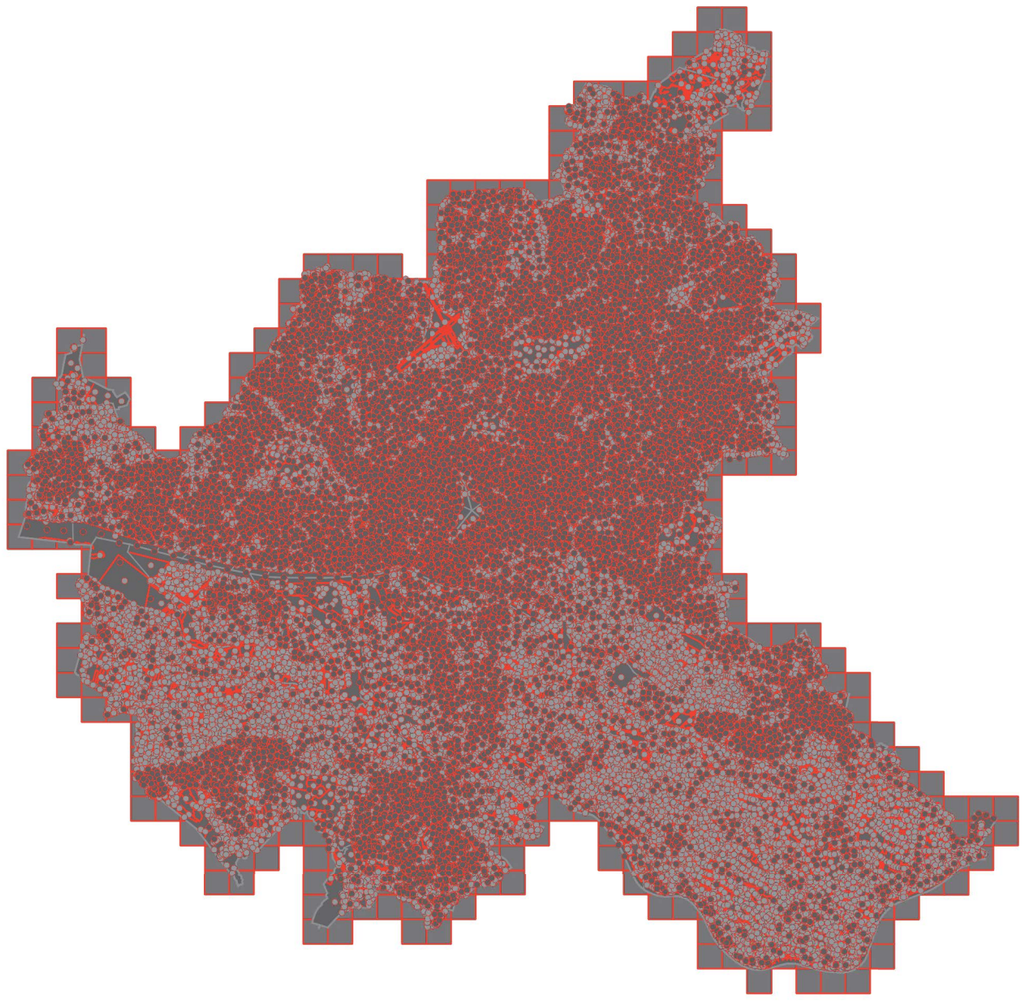

Figure 9. Visualisation of all spatial layers contained in the `ALKIS_SDP_2023.gbd`. The tile-like grid at the borders represents the extent of spatial indexing (tiling) used in the dataset. Scale 1:500.000 (author, 2025).

topography (`ALKIS__Relief_Linien`), administrative boundaries (`ALKIS__Verwaltung_Bezirke`), and infrastructure elements (`ALKIS__Bauwerke_Linien`, `Bauwerke_Punkte`), providing a robust spatial framework for urban analysis.

Figure 9 visualises all spatial layers contained in the `ALKIS_SDP_2023.gdb` for the Hamburg region, serving as a visual reference for the geodatabase content. Further details on the data layers, including their original names, English translations, and associated geometry types (Point, MultiLineString, MultiPolygon, or NoGeometry), are provided in Table 13 (Appendix A).

3.3. Dataset Review and Analytical Readiness

This section outlines the steps to prepare the spatial data for subsequent analysis. The aim is to ensure data quality and consistency, facilitating accurate urban ratio calculations. The preprocessing involves data validation and coordinate system harmonisation.

The metadata for the datasets is reviewed in two stages: first to understand the data structure and content, and subsequently to determine what information is essential for the ratio calculations and what can be excluded to optimise data processing performance, thereby ensuring that the retained data is specifically tailored for this study's requirements.

Based on the metadata review, all spatial datasets are projected using a common Coordinate Reference System (CRS) to ensure spatial consistency. Given the study's focus on Hamburg, the `ETRS89 / UTM zone 32N (EPSG:25832)` is used, as it is suited for regions between 6°E and 12°E, including Germany (Klokan Technologies, consulted April 2025). This system enables accurate area and distance measurements in meters, which are essential for reliable spatial analysis.

The data preparation process highlights a key challenge in this research: balancing speed with accuracy. The refined datasets load faster and contain only the necessary attributes for urban ratio calculations, but this creates a trade-off. While simplifying data speeds up processing, it can remove important spatial relationships needed for accurate analysis. Therefore, data preparation must be strategic, improving performance while maintaining analytical quality.

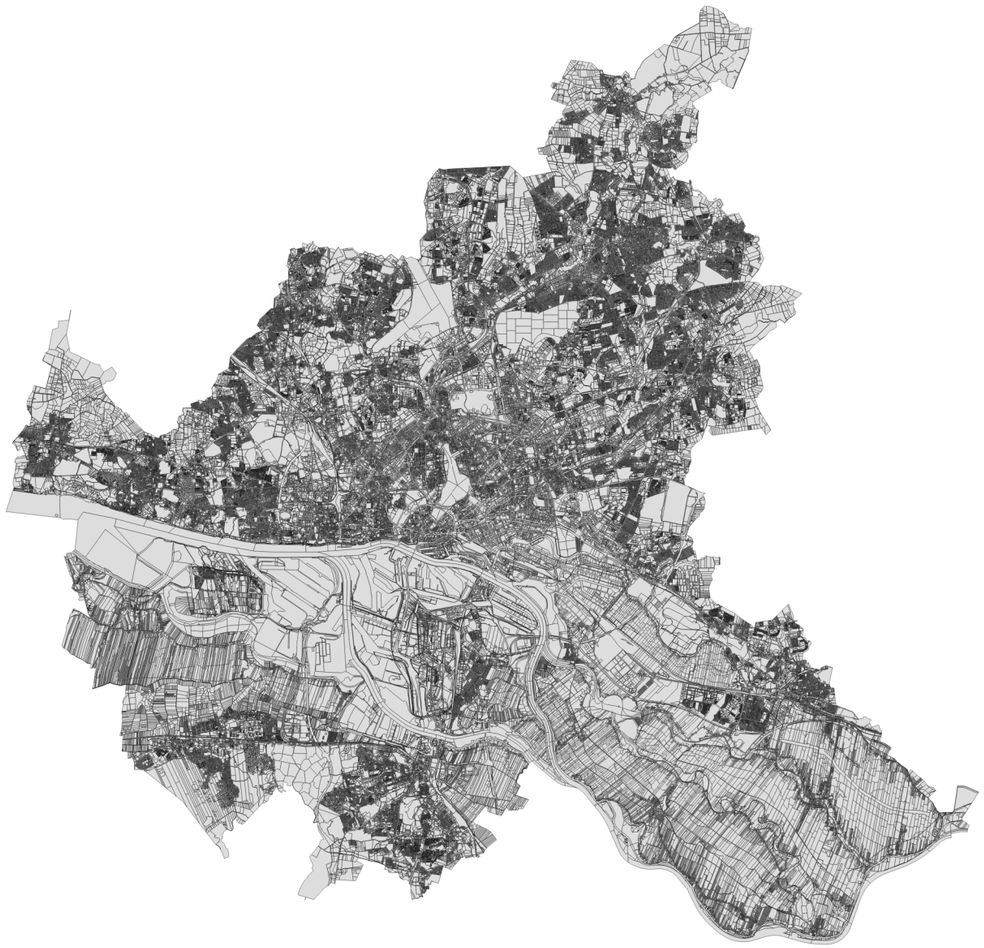

Figure 10. Cadastral parcels in Hamburg at scale 1:250.000. Large parcel clusters such as the Außenalster, the airport and Ohlsdorf Cemetery are clearly recognizable due to their size and distinctive layout (author, 2025).

3.3.1. Cadastral Parcels Dataset

This section focuses on the parcel data from the `ALKIS_SDP_2023.gdb` file. Table 3 compares the available cadastral layers by feature count and data timestamp.

The polygon layer `ALKIS__Flurstuecke_Flaechen`, illustrated in Figure 10, contains 259.734 features representing individual cadastral parcels. Each feature includes 65 attributes providing information such as official area, cadastral district, and parcel identifier. However, many attributes (e.g., `LZI/beginnt`, `AAA-Beschreibung`) appeared irrelevant to the urban ratio calculation process.

A Python script was developed to assess attribute utility through a systematic filtering approach. The initial analysis examined whether each attribute field contained data, excluding those storing only `NULL` values across all parcels. This reduced the total attributes from 65 to 50. Subsequently, the remaining fields were examined for variation. Attributes storing identical values for all parcels (e.g., `ALKIS-Kennung`, `Kreis/name`) were excluded since they provide no meaningful differentiation for analysis. The filtering criteria are documented in Table 14 (Appendix A).

Table 3. Comparison of the cadastral parcel datasets available during the research

File Source	Layer Name	Features	Timestamp
ALKIS_SDP_2023.gdb	ALKIS__Flurstuecke_Flaechen	259.734	30.12.23
Aktive_Flurstuecke_Hamburg.gdb	Flurstueck	260.419	28.10.24
ALKIS_SDP_2024.gdb	ALKIS__Flurstuecke_Flaechen	260.429	31.12.24
ALKIS_SDP_2023.gdb	ALKIS__Gebaeude_Bauteile_Flaechen	406.978	30.12.23
Gebaude_Flurstuecke.gbd	Gebaeude	403.175	28.10.24
ALKIS_SDP_2024.gdb	ALKIS__Gebaeude_Bauteile_Flaechen	409.581	31.12.24

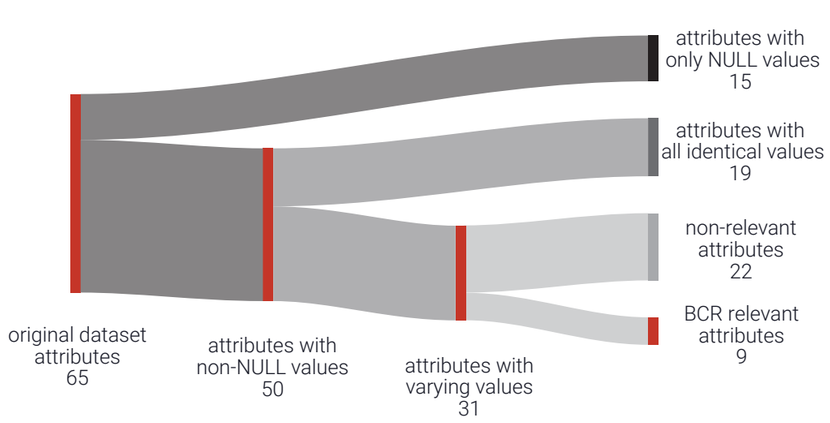

Figure 11. Attribute filtering process for the ALKIS parcel dataset, reducing 65 attributes to 9 relevant fields through null value removal and content relevance checks (author, 2025).

Figure 11 presents a Sankey diagram illustrating this attribute filtering process. The refined dataset contains only attributes identified as relevant for parcel identification and urban parameter calculations. The selected attributes are listed in Table 4. This approach produced a clearer, more efficient dataset tailored to the study objectives.

To evaluate data efficiency relative to analytical requirements, the original and pruned parcel datasets were compared using two metrics: exported CSV file size and QGIS data loading time (measured using Python's time library).

Table 4. Overview of selected ALKIS parcel attributes, including original German field names, English translations, data types, and sample values from the parcel occupied by *HafenCity University.*

Attribute Short Name	Attribute Name (German)	Attribute Name (English)	Data Type	Sample Value
AFL	AmtlicheFlaeche	Official Area	double	9171
ZAE	Flurstuecksnr/zaehler	Parcel Number/ Counter	string	2191
NAMGMK	Gemarkung/ name	Cadastral District / Name	string	Altstadt Süd
GMK	Gemarkung/ schluessel	Cadastral District / Key	string	102
BEG	LZI/beginnt	Lzi Starts	date time	09.11.20 08:49:29 (UTC)
FSK	Flurstuecks/ kennzeichen	Parcel Identifier	string	020102___02191____
UUID	Identifikator	Identifier	string	DEHHALKAJ0000HjR
ISTGEBUCHT	istGebucht-Buchungsstelle	Is Booked Booking Office	string	DEHHALKA100011nv
OBJECTID	ObjectID	ObjectID	integer	7387

The results, presented in Figure 12, demonstrate that the refined dataset file size was reduced to approximately one-quarter of the original, representing a significant storage efficiency improvement. However, loading time improvements were more modest, with the pruned dataset loading only 20% faster. This suggests that while attribute reduction meaningfully contributes

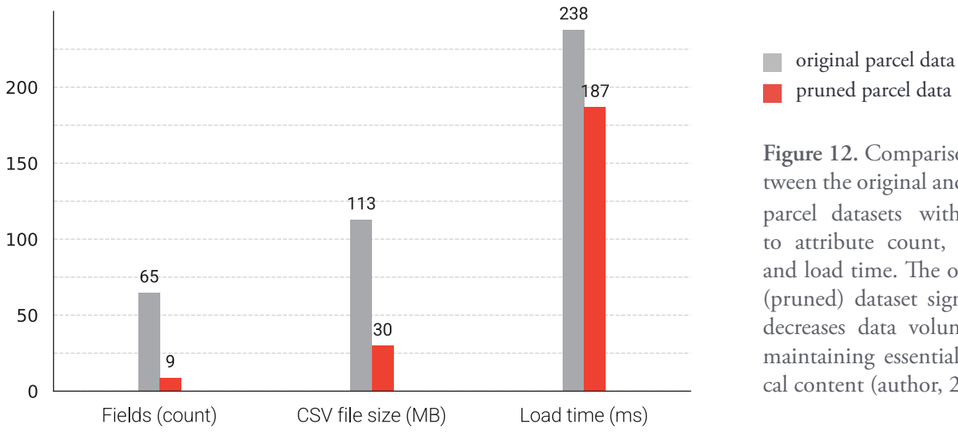

Figure 12. Comparison between the original and pruned parcel datasets with respect to attribute count, file size, and load time. The optimised (pruned) dataset significantly decreases data volume while maintaining essential analytical content (author, 2025).

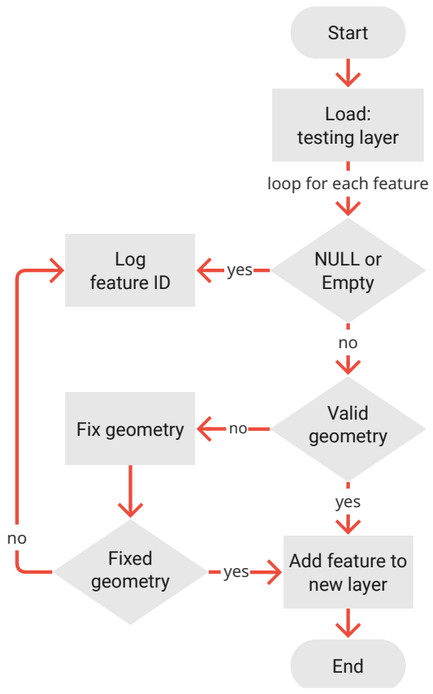

Figure 13. Flowchart illustrates the process of validating and repairing geometries in a QGIS polygon layer using Python (author, 2025).

to data size reduction, its effect on processing speed is comparatively limited, likely due to other factors such as geometry complexity.

Beyond attribute refinement, parcel geometries underwent validation to ensure spatial dataset integrity. This step is critical, as geometry errors (empty shapes, invalid polygons) can disrupt spatial operations, including intersections, area calculations, and spatial joins.

Validation was performed using a Python script (Figure 13) that evaluated each feature in the pruned parcel layer (`ALKIS__Flurstuecke_Flaechen-pruned`) for geometric validity. The script employed QGIS's `isGeosValid()` method to identify topological issues and checked for `null` or `empty` geometries that could compromise analysis completeness and reliability. Invalid features were processed using the `makeValid()` method to repair problematic geometries. Successfully corrected geometries passing the validity checks were included in the cleaned dataset, while valid geometries were transferred directly. `Null` or unfixable features were excluded.

The validation process indicated high data quality. Among more than 250.000 analysed features, none were `null` or `empty`, and only six contained invalid geometries (locations shown in Figure 14). All six were successfully repaired and included in the final cleaned dataset. This validation step ensured that data used in subsequent spatial operations, area calculations and spatial joins was free from topological errors.

The refined parcel dataset provides a solid foundation for next steps. However, the integration of this dataset with building data presents specific challenges that are addressed in the Section 3.4. (Dataset Linkage).

Figure 14. Map showing the location of the six parcels with corrected geometries within the city of Hamburg. Displayed at a scale of 1:500.000 (author, 2025).

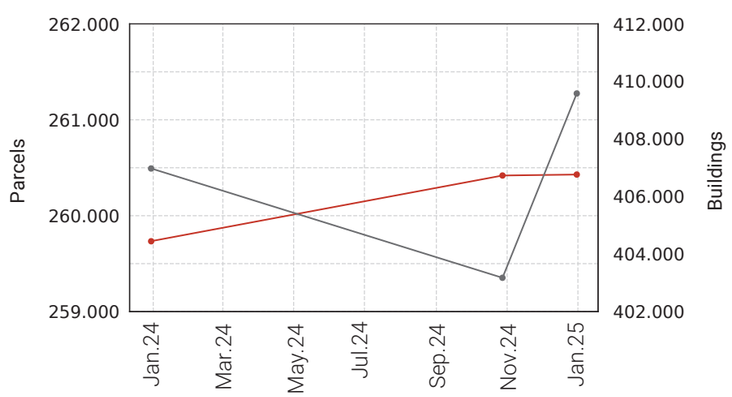

Figure 15. Timeline of feature counts for parcels and buildings. Dual-axis line chart tracks the total number of parcel and building features in the dataset over time, illustrating incremental changes and update frequencies (author, 2025).

3.3.2. Buildings Dataset

This section describes the processing of the `ALKIS__Gebaeude_Bauteile_Flaechen` dataset, which contains 406.978 polygon features. The workflow applied mirrors the methodology employed for the parcel dataset. Table 15 (Appendix A) provides the complete list of analysed attributes.

Table 3 and Figure 15 compare the available features, with the line chart illustrating the total number of parcel and building features over time.

This building layer contains 61 attributes, including potentially useful fields such as `Object Height`, `Floor Area` (for calculating FAR), and `Parcel Identifier` (which enables linking buildings to parcel geometry). However, many of these fields remain unpopulated in the current dataset version. While their presence indicates the data structure's capacity to accommodate more detailed information in future updates, the current analysis is limited by the availability of populated attributes.

Following attribute pruning, 16 attributes were selected from the original 61, as summarised in Table 5. Geometry validation used the same Python script applied to the parcel layer, successfully repairing five invalid geometries.

As the layer name indicates, the dataset includes both `AX_Gebaeude` and `AX_Bauteil` entries, distinguished by the `Aaa-Beschreibung` attribute. According to the ALKIS documentation[6] (AdV, 2022), a *Gebäude* represents a permanently constructed structure documented in the cadastre due to its legal or functional significance. In contrast, a *Bauteil* constitutes a building component that differs from the main structure in characteristics or function.

This distinction directly affects attribute completeness. **Bauteil** features generally lack essential data such as `Building Function`, `Street Name`, and `Ground Area`. Only `Location Relative to Ground Surface` remains consistently populated for Bauteile, with values including Elevated (*Aufgeständert*) or Below the Surface (*Unter der Erdoberfläche*). Conversely, **Gebäude** features exhibit complete attribute structures, with key fields like `Building Function` and `Ground Area` populated across all records, while others, such as `Additional Building Function`, contain values in approximately 3% of records.

6. The Ausleitung des ALKIS-Objektartenkatalogs DLKM (Version 7.1.2, Stand: 01.11.2022) is an official document published as part of the GeoInfoDok series, which defines and standardises object types, attributes, and classification rules used within the ALKIS cadastral information system.

Figure 16. Visualization of polygons with the attribute `AX_Gebaeude` (buildings) in dark grey at a scale of 1:30.000. The map shows the building footprints in Hamburg Altstadt (author, 2025).

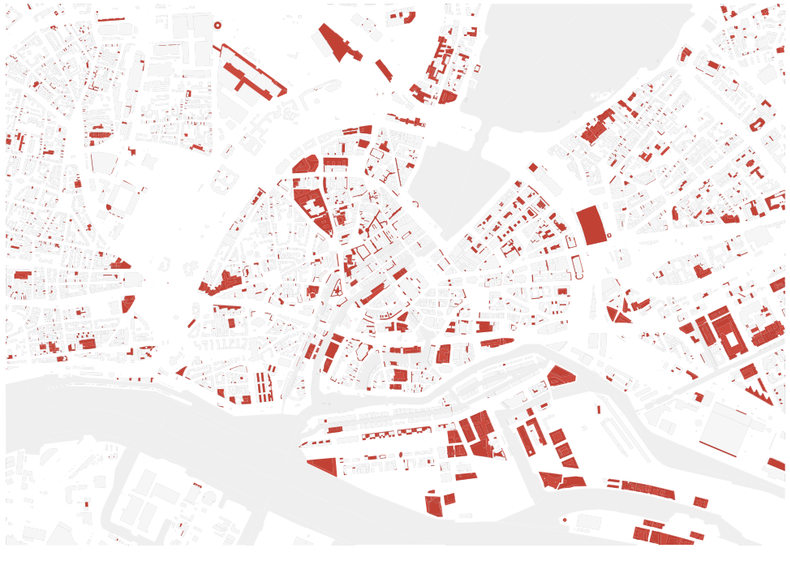

Figure 17. Visualization of polygons with the attribute `AX_Bauteil` (building components) in red at a scale of 1:30.000 (author, 2025).

Table 5. Overview of selected ALKIS builidng attributes, including original German field names, English translations, and sample values from the polygon representing the HafenCity University.

Attribute Short Name	Attribute Name (German)	Attribute Name (English)	Sample Value
UUID	Identifikator	Identifier	DEHHALKA4900003B
GFK	Gebaeudefunktion/ Schluessel	Building Function/ Code	3023
BEZGFK	Gebaeudefunktion/ Bezeichnung	Building Function	Hochschulgebäude
WGF	Weiteregebaeudefunktion/ Schluessel	Additional Building Function/Code	1060
BEZWGF	Weiteregebaeudefunktion/ Bezeichnung	Additional Building Function	Tiefgarage
OFL	Lagezurerdoberflaeche/ Schluessel	Location Relative to Ground Surface/Code	NULL
BEZOFL	Lagezurerdoberflaeche/ Bezeichnung	Location Relative to Ground Surface	NULL
BJA	Baujahr	Year of Construction	2014
NAM	Name	Name	Hafen City Universität
GRF	Grundflaeche	Ground Area	5963
NAMLAG	Strassen/Name	Street Name	Henning-Voscherau-Platz
HNR	Hausnummer	House Number	1
BEZEICH	Aaa-Beschreibung	Aaa Description	AX_Gebaeude
BEG	Lzi/Beginnt	Lzi Starts	15.12.20 10:03:15 (UTC)
OBJECTID	ObjectID	ObjectID	45521

Figures 16 and 17 present filtered visualisations of `AX_Gebäude` and `AX_Bauteil` features, respectively, revealing clear differences in data density and granularity. `AX_Gebäude` captures building footprints comprehensively across the study area, while `AX_Bauteil` features appear only in specific, limited locations with varying geometries in scale and complexity. This pattern suggests that not all buildings are subdivided into components, or that such subdivisions are recorded inconsistently.

Given these inconsistencies, only `AX_Gebäude` features were selected for urban parameter calculations due to their comprehensive and consistent data structure.

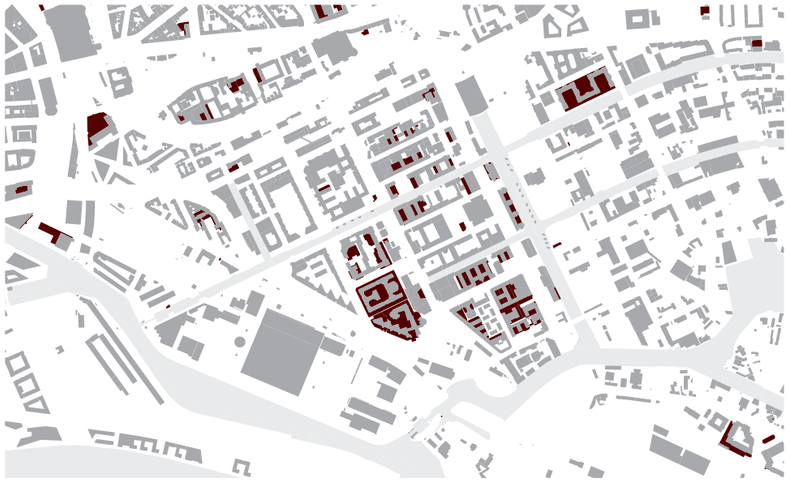

Figure 18. Visualization of polygons with the attribute `AX_Gebaeude` (buildings) in Hammerbrook at a scale of 1:20.000. Features labeled as **underground structures** are shown in dark red, while beneath aboveground structures are shown in light grey (author, 2025).

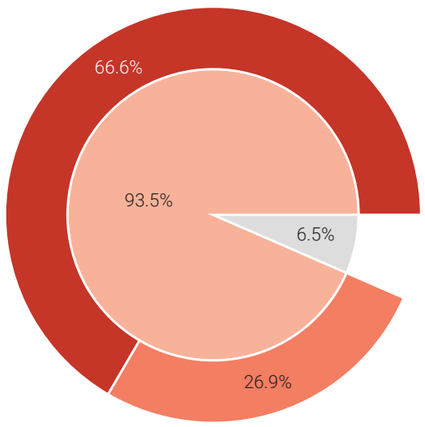

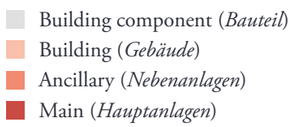

Figure 19. Hierarchical classification of building features in the ALKIS dataset. The inner pie chart distinguishes between Gebäude and Bauteil, while the outer ring breaks down Gebäude into Hauptanlagen and Nebenanlagen (author, 2025).

As outlined in Section 2.2, each building in the dataset is categorized as either a **main structure (Hauptanlage)** or an **ancillary structure (Nebenanlage im weiteren Sinne)** according to its function in terms of §19 BauNVO. In this study, we automated this classification using the ALKIS Gebäudefunktion (GFK) attribute. Table 7 shows the GFK code values corresponding to main vs. ancillary structures (see Appendix A for the full list from the ALKIS object catalog).

Table 6. Attributes and corresponding values used to identify building polygons as ancillary structures.

Attribute Short Name	Attribute Name (English)	Value (German)	Value (English)	Key (GFK)
BEZGFK	Building Function	Garage	Garage	2463
BEZGFK	Building Function	Gartenhaus	Garden shed	1313
BEZGFK	Building Function	Gewächshaus, verschiebbar	Mobile greenhouse	2742
BEZGFK	Building Function	Tiefgarage	Underground garage	2465
BEZGFK	Building Function	Treibhaus, Gewächshaus	Greenhouse	2740

The building classification approach outlined in Table 6, while methodologically consistent, carries important limitations identified during expert consultations[7]. Planning professionals confirmed that no standardized mapping exists between ALKIS `Gebäudefunktion` values and the regulatory categories of **Hauptanlagen** and **Nebenanlagen**, as these distinctions typically emerge during permitting processes based on contextual factors not captured in cadastral data. This study's reliance on `Gebäudefunktion` as a classification proxy, therefore, represents a practical compromise that enables automated analysis while acknowledging potential divergence from regulatory determinations.

Figure 18 complements this classification by comparing underground and above-ground structures, providing insight into their spatial distribution and relative prevalence.

The dataset analysis revealed the following distribution: from 406.978 original features in the `ALKIS__Gebaeude_Bauteile_Flaechen` layer, 26.588 were identified as Bauteil and 380.390 as Gebäude. Among Gebäude features, 270.958 were classified as Hauptanlagen and 109.432 as Nebenanlagen. This hierarchical breakdown (illustrated in Figure 19) demonstrates the

7. Details on the expert consultations are mentioned at the end of this section.

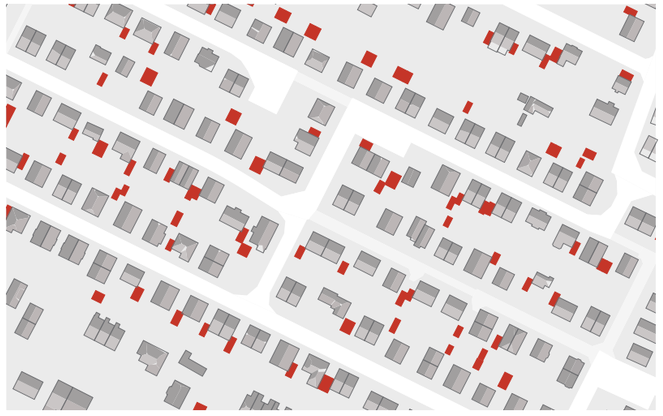

Figure 20. Visualisation comparing features labelled as *Main* and *Ancillary* in the Billstedt area, shown at a scale of 1:20.000. The distinction is clear: the ancillary units, represented in red, are typically located toward the rear façades of the parcels, indicating functions like tool sheds, greenhouses, or garden houses (author, 2025).

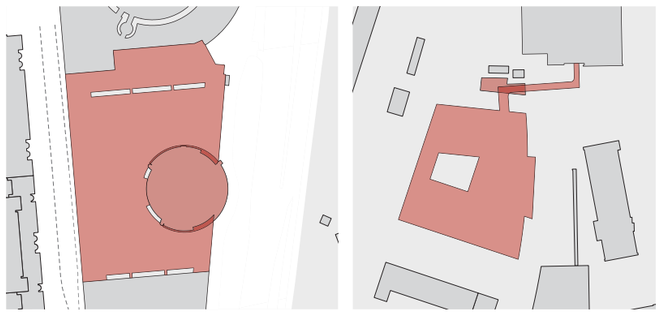

Figure 21. Examples of minor geometry intersections. *Left*: Overlapping structures near Hamburg Airport, visualised at a scale of 1:10,000. *Right*: Small bridge structure intersecting a building footprint at the University of Hamburg, Institute for Quantum Physics, shown at a scale of 1:5.000 (author, 2025).

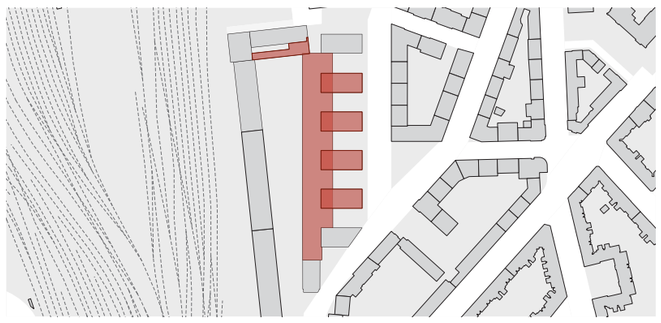

Figure 22. Intersection case involving Feature ID `DEHHALKA5XA000JA`, located near Altona Bahnhof. The feature overlaps with five others, four of which share an overlapping area of approximately 150 m² each, indicating significant spatial duplication (author, 2025).

predominance of primary structures and supports the decision to focus on `AX_Gebäude` for urban parameter calculations.

An additional validation step was performed to identify overlapping building geometries, which can cause errors in GRZ calculations by counting the same area multiple times. The analysis used a Python script to detect intersections between building features, applying a 1 m² minimum threshold to filter out insignificant overlaps caused by minor surveying inaccuracies or edge-touching geometries. Only intersections larger than this threshold were considered problematic and flagged for further investigation.

Twenty-one intersection cases were identified. As Figure 21 shows, most appear to result from slight inaccuracies in building survey data. Since `Ground Area` is stored as an attribute for each building feature, these small overlaps were deemed negligible and excluded from further consideration.

However, four intersection cases showed extensive overlapping that required further investigation. When the intersecting features were ranked by the number of intersections, four buildings stood out with high intersection counts: three buildings each overlapped with 12 other buildings, and one building overlapped with 5 other buildings. The building with five overlaps is located near Altona Bahnhof (Figure 22) has a `Building Function` value of: Storage Building (*Gebäude für Vorratshaltung*). This storage building intersects with four residential buildings and one office building.

The three highest-ranking cases, each intersecting with 11 or 12 other features, correspond to a 2021 residential development of three house rows (Figures 23 and 24). Here, building geometries appear stored twice, once as large, continuous polygons and the second time as smaller, individual units. All features share the same `Building Function` value *Wohnhaus*, but only smaller polygons include address values. The larger polygons lack this information, suggesting they represent composite or planning-level geometries. Nevertheless, all polygons maintain valid `Ground Area` values.

To determine whether these overlaps resulted from outdated data, additional available ALKIS dataset versions (Table 3) were consulted to check for updates. However, the buildings were represented identically across all versions, ruling out this explanation

Figure 23. Orthophoto of parcel `DEHHALKA70000pgU` in the Wandsbek district, showing a residential development composed of three rows of houses constructed in 2021 (author, 2025).

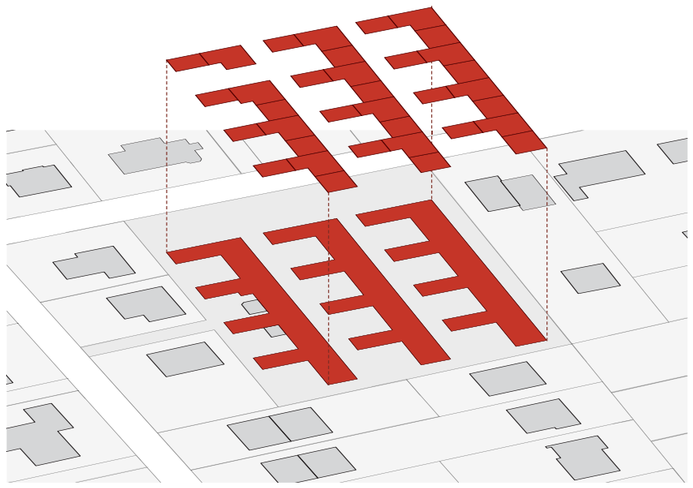

Figure 24. Visualisation of repeated building geometries on parcel `DEHHALKA70000pgU`. *Bottom*: Larger, continuous building footprints. *Top*: Individually segmented units. Shows the dual representation of the same structures (author, 2025).

Given this consistency and the absence of attribute-level errors, no features were removed or edited. Instead, the overlapping cases were documented by logging their feature IDs, and these buildings will be monitored closely during GRZ calculations. Higher-than-expected GRZ values are anticipated for the affected parcels due to the double-counting of building areas.

3.4. Dataset Linkage

Up to this point, the parcel and building datasets have been examined independently to assess their internal structure, attribute completeness, and geometric integrity. The calculation of urban morphological parameters such as GRZ, however, requires bringing these two datasets into spatial alignment.

The ALKIS data model presents a fundamental structural challenge in this regard, as its official documentation explicitly states that relational keys linking buildings to their parcels are absent. This design choice is clearly acknowledged in the documentation:

> *"Hinweise: Die Zuordnung des 'Gebäudes' zum 'Flurstück' kann durch geometrische Verschneidungsoperationen realisiert werden; das explizite Führen von Relationen zwischen den beiden Objektarten unterbleibt."*
>
> - AdV, 2022, p. 191

This absence of explicit linkage introduces both analytical and computational complexity, necessitating the use of spatial operations, specifically geometric intersections, to establish relationships between the two datasets. The implications of this limitation are substantial and inform the methodological approaches developed in the subsequent sections.

3.4.1. Building-Parcel Geometric Relation

Establishing spatial relationships between buildings and parcels is essential. These associations must be inferred through geometric operations, most commonly by evaluating whether a building polygon intersects a parcel polygon.

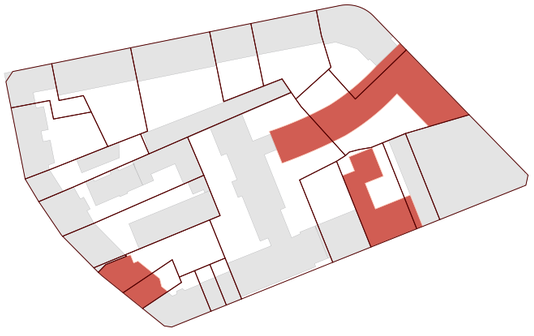

Figure 25. Multi-parcel building footprints in the Behringstraße 29 Block (Ottensen, Hamburg). Several building footprints (shown in red) extend across multiple cadastral parcels (outlined in dark) (author, 2025).

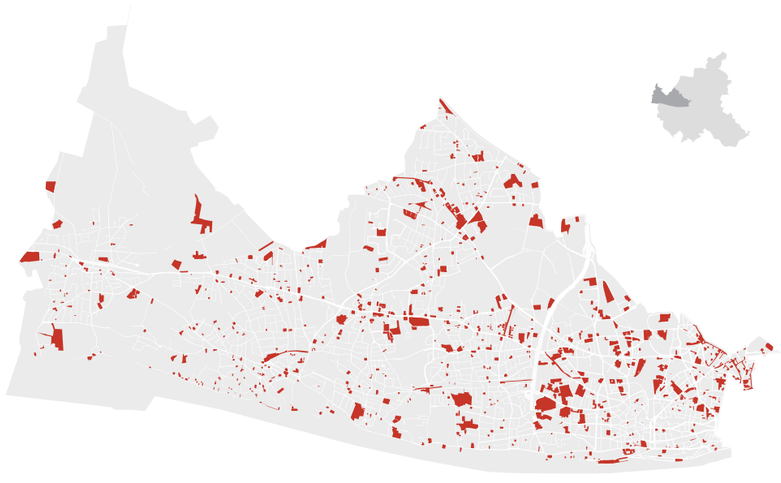

Figure 26. Map of Altona distric showing in red the parcels that share builidng geometries (author, 2025).

Initial visual inspections of the spatial data revealed a key complexity: while most buildings are entirely contained within single parcel boundaries, a significant number of buildings span across multiple parcels. Figure 25 illustrates an urban block where this occurs. Such overlaps introduce analytical ambiguity into GRZ calculations because it becomes unclear how to attribute building areas when a single structure spans multiple parcels. This ambiguity prompted further investigation to determine the scope and spatial distribution of these overlapping cases.

To quantify this phenomenon, a comprehensive spatial analysis was conducted on the district Altona, selected as a representative sample of Hamburg's urban morphology. The analysis identified building footprints intersecting more than one parcel boundary. The results showed that 4.110 out of 58.158 buildings (approximately 7,0 %) intersect multiple parcels, thereby constituting non-trivial cases for standard per-parcel GRZ calculations (see Figure 26).

Although this 7,0 % proportion represents a minority, the absolute number of affected structures is substantial and requires specialised analytical treatment. Moreover, the geometric characteristics of these overlaps vary significantly. In some cases, buildings only slightly exceed parcel boundaries, possibly due to digitisation discrepancies or coordinate precision errors. While in others, substantial structures span several legal parcels. This variability necessitates a refined approach capable of distinguishing between meaningful spatial relationships and spurious geometric artefacts.

These findings raised a key methodological question: how should GRZ be calculated when a single building footprint overlaps multiple parcels? Two potential strategies were considered:

1. **Proportional Allocation**: Divide the building's footprint area among intersecting parcels based on the percentage of overlap.
2. **Parcel Clustering**: Treat the affected parcels as a single analytical unit in cases where overlaps occur.

To assess the feasibility and regulatory validity of these alternatives, consultations were held with planning professionals and additional quantitative tests were conducted. The author consulted with representatives from the Landesbetrieb Geoinformation und Vermessung (LGV), while Benjamin Dally consulted with the Bezirksamt Altona, Zentrum für Wirtschaft, Bauen und Umwelt. Both consultations were conducted within the HCU–LIG research collaboration project. The feedback on this consulations can be summarised as follows:

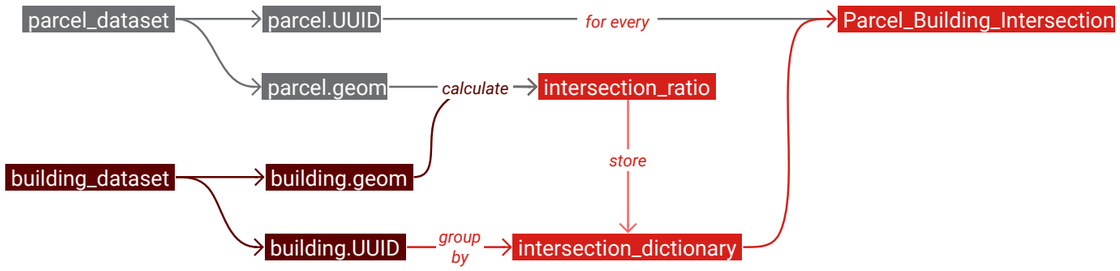

Figure 27. Diagram for the dictionary-based workflow for Parcel–Building intersection analysis (author, 2025).

Standard Practice: GRZ is generally calculated per parcel.

Legal Complexity: In certain cases, multiple parcels may functionally act as a single building lot (Baugrundstück), particularly when listed under the same land registry sheet (Grundbuchblatt) and held in common ownership. In such instances, GRZ may be calculated over the combined area.

Data Ambiguity: These legal groupings are not consistently recorded within the ALKIS dataset, as they are governed by separate legal instruments (e.g., Baulasten) that are not always accessible via spatial data systems.

In light of these complexities, this thesis adopts a pragmatic and methodologically consistent approach: GRZ is calculated per parcel, with the area of intersecting buildings divided proportionally according to the degree of geometric overlap (see Figure 27). This method ensures transparency, aligns with prevailing regulatory interpretations, and enables a scalable, repeatable pipeline for large-scale urban analysis.

3.5. Building Coverage Ratio Calculation Method

This section outlines the automated methodology for calculating the Building Coverage Ratio (Grundflächenzahl, GRZ). Following the building classification approach detailed in Section 3.3.2, two GRZ values are computed: GRZ_main (main buildings only) and GRZ_aux (all building types).

$$\text{GRZmain} = \frac{B_{\text{main}}}{P} \tag{1}$$

$$\text{GRZaux} = \frac{B_{\text{main}} + B_{\text{aux}}}{P} \tag{2}$$

The calculation process establishes spatial associations between parcels and buildings through automated Python and SQL workflows, then sums relevant building footprint areas per parcel. This two parallel methods are applied to the `ALKIS_SDP_2023.gdb` dataset to ensure comparable results.

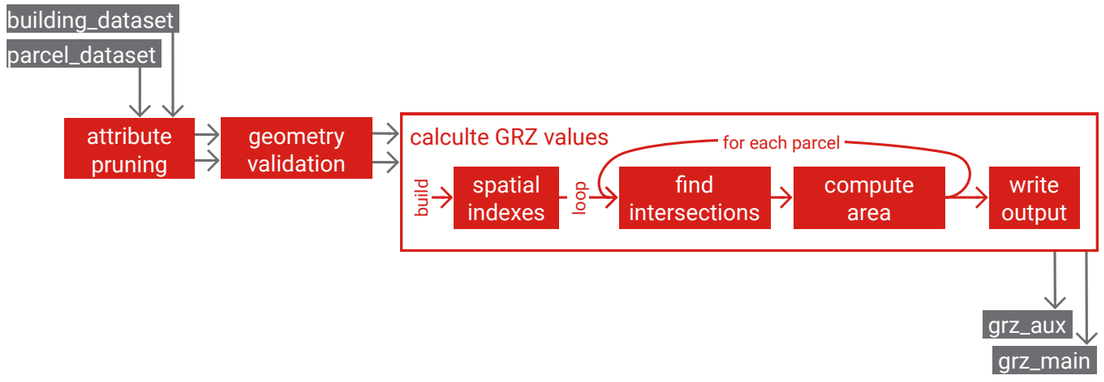

Figure 28. Flowchart illustrating the complete GRZ calculation workflow in QGIS (author, 2025).

```
main_area = sum(
    feat.geometry().intersection(parcel_geom).area()
    for feat in main_feats
    if not feat.geometry().intersection(parcel_geom).isEmpty()
           and inter. area() > 1.0
)
```

Listing 1. Code snippet of Listing 5 (Apendix B) focused in area calculation of main building intersections (excluding empty geometries and intersections smaller than 1 m²).

3.5.1. Calculation using GIS Workflows

This workflow was implemented in QGIS version 3.34.4 and combines graphical tools with custom Python scripting. After loading and validating the parcel and building datasets (as described in Sections 3.3.1 and 3.3.2), the analysis filters features to include only `AX_Gebaeude`, which are then classified into `main` and `ancillary` types. Once classification is complete, the spatial analysis proceeds with calculations based on actual geometric relationships between buildings and parcels.

To perform the analysis, a custom Python script was developed and executed within the QGIS environment. The first step involves creating spatial indexes for both layers. These indices significantly speed up the spatial queries by enabling quick identification of building features that are likely to intersect each parcel's geometry[8]

The script then iterates through each parcel in the dataset, retrieving its geometry and total area. For each parcel, the script uses the spatial indexes to identify candidate building features whose bounding boxes intersect the parcel. These candidates are further filtered by testing for actual geometric intersections. If an intersection exists, the overlapping area between the parcel and each building footprint is calculated (see code Snippet in Listing 1).

Two separate calculations are carried out for each parcel: `GRZ_main` and `GRZ_aux` (as defined in Section 3.5). Both GRZ values are rounded to two decimal places and stored in a newly created output layer. Each feature in this layer preserves the original parcel geometry and attributes, along with the two new GRZ metrics. Finally, the script records the total execution time using Python's time module, providing a useful benchmark for evaluating the workflow's performance. The complete sequence of steps (ranging from geometry validation to GRZ computation) is visualised in Figure 28 (see code snippet in Listing 1; full script available in Appendix B, Listing 5).

Unlike methods that rely on existing attribute fields such as `Ground Area`, this workflow dynamically calculates coverage based on actual geometry. While this approach ensures geometric consistency by calculating coverage based on actual spatial intersections, it also requires more processing time, as every parcel-building intersection must be evaluated individually.

8. As a comparison, the version of the script that included spatial indexing completed the task in approximately 7 minutes. In contrast, the same script without indexing was still running after more than 45 minutes and was manually aborted.

3.5.2. Calculation using Spatial Query Methods

The PostGIS-based method uses SQL queries within a PostgreSQL database to calculate the Building Coverage Ratio (`GRZ_main` and `GRZ_aux`) on spatial datasets. The workflow operates through automated SQL scripts that perform all required steps, from data validation to spatial analysis and ratio computation, without manual intervention during execution. This contributes to full automation in this workflow by eliminating manual steps during execution, significantly enhancing its reproducibility and reliability for urban analysis.

Although the current implementation requires manually downloading and importing the ALKIS dataset into the PostgreSQL database, the method is designed with full automation in mind. In the context of the HCU–LIG collaboration, future iterations of this workflow will integrate direct data access via an `OGC API`, allowing seamless, real-time updates of spatial data in the database.

The process begins by importing the raw ALKIS datasets (parcels and building footprints) into a PostgreSQL database with the PostGIS extension enabled. Geometry columns are indexed in this process to improve query performance. Unlike file-based tools such as QGIS or Python, where redundant attributes can burden performance, PostgreSQL dynamically retrieves only the fields needed for analysis. As such, attribute trimming is not required; instead, the focus of data preparation shifts to ensuring geometric integrity.

Geometry validation steps follow the same logic as described in Section 3.3.2, using here PostGIS functions to ensure clean spatial data. Invalid or empty geometries are logged and removed from the analysis. Buildings are classified into main and ancillary types using the approach established in Section 3.3.2. The classification is stored as a new field for downstream calculations.

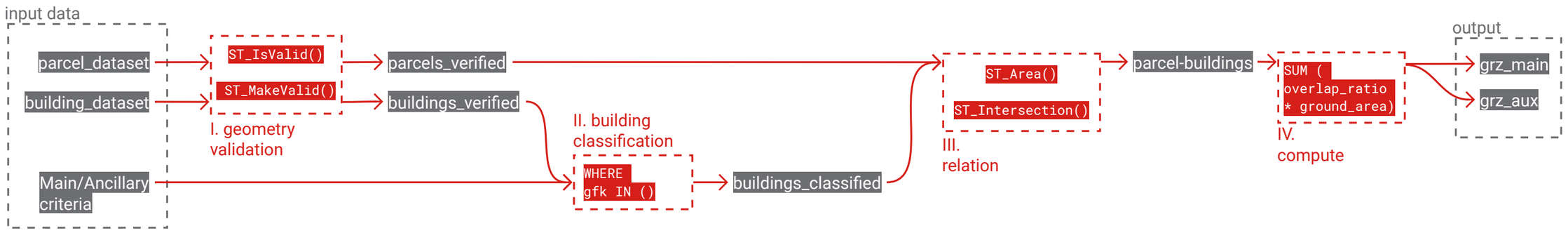

Figure 29. Workflow diagram for `GRZ_main` and `GRZ_aux` calculation using PostGIS extension (author, 2025).

```sql
-- STEP 3 : parcels-buildings relation
ALTER TABLE public.flurstuecke
ADD COLUMN IF NOT EXISTS b_ratios JSONB;

-- filter relevant buildings and precompute their area
WITH filtered_buildings AS (
    SELECT uuid, geom, ST_Area(geom) AS b_area
    FROM public.gebaeude_bauteile
    WHERE bezeich = 'AX_Gebaeude'),

-- compute intersection area between each building and parcel
intersections AS (
    SELECT
        p.uuid AS parcel_uuid,
        b.uuid AS building_uuid,
        ST_Area(ST_Intersection(b.geom, p.geom)) AS intersection_area,
        b.b_area
    FROM public.flurstuecke p
    JOIN filtered_buildings b
      ON ST_DWithin(p.geom, b.geom, 1.0)
   WHERE ST_Intersects(p.geom, b.geom)),

-- calculate relative overlap ratios and format as a JSONB object
ratios AS (
    SELECT
        parcel_uuid,
        jsonb_object_agg(
            building_uuid,
            ROUND(
                CASE
                    WHEN intersection_area / NULLIF(b_area, 0) > 0.95 THEN 1.0
                    WHEN intersection_area / NULLIF(b_area, 0) < 0.05 THEN 0.0
                    ELSE intersection_area / NULLIF(b_area, 0)
                END::numeric,
                2
            )
        ) AS json_result
    FROM intersections
    GROUP BY parcel_uuid
)
UPDATE public.flurstuecke AS parcels
SET b_ratios = ratios.json_result
FROM ratios
WHERE parcels.uuid = ratios.parcel_uuid;
```

Listing 2. SQL query for calculating parcel-building overlap ratios and storing results in JSONB format

Spatial relationships are then determined using intersection queries. For each parcel, the workflow calculates the intersection area with overlapping buildings and compares it to the full building footprint to determine the overlap ratio. A rule-based filter is applied: intersections covering less than 5% of a building's area are discarded, and those greater than 95% are treated as full overlaps.

Listing 2 presents the SQL code for step 3 (parcel-building relations), with the complete SQL query provided in Listing 10 (Appendix B).

The selection of these threshold values represents a critical methodological decision that balances computational efficiency with analytical precision. The 5% lower threshold eliminates spurious intersections caused by minor geometric overlaps, edge effects, or coordinate precision limitations that are common in large-scale cadastral datasets. On the other hand, the 95% upper threshold accounts for small geometric discrepancies between building footprints and parcel boundaries that may result from digitisation errors, coordinate transformations, or temporal misalignments between dataset updates. These thresholds effectively create a tolerance band that accommodates the inherent uncertainties in spatial data while maintaining the integrity of the spatial analysis.

The rationale for these specific percentage values is based on empirical observations from the Hamburg dataset, where preliminary analysis revealed that the majority of meaningful building-parcel relationships fell outside these boundary ranges. A detailed sensitivity analysis of these thresholds, including their impact on overall GRZ calculations, is provided in Chapter 5.

The resulting ratios are stored in a dictionary-like structure, using building UUIDs as keys and overlap percentages as values, enabling efficient lookup operations during subsequent GRZ calculations. Using this structure, GRZ values are calculated. Each building's overlap ratio is multiplied by its official ground floor area (`GRF`), and the adjusted areas are aggregated per parcel. The method outputs both GRZ variants. The final values are written to the parcel layer as two new columns.

The PostgreSQL instance used for this analysis was hosted within a Docker container, using the official `postgis/postgis:15-3.3` image for AMD64 architectures. This configuration offered several technical advantages. It enabled consistent deployment across machines, eliminated system-level dependency conflicts, and provided a lightweight environment for managing spatial operations.

Docker's versioning features also allowed for structured experimentation with different processing strategies during the workflow design phase. This setup formed a robust platform for managing and querying ALKIS data at the city scale.

This method represents a solution for morphological analysis in urban planning, loading raw ALKIS data, validating geometries, classifying structures, calculating spatial intersections, and computing GRZ values entirely within the database environment. From a learning perspective, developing this method provided valuable insights into relational database design, spatial indexing, and SQL-based geospatial workflows. It reflects broader trends in planning practice, where, transparent and reproducible methods are increasingly necessary for managing large, frequently updated spatial datasets. In this context, PostGIS emerges as a foundational tool for institutional and research-oriented urban morphology.

3.6. Comparative Analysis Setup

This section presents a comparison of the QGIS and PostGIS workflows developed to calculate `GRZ_main`. The comparative framework is structured around two key aspects: agreement of results and computational efficiency. These criteria were selected to evaluate both the technical consistency of the outputs and the practical feasibility of implementing each method in real-world urban research applications.

Since no ground truth data is available for validation, the accuracy assessment focuses on measuring the agreement between the two workflows. A paired dataset is created, in which each parcel is assigned the GRZ values produced by the QGIS and PostGIS methods. This allows for a direct statistical comparison of the results.

The agreement analysis is carried out through the steps listed in Table 7. These analyses provide an evaluation of how closely the two workflows align. They help identify potential discrepancies that may arise from differences in spatial processing, such as the use of **actual polygon intersections** in QGIS versus **attribute-based computations** in PostGIS.

For efficiency evaluation, processing time for major steps in both workflows is tracked and analysed. Key steps include data import/loading, spatial linkage (parcel-to-building intersection), and GRZ calculation (main and auxiliary). For QGIS, timing is captured using Python's `time` module, while for PostGIS, timing and query performance are analysed using `EXPLAIN ANALYZE`. This allows for a structured comparison of runtime performance, memory/CPU usage, and overall responsiveness across varying data sizes.

Table 7. Summary of statistical metrics used to evaluate the agreement between GRZ values calculated in QGIS and PostGIS.

Metric / Plot	Description	Purpose / Insight
Mean Difference	Computes the average difference between QGIS and PostGIS GRZ values across all parcels	Identifies whether one method consistently over- or underestimates GRZ compared to the other
Standard Deviation of Differences	Measures how much the differences between the two methods vary from parcel to parcel	Assesses consistency of agreement; large SD suggests unstable or uneven differences
Bland–Altman Plot	Plots the difference vs. the average of the two methods, showing bias and limits of agreement	Visualizes both systematic bias and spread of differences, highlighting potential outliers or trends

Qualitative factors such as user-friendliness, transparency, and workflow flexibility are also considered, for example, an intuitive GUI that supports experimentation and visual validation, or robust, fully automated solutions requiring proficiency in database management.

This structured comparison offers a comprehensive understanding of the trade-offs between visual interface-based spatial analysis and automated, database-driven spatial computing, supporting the broader goal of evaluating tools for urban morphological analysis.

3.7. Data Visualisation and Interpretation

Visualisation plays a central role in this study, serving both to validate spatial logic and to interpret urban morphological patterns. The `GRZ_main` values calculated through both workflows are visualised using a combination of maps, charts, and statistical graphics. These visualisations highlight spatial trends, reveal potential inconsistencies, and support comparative analysis.

Table 8 presents the different types of visualisations employed in the study. Each is designed to fulfil a specific analytical purpose, from identifying spatial patterns and comparing calculation methods to detecting anomalies within the data.

Table 8. Overview of visualization types used to analyze and compare parcel-level GRZ calculations. Each visualization supports a specific analytical goal, from spatial pattern recognition to method comparison and anomaly detection.

Visualisation	Description	Purpose / Insight
Color-coded maps	Showing parcel-level GRZ_main and GRZ_aux values using graduated symbology across the study area	Reveal spatial variation in building coverage ratios (main vs. ancillary structures)
Scatter plots	Comparing QGIS and PostGIS outputs for matched parcels	Identify differences or alignment between calculation methods
Histograms	Displaying the distribution of GRZ values within each workflow	Understand frequency and spread of GRZ outcomes
Flagged parcel maps	Highlighting parcels exceeding GRZ thresholds or showing notable discrepancies between methods	Detect anomalies or parcels with potential data or planning issues

All spatial maps are generated using QGIS, while statistical graphics are produced with Python's `matplotlib` library. Beyond their illustrative function, these visual outputs contribute to a more comprehensive understanding of urban form and density distribution across Hamburg. They also form the foundation for the comparative analysis in Chapter 4, Results, supporting conclusions about the strengths, limitations, and planning relevance of each calculation method.

The approach to visualisation in this thesis was not developed in isolation. It was significantly shaped by the visual and analytical style presented in *SPACEMATRIX: Space, Density and Urban Form* by Berghauser Pont and Haupt (2021), published by TU Delft OPEN. The report's emphasis on structured design, clarity of communication, and integration of spatial metrics served as both a conceptual and aesthetic reference.

3.8. Methodological and Data Limitations

The workflows developed in this study offer practical approaches for calculating GRZ values, but several technical and procedural limitations affect their reproducibility, automation potential, and data handling robustness.

The QGIS-based method, while suitable for spatial exploration, is constrained by its manual nature. Each step, from data preparation to spatial analysis, requires user interaction. This limits repeatability and increases the risk of human error. While QGIS offers partial scripting capabilities, it lacks full pipeline automation, making it better suited for one-off or exploratory tasks than for standardised batch processing.

The PostGIS workflow is more structured but still presents methodological constraints. The classification of buildings into `main` and `ancillary` categories relies on hardcoded `GFK` codes embedded in SQL (captured as pseudocode in Listing 3). This limits flexibility, transparency, and adaptability to changes in schema. A maintainable solution would involve a separate lookup table to allow more dynamic classification logic.

Both methods depend on the integrity and accuracy of the ALKIS dataset. Errors such as outdated geometries, topological inconsistencies, or misclassified attributes can compromise workflow outputs. In particular, the use of the official `Ground Area` attribute in the PostGIS workflow may not reflect the actual building footprint, while the QGIS method relies on geometry-based calculations that demand valid and accurate spatial data.

Workflow robustness also depends on empirically determined thresholds. For example, the PostGIS method excludes overlaps below 5% and treats those above 95% as full containment. While these thresholds were tuned during testing, they remain assumptions and may not generalise across all urban morphologies or data qualities.

Understanding these methodological and data constraints is essential for interpreting workflow results. The following chapter presents the practical outcomes of both the QGIS and PostGIS workflows, examining spatial patterns, identifying data anomalies, and comparing the methods' performance to validate these approaches and inform the broader conceptual limitations discussed in Chapter 5

```
building_feature is considered a Ancillary_Building if:
    building.GFK = 2463 // Garage
    OR building.GFK = 2465 // Tiefgarage (Underground Garage)
    OR building.GFK = 1313 // Gartenhaus (Garden house)
    OR building.GFK = 2742 // Gewächshaus, verschiebbar (Mobile Greenhouse)
    OR building.GFK = 2462 // Treibhaus, Gewächshaus (Greenhouse)

else:
    building_feature is considered a Main_Building.
```

Listing 3. Pseudocode for classifying building as `main` or `ancillary`. Logic assigns the label based on specific GFK (Building Function) codes.

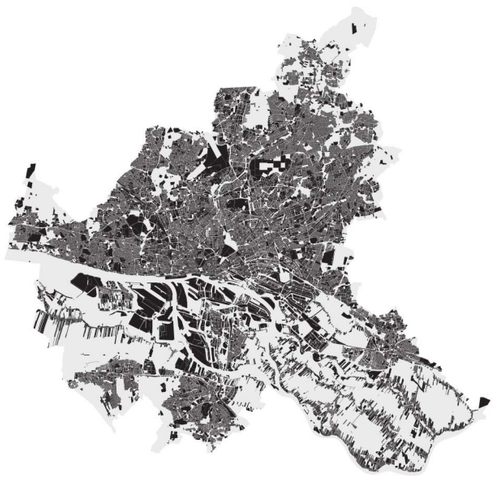

Figure 30. Parcels in Hamburg with calculated `GRZ_main` values greater than zero (manual GIS workflow). Map scale: 1:500.000 (author, 2025).

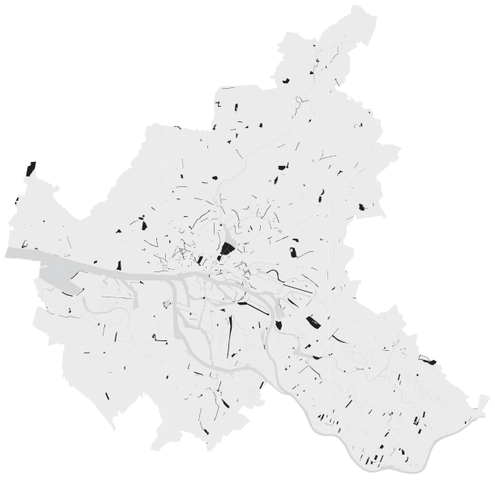

Figure 31. Parcels in Hamburg with `GRZ_main` values between 0 and 0,001 (manual GIS workflow). Map scale: 1:500.000 (author, 2025).

4. Results

This chapter presents the practical outcomes of the methodological workflows described in Chapter 3. It highlights spatial patterns, identifies anomalies, and compares the methods in terms of agreement of results and efficiency to support the discussion in the next chapter.

4.1. GRZ Results from GIS Workflows

This section presents the spatial results of the manually computed `GRZ_main` values. The objective is to assess building coverage patterns across Hamburg at the parcel level, focusing on spatial distribution characteristics, data anomalies, and the identification of underutilized land through citywide visualization approaches.

4.1.1. Citywide Building Coverage Distribution

Figure 30 demonstrates all parcels in Hamburg where manually calculated `GRZ_main` exceeds zero, indicating building footprint presence. The spatial distribution reveals developed parcels as darker areas, while lighter regions indicate no detected building coverage. Notable anomalies emerge immediately, particularly parcels marked as developed within water bodies such as the Außenalster. These irregularities result from minor edge overlaps where adjacent buildings are incorrectly attributed to parcels, demonstrating the sensitivity of manual workflows and emphasizing the necessity for post-processing validation and thresholding procedures.

Data Quality Assessment: Figure 31 provides further detail by isolating parcels with `GRZ_main` values between 0 and 0,001. The objective was to detect parcels with small building overlap, essentially parcels that are empty but which the current algorithm marks as occupied due to small intersections. Many of these parcels are narrow and elongated, typically corresponding to transportation infrastructure such as roads or rail corridors. Even minimal contact between a building and such parcels can result in a non-zero GRZ value, despite the parcel being functionally unrelated to built development.

A second quality check involved identifying parcels with `GRZ_main` values greater than 1,0. A physically impossible outcome that indicates data quality issues. GRZ values cannot exceed 1,0

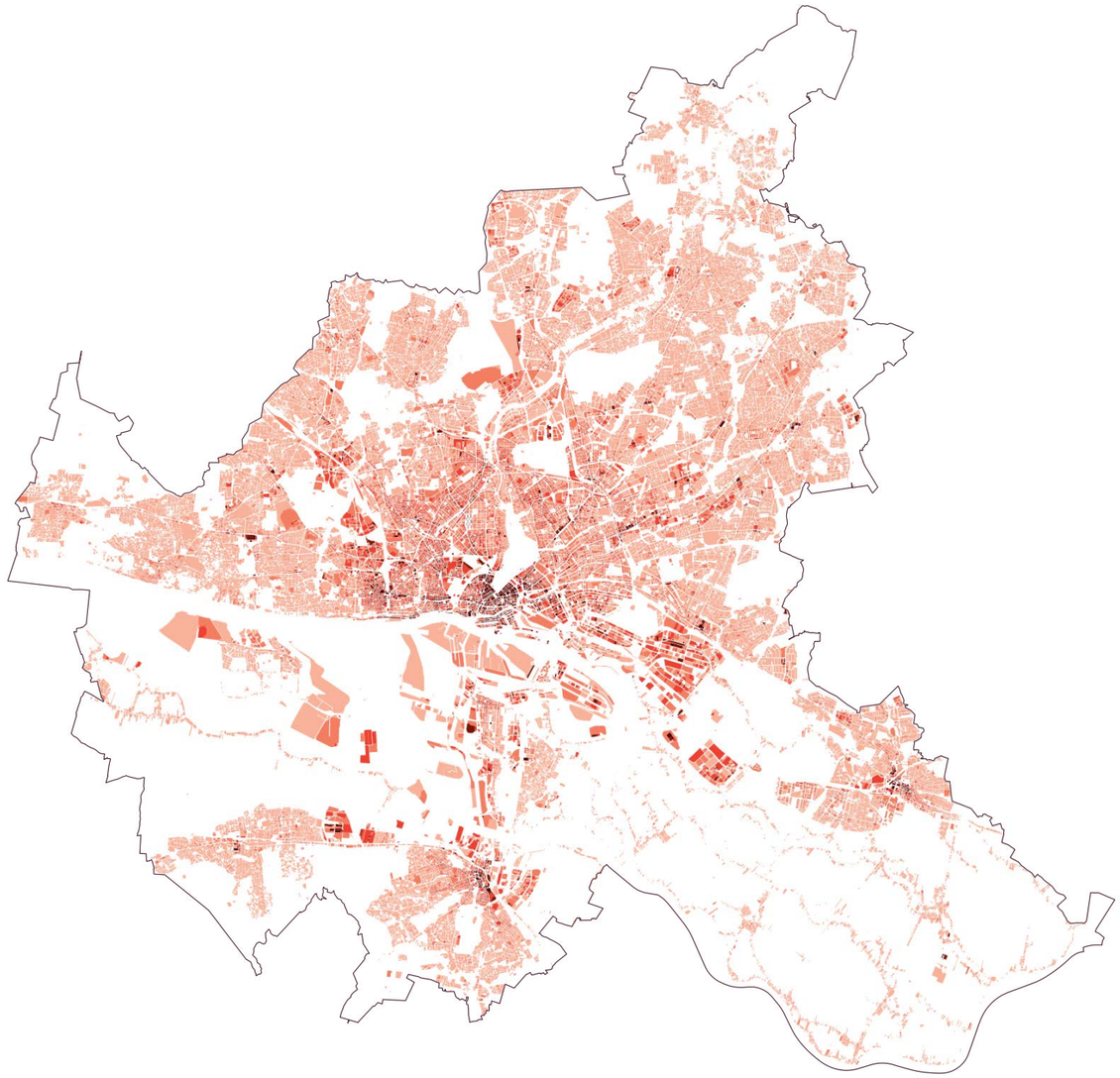

Figure 32. `GRZ_main` values across Hamburg, classified into six intervals. The interval classification begins at `GRZ_main>0,05` to suppress noise from minimal geometric intersections. (manual GIS workflow) (author, 2025).

since this would mean building footprints cover more than 100% of the parcel area. Although values higher than 1,0 are rare and not detectable at the citywide scale due to their limited occurrence, they represent critical data anomalies that require investigation.

Figure 33 zooms in on one such example near Hamburg Airport, where a parcel exhibits a GRZ_main value exceeding 1,0. This specific anomaly was previously identified and discussed in Section 3.3.2, with the underlying cause visualized in Figure 21. The error stems from overlapping building geometries within the ALKIS dataset. In this particular case, building polygons representing closely related structures are stored as separate, overlapping features, causing the algorithm to sum their areas and attribute the total to the intersecting parcel.

This example demonstrates how unresolved data quality issues can significantly distort parcel-based analyses, particularly in large infrastructure areas where complex building arrangements are common. Such facilities often contain multiple interconnected structures that may be digitized inconsistently in cadastral systems, leading to geometric overlaps that propagate through automated calculations. While these cases represent a small fraction of the total dataset, their impact on individual parcel analyses can be substantial, highlighting the importance of data validation and quality assessment in automated urban parameter calculations.

Classification Analysis: To explore general trends in building coverage across the study area, `GRZ_main` values were spatially visualized using a five-class color ramp classification system (Figure 32). A lower threshold of 0,05 was applied to exclude marginal intersections that might result from minor geometric overlaps or digitization inaccuracies, ensuring that only meaningful building-parcel relationships are represented in the analysis.

The classification intervals were strategically selected to provide a comparative overview of building intensity while minimizing potential distortion from statistical outliers. This approach enables clear differentiation between density categories while maintaining analytical robustness across the diverse urban morphologies present in Hamburg.

The resulting choropleth map reveals distinct structural patterns that reflect Hamburg's urban development history and planning policies. Particularly striking is the division between the northern and southern halves of the district. Higher GRZ_main values concentrate in the northern portion of the study area, forming a distinctive separation characterized by intensive land use.

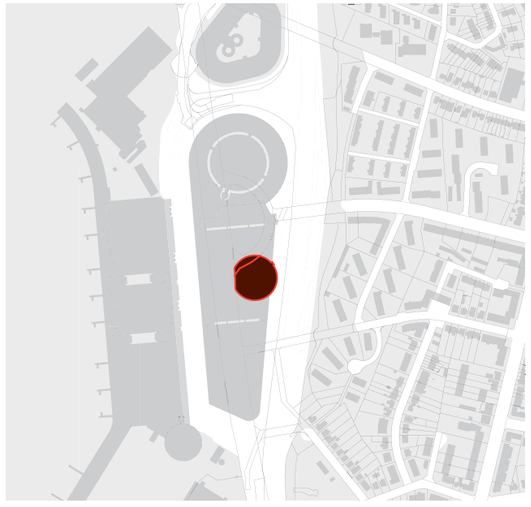

Figure 33. Parcels with `GRZ_main>1,0` in the Hamburg Airport complex, shown with cadastral boundaries (outlined), building footprints (light grey), and the affected parcel highlighted in dark (manual GIS workflow). Map scale of 1:10.000 (author, 2025).

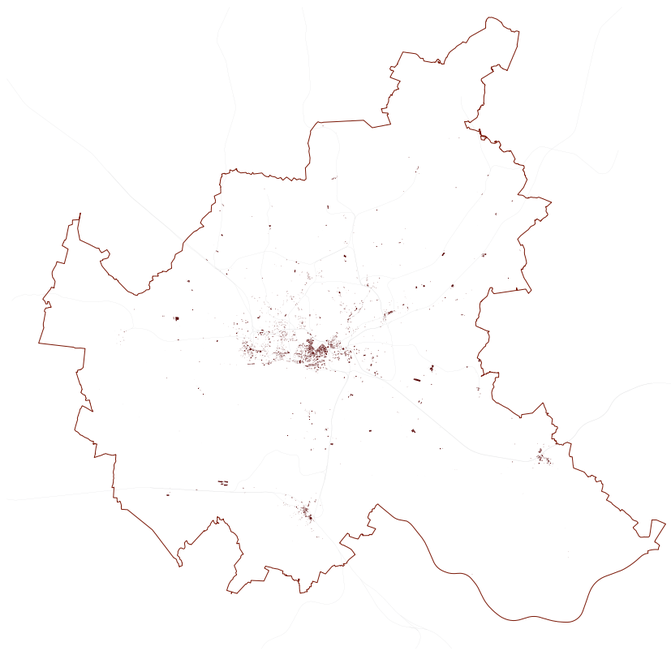

Figure 34. Parcels in Hamburg with `GRZ_main` values greater than 0,8 (manual GIS workflow). Representing zones of very high spatial intensity. The pattern illustrate Hamburg's polycentric morphology in relation to the city's rail system. Map scale: 1:500.000 (author, 2025).

Notable linear patterns of moderate to high building coverage appear along watercourses, particularly visible as continuous strips of development that follow the natural geography. This reflects Hamburg's historic relationship with its waterways and port-related development patterns. Linear patterns of varying intensity suggest the influence of major transportation corridors in shaping development patterns, with denser development often appearing to follow main routes through the district.

4.1.2. High-Density Development Patterns

Figure 34 focuses on parcels with `GRZ_main` values above 0,8, revealing Hamburg's distinctive polycentric urban structure through the spatial distribution of high-density development. The analysis demonstrates several key characteristics of the city's morphology that extend beyond simple density mapping.

The most prominent concentration appears in Hamburg's historic core, particularly in Altstadt, Neustadt, and St. Georg, where the dense constellation of high-GRZ parcels reflects centuries of incremental urban development. This central concentration exemplifies the typical European city pattern where medieval cores maintain the highest building densities due to historical plot subdivisions and continuous redevelopment pressure.

Beyond this historic concentration, the overlay of the rail system reveals a strong correlation between high-GRZ parcels and transportation infrastructure. Clusters consistently appear near major railway stations and junctions, confirming the relationship between accessibility and development intensity. This transit-oriented pattern is particularly evident in Hamburg's central station area, Altona station surroundings, Harburg's station area, and Bergedorf's rail-adjacent areas.

Rather than showing a simple monocentric pattern radiating from Hamburg's center, the distribution demonstrates a clear polycentric structure reflecting the city's historical development. Each former independent municipality maintains distinct characteristics while contributing to the overall urban fabric.

In Altona, high-GRZ parcels cluster around Altona-Altstadt and Ottensen, reflecting compact, mixed-use historical development that maintains its distinct urban character. In Harburg, a moderate cluster appears near the harbor and train station, combining residential and transport-related land uses in a pattern that reflects this district's role as a former independent town. In

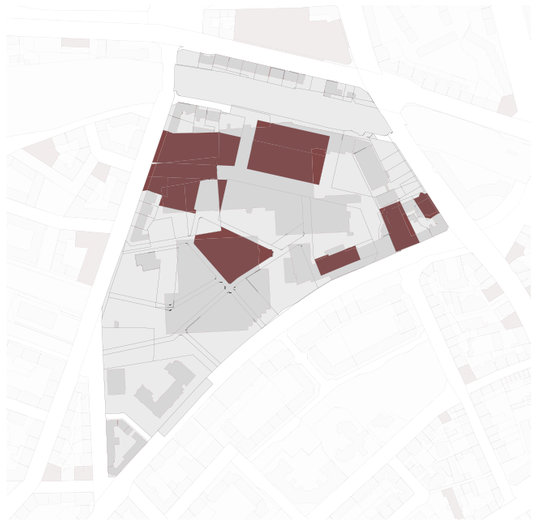

Figure 35. Close-up view of parcels with `GRZ_main>0,8` in Altona-Nord (manual GIS workflow). Parcels with high GRZ values are shown in darker, with parcel outlines and building footprints overlaid. The view shows a series of smaller adjacent parcels, some with individually high GRZ values. Map scale: 1:8.000 (author, 2025).

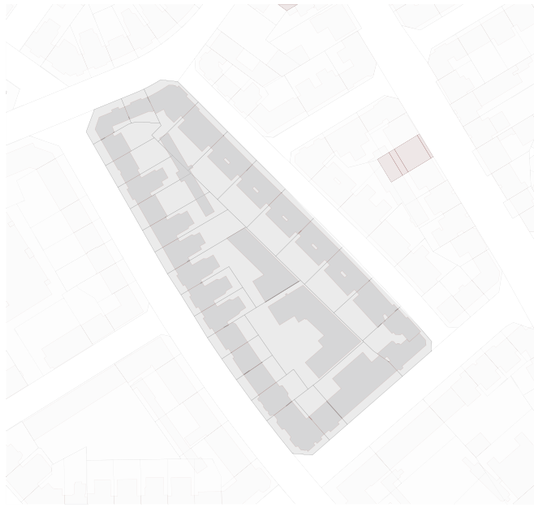

Figure 36. Example of a cadastral layout where most building footprints are fully contained within individual parcels. Map scale: 1:4.000 (author, 2025).

Bergedorf, a smaller cluster aligns with the historic center's denser urban fabric, maintaining the characteristics of its pre-incorporation identity.

Each of these former independent towns (Altona, Harburg, Bergedorf) maintains its own high-density cluster, demonstrating how historical municipal boundaries continue to influence contemporary development patterns even after administrative consolidation into greater Hamburg.

The influence of Hamburg's economic functions extends beyond historical and transit factors. Some high-GRZ clusters appear along the Elbe River, particularly in port-adjacent areas, suggesting the continued influence of Hamburg's maritime economy on land use intensity patterns. This waterfront influence adds another layer to the city's complex density distribution, where economic functions drive development intensity independently of historical or transit-related factors.

Beyond these clustered patterns, some isolated high-GRZ parcels were identified throughout the analysis. These correspond either to large-scale, single-use facilities such as logistics centers or warehouses that nearly cover their entire parcels, or to clusters of adjacent parcels that appear to function as unified lots due to continuous building footprints.

As illustrated in Figure 35, these configurations may result from ongoing redevelopment processes where parcels have been subdivided or consolidated in preparation for future construction, while existing buildings have not yet been demolished or modified. In such cases, GRZ is artificially inflated due to the disconnect between new parcel boundaries and legacy building footprints[9]. This reveals how simple parcel-based GRZ calculations may not fully capture development reality in areas undergoing transformation.

These observations from the spatial analysis carry important implications for urban planning practice and future research methodology. The contrast between city-wide patterns (Figure 34) and parcel-level analysis (Figure 35) demonstrates that GRZ analysis must consider multiple scales to be meaningful. City-wide patterns reveal structural relationships with infrastructure and historical development, while parcel-level analysis exposes the complexities of contemporary development processes that require different analytical approaches.

---

9. This specific example reflects the Holsten-Quartier redevelopment project (Bebauungsplan Altona Nord 28), transforming a 9.6-hectare former brewery site into mixed-use development including residential, commercial, and public spaces. The development plan establishes new parcel boundaries for planned construction while preserving existing brewery buildings for integration into the new quarter design. The preliminary zoning plan (Bebauungsplan-Entwurf) is provided in Entry 5 (W D).

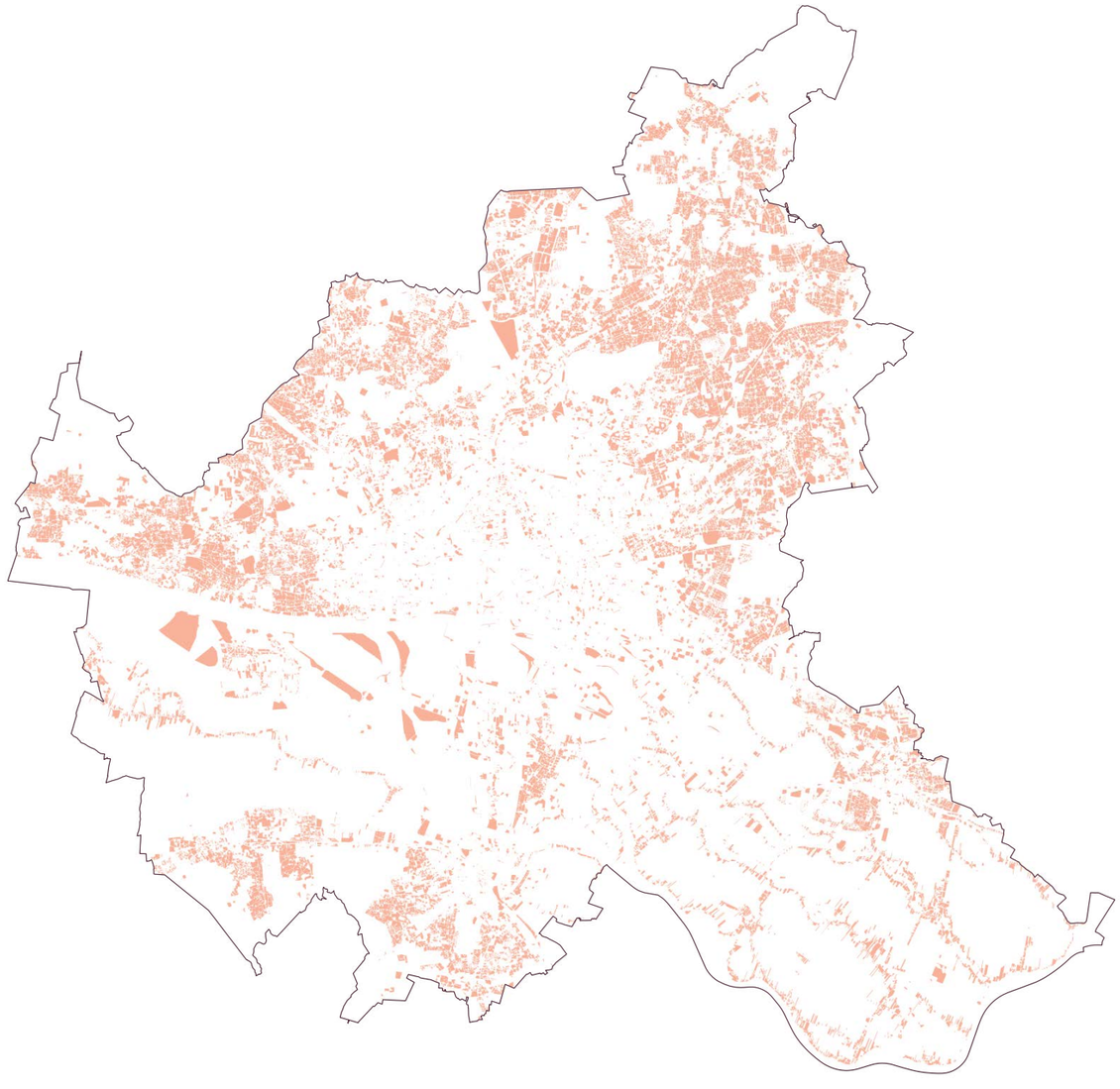

Figure 37. Parcels in Hamburg with `GRZ_main` between 0,05 and 0,2 (manual GIS workflow). Highlights buildable parcels with low ground coverage, relevant for identifying urban infill or densification potential. (author, 2025).

From a methodological perspective, aggregating parcels at the lot level would likely provide a more accurate representation of spatial intensity, particularly in areas experiencing active redevelopment. This approach would address the temporal misalignments between cadastral boundaries and physical development that currently distort individual parcel calculations.

Furthermore, the correlation between rail infrastructure and high-GRZ clusters reinforces the importance of coordinated transportation and land use planning in managing urban density and development patterns. This relationship suggests that future density planning should explicitly consider proximity to transit infrastructure as a key factor in determining appropriate development intensities.

While high-density zones provide crucial insights into urban cores and development pressures, (visually)the majority of parcels in Hamburg fall within the low to moderate GRZ range, representing significant latent development capacity. Understanding these underutilized areas is essential for comprehensive urban planning and sustainable densification strategies.

4.1.3. City-Wide Low-Density Distribution

Figure 37 highlights parcels with `GRZ_main` values between 0.05 and 0.2, indicating plots with relatively minimal building coverage that are especially relevant for assessing development potential. This city-wide analysis reveals a clear spatial pattern where clusters of low-GRZ parcels concentrate in Hamburg's outer districts, particularly in Wandsbek, Rahlstedt, Jenfeld, and parts of Harburg. These areas represent the city's suburban periphery, where lower development densities reflect both historical settlement patterns and current zoning regulations that favor single-family residential development[10].

The distribution also reveals scattered low-GRZ parcels within the inner city, which may reflect temporary vacancies, underutilized industrial sites, or properties awaiting redevelopment. These inner-city parcels are particularly significant from a planning perspective, as they represent immediate opportunities for infill development within established urban infrastructure networks.

10. For example, the Baustufenplan for the Farmsen area (Entry 6, Appendix D) and the Bebauungsplan Wellingsbüttel 16 (Entry 7, Appendix D) outline zoning provisions that reflect these low-density development principles

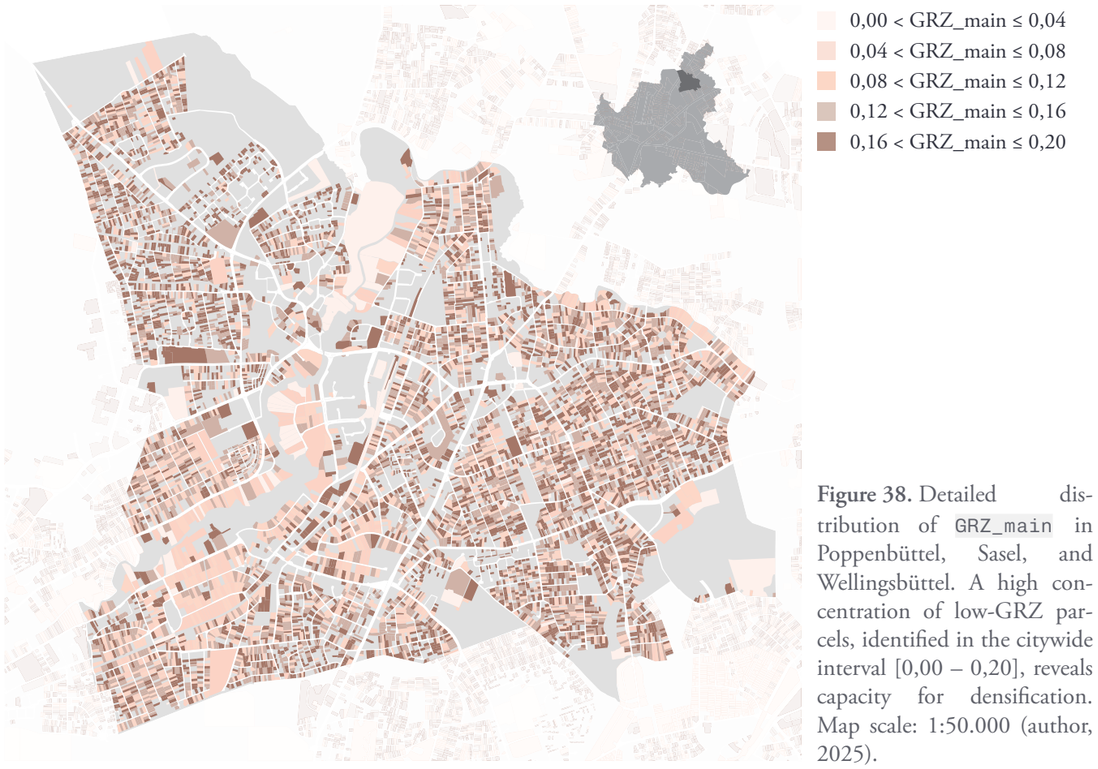

Figure 38. Detailed distribution of `GRZ_main` in Poppenbüttel, Sasel, and Wellingsbüttel. A high concentration of low-GRZ parcels, identified in the citywide interval [0,00 – 0,20], reveals capacity for densification. Map scale: 1:50.000 (author, 2025).

Wandsbek Case Study: To examine this development potential more closely, a finer `GRZ_main` classification was applied to a representative subset of Bezirk Wandsbek, focusing on the Stadtteile of Poppenbüttel, Sasel, and Wellingsbüttel. Figure 38 visualizes this region using five narrow GRZ intervals within the 0,00–0,20 range, revealing the fine-grained variation in development intensity that characterizes Hamburg's suburban landscape.

This detailed analysis highlights a low-density suburban environment dominated by detached homes on spacious lots. The granular classification reveals subtle but important variations in land use intensity, with some parcels showing minimal coverage (approaching 0,00) while others approach the 0,20 threshold, suggesting different development phases or varying lot sizes within the same neighborhood context.

The spatial clustering of similar GRZ values indicates coherent development patterns, reflecting common zoning regulations. This pattern-based analysis provides an understanding of where modest densification might be most appropriate and socially acceptable.

Visual Pattern Recognition Technique: Figure 39 employs visual technique to emphasize spatial patterns and development opportunities. By rendering all parcels with GRZ_main values above 0.20 in the same dark brown tone used for road infrastructure, this approach effectively suppresses areas with already substantial building coverage and draws visual attention to lighter parcels with lower development ratios.

This cartographic technique creates a visual hierarchy where underutilized parcels emerge as spatial gaps in the urban fabric. The lighter areas represent plots that are already built but currently exhibit low land use intensity compared to their neighbors, making them immediately identifiable as potential soft development opportunities within established neighborhoods.

The method proves particularly effective in identifying parcels that might be suitable for gentle densification strategies, such as accessory dwelling units, lot splitting, or modest building additions, without requiring the wholesale redevelopment associated with high-density projects. These opportunities are especially valuable in contexts where community acceptance of change is crucial for successful implementation.

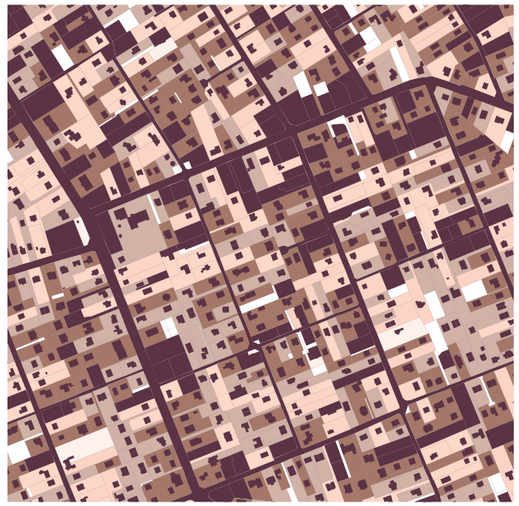

Figure 39. Extract from *Sasel* showing `GRZ_main` distribution with visual emphasis on underbuilt parcels. All parcels with `GRZ_main>0,20` are rendered in the same dark brown as road infrastructure, allowing parcels with lower coverage ratios to stand out. Map scale: 1:50.000 (author, 2025).

4.1.4. Planning Implications for Sustainable Densification

This analysis of low-GRZ parcels reveals several important considerations for sustainable urban development. The concentration of development potential in outer districts suggests opportunities for strategic densification that could support public transit investments and reduce urban sprawl pressures. However, the scattered nature of many low-GRZ parcels indicates that successful densification will require careful, site-specific approaches rather than broad-brush zoning changes.

The detailed suburban analysis demonstrates that even within low-density areas, there exists a spectrum of development intensities that can guide targeted interventions. Understanding these gradations allows researchers to identify where modest increases in density might be most appropriate and least disruptive to existing neighborhood character.

Furthermore, the visual pattern recognition technique provides a practical tool for communicating development potential to stakeholders and communities, making abstract density calculations more accessible and spatially comprehensible. This approach supports more informed public participation in planning processes and helps build consensus around appropriate development strategies.

4.2. GRZ Results from Spatial Query Methods

This section presents the results of calculating `GRZ_main` using SQL queries within a PostgreSQL database environment enhanced with PostGIS spatial extensions. Unlike the visual workflow described in Section 4.1, this approach emphasizes structured, query-based spatial analysis that enables systematic examination of building-parcel relationships across Hamburg's entire urban fabric. The objective is to evaluate whether comparable spatial insights can be obtained through automated database operations while making use of the computational advantages of SQL for large-scale urban morphology analysis.

The PostGIS framework enables advanced spatial functions that would be time-consuming or impractical to perform manually in traditional GIS environments, offering a scalable alternative for metropolitan-level urban parameter calculations. All SQL queries used in this analysis, along with their execution times and performance metrics, are compiled in Appendix B as code listings, providing methodological transparency and reproducibility.

4.2.1. Citywide Distribution Analysis

The analytical process began with systematic database queries to establish citywide GRZ distribution patterns. Using SQL aggregation functions (see Listing 6), `GRZ_main` values were grouped by Stadtteil to identify broad spatial patterns and statistical characteristics across Hamburg's 104 administrative districts. The results are plotted in the line chart shown in Figure 40.

As anticipated from the visual analysis, Hamburg's dense urban core districts (Altstadt, Neustadt, HafenCity, and St. Georg) recorded the highest average GRZ values, typically exceeding 0,7. These historically developed environments reflect minimal open space relative to building footprints. Nevertheless, it was somewhat surprising to find the newly developed HafenCity, among this group. The observed values closely align with the patterns shown in Figure 34 from the GIS workflow analysis, demonstrating consistency between the two methodological approaches.

In stark contrast, peripheral districts such as Reitbrook or Spadenland showed average GRZ values below 0,1, indicative of agricultural land use, nature conservation areas, or extremely low-density residential development. The full statistical overview, for all districts, is provided in Table 17 in Appendix C.

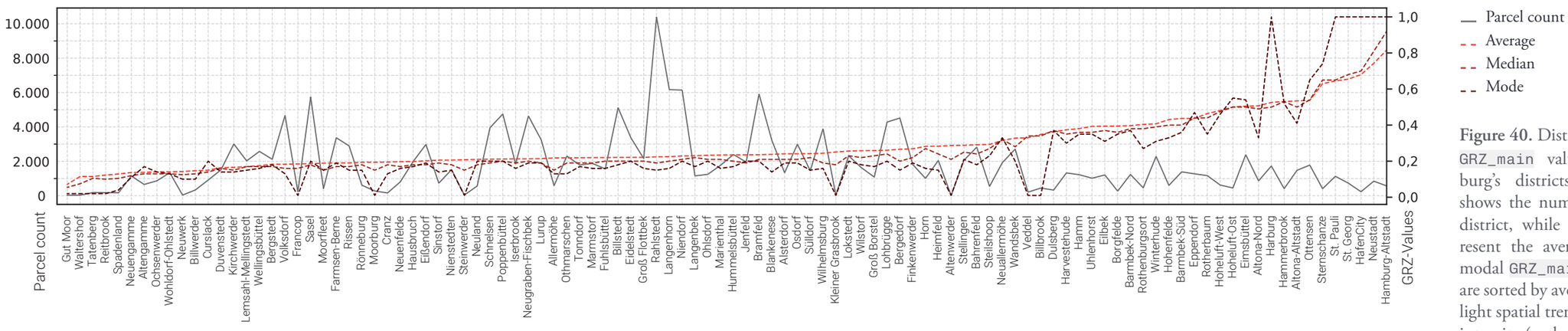

Figure 40. Distribution of `GRZ_main` values across Hamburg's districts. The grey line shows the number of parcels per district, while the red lines represent the average, median, and modal `GRZ_main` values. Districts are sorted by average value to highlight spatial trends in development intensity (author, 2025).

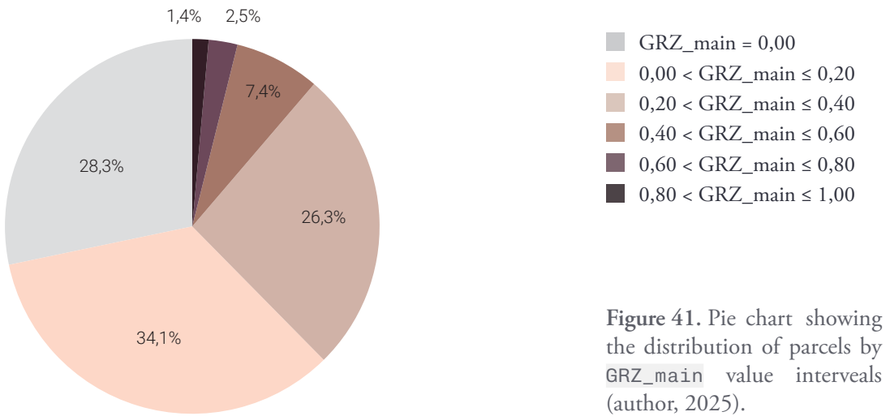

Figure 41. Pie chart showing the distribution of parcels by `GRZ_main` value interveals (author, 2025).

4.2.2. Frequency Distribution

To complement the district-level aggregation, a comprehensive frequency analysis was conducted using histogram generation queries (see Listing 7). This analysis revealed the precise distribution of `GRZ_main` values across Hamburg's approximately 258.000 cadastral parcels, providing quantitative validation of the patterns observed in the visual workflow.

The results demonstrate that approximately 73.000 parcels (28,3%) reported a `GRZ_main` value of exactly 0,00. Indicating either undeveloped land or parcels where buildings are not permitted. The largest single category, encompassing around 34,1% of all parcels, fell within the 0,00–0,20 range, representing low-density residential areas, agricultural plots with minimal structures, or parcels with small buildings.

Moderate development intensity (0,20–0,40 GRZ range) characterized 26,3% of parcels, typically corresponding to suburban residential neighborhoods with detached or semi-detached housing. Higher density categories showed progressively smaller representation: 7,4% of parcels fell within the 0,40–0,60 range, 2,5% within 0,60–0,80, and only 1,4% exceeded 0.80 GRZ values.

This distribution confirms the rarity of full-coverage development in Hamburg, with less than 2% of parcels approaching or exceeding 80% building coverage. The frequency distribution was visualized using the pie chart representation shown in Figure 41, highlighting the relative proportion of each value range and confirming Hamburg's predominantly low-to-moderate development density profile.

4.2.3. Building-Parcel Relationship

Beyond general distributional trends, the SQL-based approach enabled systematic analysis of building-parcel relationships that would be extremely difficult to assess through visual methods alone. Using complex spatial join queries (see Listing 9), the analysis examined the distribution of buildings per parcel across the entire dataset, revealing significant structural complexities in Hamburg's urban fabric.

The results demonstrate substantial variation in building-parcel associations. Approximately 78.000 parcels were linked to a single building. Nearly 52.000 parcels contained exactly two buildings, often indicating main buildings with detached structures

Figure 42. Schematic overview of SQL-based workflow for detecting underdeveloped parcels by GRZ comparison (author, 2025).

More complex configurations emerged in the analysis, with over 40.000 parcels associated with three buildings, and increasingly smaller numbers containing four, five, or more structures. The complete statistical breakdown is presented in Table 18 in Appendix C, illustrating the full spectrum of building density variations across Hamburg's parcel inventory.

The database analysis identified, as well, several extreme cases that requiered detailed examination. Eight individual parcels were found to be associated with more than 100 buildings each, with the most exceptional instance involving 180 separate structures attributed to a single parcel. Through spatial query verification, this particular case was identified as corresponding to the research complex of the Deutsches Elektronen-Synchrotron (DESY), where the parcel encompasses an area roughly equivalent in size to the Binnenalster and contains numerous specialized research facilities, laboratories, and support structures.

These extreme cases highlight both the analytical power of SQL-based approaches for identifying edge-cases and the importance of contextual interpretation when evaluating automated urban parameter calculations. While such high building counts might initially suggest data errors, they often reflect legitimate land use patterns in specialized institutional, industrial, or research contexts.

4.2.4. Cross-Parcel Building Analysis

A complementary analysis examined the inverse relationship: buildings associated with multiple parcels. This query revealed over 130,000 building-parcel links where individual building footprints intersected multiple cadastral parcels, indicating significant geometric complexity in Hamburg's built environment. The most extreme case identified a single building geometry associated with 31 separate parcels. Through spatial verification, this instance was confirmed to correspond to the Holsten-Quartier redevelopment project, which was previously identified during the visual analysis in the QGIS workflow and illustrated in Figure 35. This large-scale mixed-use development exemplifies the challenges posed by contemporary urban projects that span multiple traditional parcel boundaries.

Such geometric complexities may arise from several factors, already mentioned in the previous section. These findings expose once again a fundamental methodological limitation inherent in parcel-based GRZ calculations: the assumption that building geometries align neatly with legal parcel boundaries.

Step 1: Base Table Input

Start with: public.PostGIS_GRZ
Fields used: uuid, geom, grz_main

Step 2: neighbours

Self-join PostGIS_GRZ as test_parcel and neighbor
→ Filter by: ST_DWithin(p.geom, n.geom, 0.1)
→ Exclude self-pairs (p.uuid ≠ n.uuid)
→ Only include: test_parcel.grz_main ≥ 0.1 AND
neighbor.grz_main > 0

Output: List of valid test_parcel - neighbor pairs

Step 3: comparison

Aggregate per center_uuid:
→ COUNT(*)
as total_neighbors
→ COUNT(*) WHERE neighbor.grz ≥ test_parcel.grz + 0.3
as higher_neighbors

Output: Summary stats per test_parcel

Step 4: filtered

Filter center parcels where:
→ total_neighbors > 0
→ higher_neighbors > total_neighbors / 2A

Final Output: List of underdeveloped parcels by GRZ

Figure 43. SQL-based workflow for detecting underdeveloped parcels based on local GRZ contrast (author, 2025).

4.2.5. Data Integrity Validation

The systematic nature of SQL queries enabled comprehensive data quality assessment that would be impractical through visual inspection alone. Validation queries identified six parcels with GRZ_main values exceeding 1,0 a physically impossible outcome that indicates geometric inconsistencies in the underlying datasets.

Notably, this automated approach identified fewer impossible GRZ values compared to those detected through the GIS workflow analysis, suggesting that the SQL-based spatial operations may handle certain geometric edge cases more robustly, or alternatively, that different calculation methodologies produce varying sensitivities to data anomalies.

Additional diagnostic queries flagged 5.139 parcels containing only ancillary structures (such as garden houses, storage sheds, or other secondary buildings) These parcels, which appear undeveloped under the `GRZ_main` calculation, highlight the importance of interpreting GRZ values based not only on geometric relationships but also on building function and classification codes within the ALKIS dataset.

4.2.6. Automated Densification Potential Assessment

Tapping into the precision and scalability of SQL-based spatial analysis, this study explored the potential for automatically identifying parcels suitable for densification through comparative neighborhood analysis. A prototype query was developed to detect parcels with significantly lower `GRZ_main` values than their immediate spatial neighbors (see Listing 8 in Appendix B).

The conceptual workflow, illustrated in Figures 42 and 43, employs spatial buffering operations to identify neighboring parcels within specified distance thresholds, calculates average of surrounding GRZ values, and flags parcels that fall below defined percentile thresholds relative to their local context.

While the initial implementation did not fully meet analytical expectations and revealed the need for more sophisticated query logic incorporating parcel size, the experiment demonstrates a promising direction for automated urban planning support tools. The approach highlights how database-driven spatial analysis can move beyond descriptive statistics toward predictive and prescriptive applications in urban development planning.

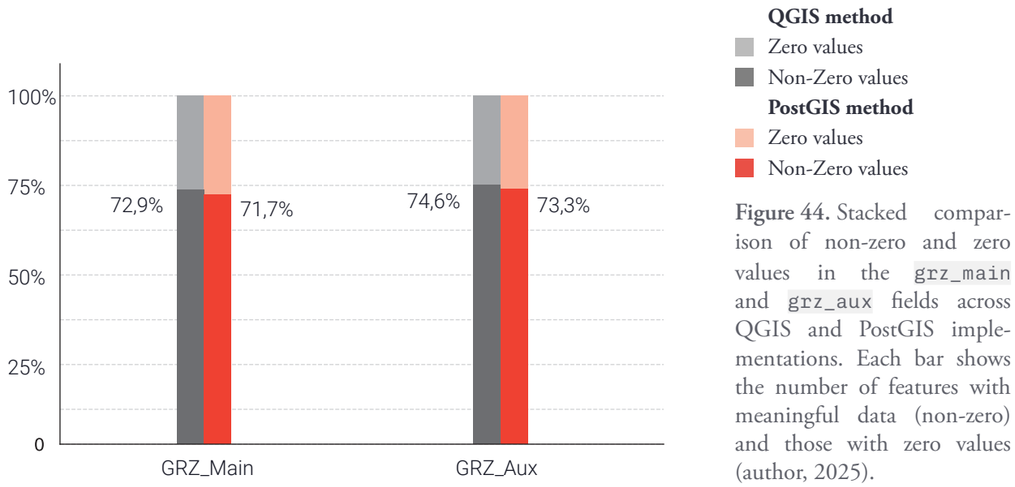

Figure 44. Stacked comparison of non-zero and zero values in the `grz_main` and `grz_aux` fields across QGIS and PostGIS implementations. Each bar shows the number of features with meaningful data (non-zero) and those with zero values (author, 2025).

4.3. Workflow Comparison Results

In line with the research questions outlined in Section 1.2, this section compares the **QGIS** and **PostGIS** workflows in terms of their processing efficiency and the consistency of the GRZ results they produce. We analyze how closely the two methods agree on parcel-level GRZ values and examine the performance (speed and scalability) of each approach when applied at city scale..

4.3.1. Data Completeness and Integrity

Before examining error metrics and visual comparisons, it is crucial to assess the underlying data integrity. Both QGIS and PostGIS datasets (n = 259.734 parcels each) show 100% non-null values for `GRZ_main` and `GRZ_aux`. Notable proportions of the GRZ values are exactly zero, which reflect legal or functional realities (e.g., undeveloped parcels, parcels where no buildings are permitted).

Table 9. Distribution of values for GRZ calculaiton (QGIS and PostGIS implementations).

Column	Non-Zero	Zero
QGIS GRZ_main	189.415	70.319
PostGIS GRZ_main	186,261	73,473
QGIS GRZ_aux	193,542	66,192
PostGIS GRZ_aux	190,453	69,281

As presented in Table 9 and visualized in Figure 44, the stacked bar comparison reveals high alignment between methods, with only marginal differences in zero-value distributions. For `GRZ_main`, QGIS recorded 189.415 non-zero values compared to PostGIS's 186.261, a difference of only 3.154 parcels (approximately 1,2% of the total dataset). Similarly, for `GRZ_aux`, the difference was 3.089 parcels. The visualization clearly demonstrates that both methods maintain consistent proportions of meaningful data versus zero values, with non-zero values representing approximately 73-75% of all parcels in both implementations.

These results suggest that the core spatial logic in both workflows is comparable, though the PostGIS workflow produces marginally more zero values. This pattern potentially indicates stricter

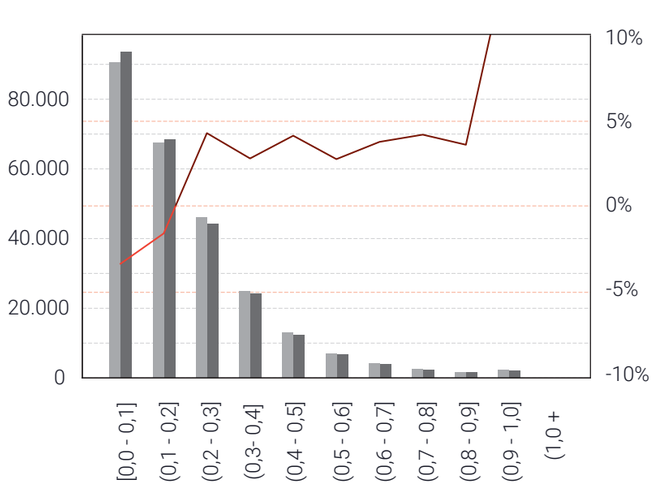

Figure 45. Comparison of `GRZ_main` distribution across QGIS and PostGIS implementations. The grouped bars show the number of features within each GRZ interval for both platforms (left axis), while the red line represents the percentage difference between them (right axis) (author, 2025).

spatial thresholds in the PostGIS implementation or more conservative handling of partial building overlaps, where ambiguous intersections are excluded rather than included.

4.3.2.Values Distribution

To explore the degree of alignment between the QGIS and PostGIS workflows, the `GRZ_main` values were grouped into frequency intervals. This step provides a view of how each method distributes GRZ values across the urban fabric, with particular attention to end values, 0 and 1. These extremes are especially relevant, as they can reflect the practical implications of the spatial thresholds applied in the second workflow.

Table 10. Frequency distribution of `GRZ_main` values across predefined intervals for QGIS and PostGIS workflows.

GRZ Range	QGIS Count	PostGIS Count	Difference	Comment
[0,0–0,1]	90.508	93.538	-3.030	More near-zero in PostGIS
(0,1–0,2]	67.434	68.501	-1.067	Very close
(0,2–0,3]	46.119	44.147	1.972	Slightly more mid-density in QGIS
(0,3–0,4]	24.978	24.278	700	Similar
(0,4–0,5]	12.945	12.411	534	Slight edge to QGIS
(0,5–0,6]	6.953	6.761	192	Nearly identical
(0,6–0,7]	4.239	4.079	160	Nearly identical
(0,7–0,8]	2.484	2.380	104	Nearly identical
(0,8–0,9]	1.667	1.607	60	Nearly identical
(0,9–1,0]	2.382	2.026	356	More high-density values in QGIS

The results of this process are presented in Table 10 and visualized in Figure 45. The grouped bar chart displays the number of parcels within each interval for both workflows, while a red line overlays the percentage difference between them. The analysis reveals several key distribution patterns that illuminate the methodological differences between approaches.

Both workflows display highly similar patterns across all intervals, confirming their general consistency. The largest proportion of parcels falls within the [0,0–0,1] interval in both datasets,

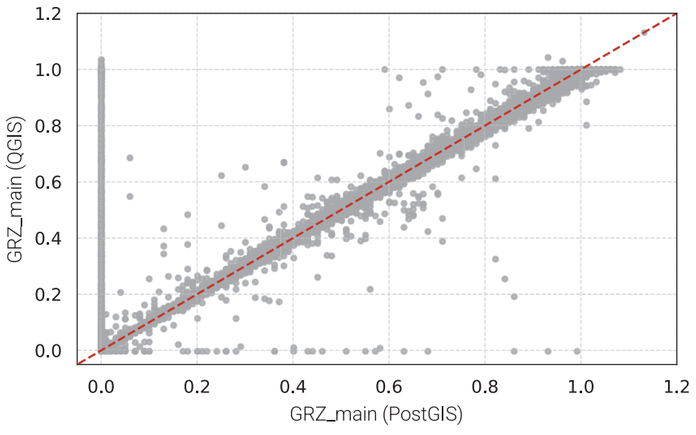

Figure 46. Scatter plot comparing the `GRZ_main` values. Each point represents a parcel, with coordinates reflecting the GRZ values calculated by both methods. The diagonal (x = y) is the reference line for perfect agreement between methods (author, 2025).

with 90.508 parcels in QGIS and 93.538 in PostGIS, reflecting the dominance of low-density development in Hamburg's urban fabric. This represents approximately 35-36% of all parcels.

However, the distribution analysis reveals systematic differences that illuminate each method's handling of edge cases. The PostGIS method records 3.030 more parcels in the [0,0–0,1] range, representing the most significant absolute difference across all intervals. This elevated count suggests that PostGIS filters marginal building overlaps more conservatively, potentially treating small or imprecise intersections as non-coverage.

Conversely, QGIS demonstrates higher counts in several mid-to-high density intervals. In the (0,2–0,3) range, QGIS records 1.972 more parcels, while in the highest density interval (0,9–1,0) QGIS shows 356 more parcels than PostGIS. This pattern suggests that QGIS is more inclusive of partial overlaps and building extensions, resulting in higher GRZ calculations for parcels that PostGIS might classify as having lower coverage ratios.

The convergence pattern in the mid-density ranges (0,3–0,7) is particularly noteworthy, with differences consistently below 1.000 parcels and percentage differences under 3%. This convergence reinforces that both workflows implement comparable core logic for typical urban configurations, with discrepancies primarily emerging at the distribution extremes where geometric interpretation becomes more critical.

4.3.3. Agreement of Results

The agreement between the two workflows was assessed using multiple analytical approaches that reveal both the overall concordance and specific patterns of disagreement between methods.

Statistical Agreement Measures: The analysis begins with the *mean difference* (3), which quantifies the average discrepancy between GRZ values calculated using QGIS and PostGIS. For the main building footprint ratio (`GRZ_main`), the *mean difference* is 0,0022. This value is extremely small and can be considered negligible, given that GRZ values range from 0 to 1. In practical terms, the QGIS workflow tends to produce slightly higher GRZ_main values on average.

$$\text{Mean Difference} = \frac{1}{n}\sum_{i=1}^{n}(\text{GRZ}_{QGIS} - \text{GRZ}_{PostGIS}) \tag{3}$$

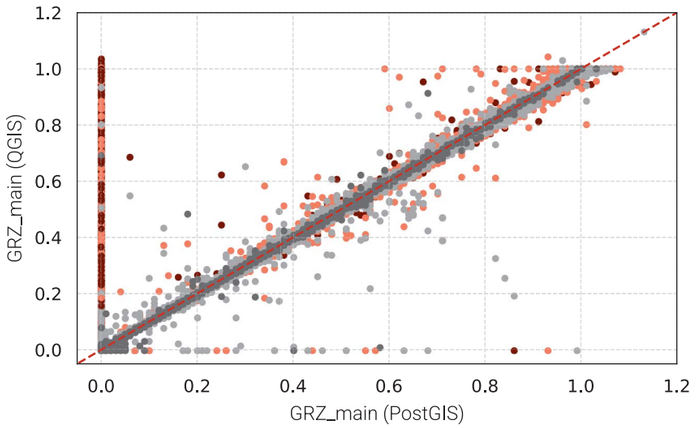

Figure 47. Area-based refinement of the `GRZ_main` comparison shown in Figure 46. Parcels are color-coded by size category, revealing that the most pronounced deviations from the diagonal reference line occur among smaller parcels (≤ 100 m² and ≤ 500 m²) (author, 2025).

While the *mean difference* suggests strong alignment between workflows, a more detailed view is provided by the *Standard Deviation of Differences* (4), based on the comparison of 259.734 matched parcels. The *standard deviation* for `GRZ_main` is 0,0419. Although these deviations remain relatively small relative to the full GRZ scale, they are significantly larger than the mean bias, indicating occasional discrepancies between methods that warrant further investigation.

$$\text{SSD} = \sqrt{\frac{1}{n-1}\sum_{i=1}^{n}\left[(\text{GRZ}_{\text{QGIS}} - \text{GRZ}_{\text{PostGIS}}) - \text{Mean Difference}\right]^2} \qquad (4)$$

Scatter Plot Analysis: Figure 46 presents a comprehensive scatter plot comparing `GRZ_main` values between QGIS and PostGIS implementations. The visualization reveals several critical patterns in the data agreement. The strong concentration of points along the y = x diagonal confirms overall alignment between methods, with the majority of parcels showing nearly identical GRZ calculations across both workflows.

However, the scatter plot reveals a distinctive pattern that explains much of the observed variance: a prominent vertical cluster at `GRZ_main(PostGIS)=0`. This cluster represents parcels where PostGIS assigns zero coverage while QGIS calculates positive GRZ values, creating the characteristic vertical striping pattern visible in the plot. These systematic disagreements are not random but reflect fundamental differences in how each workflow handles specific geometric configurations.

The scatter plot also shows a less pronounced but notable horizontal cluster where `GRZ_main(QGIS)=0` and PostGIS has positive values, though this pattern is considerably less frequent than its vertical counterpart. This asymmetry in disagreement patterns provides insights into the relative conservatism of each method's spatial intersection logic.

Area-Based Refinement Analysis: Figure 47 provides crucial insights by color-coding parcels according to their size categories, revealing that parcel area is a primary determinant of agreement between workflows. The area-based analysis demonstrates that the most pronounced deviations from the diagonal reference line occur among smaller parcels, particularly those ≤ 100 m² (shown in the shades of red color coding).

Small parcels (≤ 100 m²) show the greatest scatter and most frequent non-agreement cases, with many instances of zero PostGIS values paired with positive QGIS values. Medium-sized

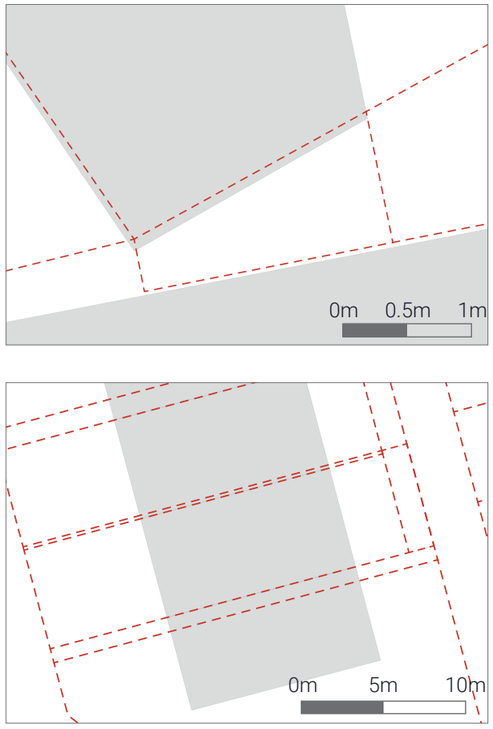

Figure 48. Two examples where parcels intersect with building polygons that span multiple parcels. The solid grey area represents the building footprint, while the dashed red lines outline parcel boundaries (author, 2025).

parcels (≤ 500 m²) display improved but still notable scatter, while larger parcels (> 5,000 m²) demonstrate strong adherence to the diagonal, indicating high agreement between methods.

This pattern highlights that smaller parcels are more sensitive to how building geometries are intersected and attributed, likely due to their higher perimeter-to-area ratio making them more susceptible to boundary effects and geometric ambiguities. These smaller parcels are more sensitive to how building geometries are intersected and attributed. This pattern highlights parcel size as a significant factor influencing agreement between workflows and underlines the importance of geometry-handling choices in fine-scale spatial analyses.

Geometric Configuration Analysis: The systematic disagreements observed in smaller parcels are explained by Figure 48, which illustrates two representative examples where small parcels intersect with building polygons that span multiple parcels. The solid grey areas represent building footprints that extend across parcel boundaries, creating ambiguous spatial relationships that each workflow resolves differently.

In such configurations, the PostGIS workflow, due to implemented spatial thresholding rules, assigns the full building footprint to the larger or primary parcel and attributes zero GRZ to smaller adjacent parcels. This approach prioritizes geometric clarity and avoids double-counting of building areas across parcel boundaries. In contrast, the QGIS workflow includes all partial overlaps proportionally, resulting in non-zero GRZ calculations for smaller parcels even when building coverage is minimal.

This methodological difference explains many of the larger outliers observed in the scatter plot analysis and contributes significantly to the increased variance seen in GRZ_main comparisons. The geometric examples demonstrate that these disagreements are not errors but rather reflect different approaches to handling ambiguous spatial relationships.

Bland-Altman Analysis: Figure 49 presents a Bland-Altman plot that provides a complementary perspective on the agreement between methods by plotting the difference against the mean of both measurements. The plot reveals several important characteristics of the inter-method agreement.

The central red line represents the mean difference (-0,002), plotting the minimal systematic bias between methods. The distribution of points around this mean line is relatively symmetric,

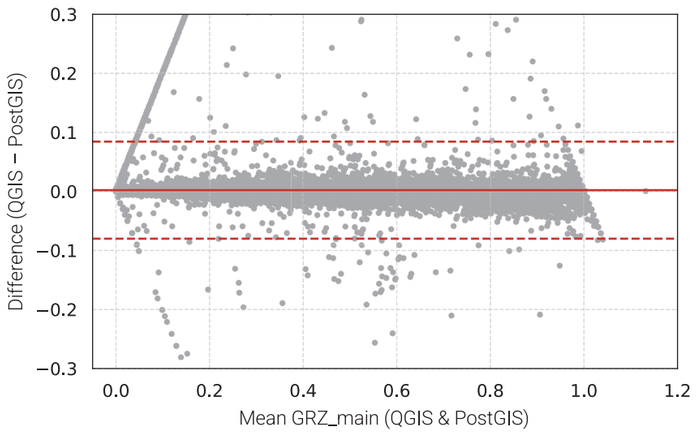

Figure 49. Bland–Altman plot comparing `GRZ_main` values. The solid red line indicates the mean (≈ 0,002), and dashed lines mark the 95% limits of agreement. The plot is vertically limited to a y-axis range of –0,3 to +0,3 to focus on the distribution where the vast majority of observations fall (author, 2025).

indicating that while individual differences occur, they do not follow a consistent directional pattern across the `GRZ_main` range.

The 95% limits of agreement, marked by dashed lines, range from approximately -0.12 to +0.13, encompassing the vast majority of parcel comparisons. This range represents the boundaries within which 95% of differences between methods fall, providing a practical assessment of expected variation. The relatively narrow bounds confirm strong consistency overall between workflows.

However, the Bland-Altman plot also reveals the presence of notable outliers beyond the 95% limits, particularly in the negative direction where PostGIS values significantly exceed QGIS values. These outliers correspond to the specific geometric configurations identified in the scatter plot analysis, where methodological differences in handling building-parcel intersections result in substantial disagreements.

The plot's horizontal distribution shows that differences are not systematically related to the magnitude of GRZ values, indicating that the observed disagreements are primarily driven by geometric configuration rather than by the absolute level of building coverage.

This sensitivity in small parcels has practical implications for urban planning applications, particularly when assessing development potential in densely subdivided historic districts or identifying infill opportunities in constrained urban environments.

4.3.4. Practical Efficiency

This section evaluates the practical efficiency of the two workflows, QGIS and PostGIS, focusing on four key aspects: processing time, scalability, automation and repeatability, and ease of use. System performance was stable in both environments. No crashes or significant slowdowns were observed during testing, which was conducted on a MacBook Pro equipped with an Apple M1 Max chip (10-core CPU, 2.06–3,22 GHz) and 32 GB of RAM.

Processing Time Analysis: Processing time was measured by assessing how long each workflow took to prepare data, perform spatial operations, and compute GRZ values. Data loading times were excluded from the comparison due to the inherent differences between QGIS's file-based architecture and PostgreSQL's database-driven structure. In both cases, however, loading was fast and had no noticeable impact on overall performance.

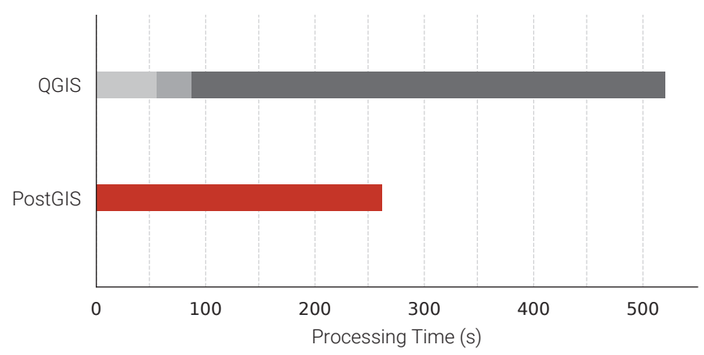

Figure 50. Comparison of GRZ workflow execution times in QGIS and PostgreSQL/PostGIS. The SQL-based execution in PostGIS achieved a 43% reduction in runtime (author, 2025).

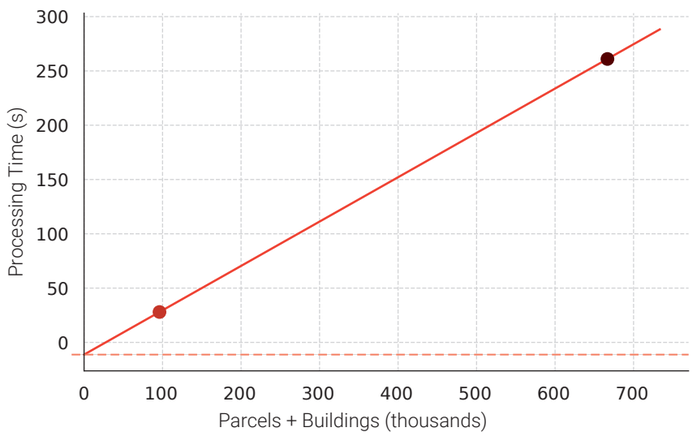

Figure 51. Processing time vs. dataset size for the PostGIS workflow. The graph compares processing times for two datasets, Altona (district-level) and Hamburg (full city) (author, 2025).

Table 11 provides a detailed breakdown of processing times for key steps in the manual GIS workflow. The analysis reveals significant variations in computational demands across different operations. Attribute pruning operations were relatively fast, requiring 19,13 seconds for parcel data (259.734 features) and 36,43 seconds for building data (406,978 features). Geometry validation showed similar efficiency, completing in 12,29 seconds for parcels and 19,20 seconds for buildings.

Table 11. Processing times for key steps in the Manual GIS Workflow

Step	Features	Step Time (sec)
Attribute Pruning - Flurstuecke_Flaechen	259.734	19,13
Attribute Pruning - Gebaeude_Bauteile_Flaechen	406.978	36,43
Geometry Validation - Flurstuecke_Flaechen	259.734	12,29
Geometry Validation - Gebaeude_Bauteile_Flaechen	406.978	19,20
GRZ Calculation (intersection + computation)	666.712	432,93 (~7 min)

However, the GRZ calculation step, involving spatial intersection and computation operations on the combined dataset of 666.712 features, required substantially more time at 432,93 seconds (approximately 7 minutes). This step represents the computational bottleneck in the QGIS workflow, accounting for nearly 87% of the total processing time. The cumulative script execution time for the complete QGIS workflow totaled approximately 497 seconds (about 8 minutes and 17 seconds).

By contrast, the PostGIS workflow demonstrated significant performance advantages. Once imported into the database, the full calculation pipeline (geometry validation, classification, and GRZ computation) executed within a single SQL query, completing in 4 minutes and 21 seconds. This represents a 43% reduction in processing time compared to the QGIS approach, highlighting the computational efficiency of conducting all operations within the PostgreSQL database environment.

Scalability Assessment: Scalability was further tested by applying the PostGIS workflow to the district of Altona, a subset including 37.944 parcels and 58.158 buildings (roughly 15% of Hamburg's full dataset). This reduced dataset completed processing in just 28 seconds, demonstrating exceptional scalability characteristics.

Figure 51 visualizes the relationship between dataset size and processing time for the PostGIS workflow. The graph plots processing time against the total number of features (parcels + buildings) for both Hamburg (full city) and Altona (district-level) datasets. The relationship suggested by connecting these two data points reveals favorable scaling properties, with the trend line intersecting the Y-axis close to zero, indicating minimal fixed overhead for smaller datasets.

This scalability characteristic suggests that the PostGIS approach is well-suited for both city-wide comprehensive analyses and focused district-level studies, enabling flexible analytical scope depending on research requirements. The suggested near-linear scaling also implies predictable performance for intermediate dataset sizes, facilitating resource planning for different analytical scenarios.

Workflow Comparison Summary: Table 12 provides a comprehensive comparison of key workflow steps between manual GIS (QGIS) and automated (PostGIS) approaches. The comparison highlights fundamental differences in architectural approach and operational efficiency.

Table 12. Comparative overview of key workflow steps in manual GIS (QGIS) vs. automated (PostGIS) approaches.

Workflow Step	Manual GIS (QGIS)	Automated (PostGIS)
Data cleaning	Done manually and semi-manually	Handled in the database logic
Geometry validation	Python script run in QGIS	SQL-based validation inside database
Spatial join (parcel-buildings)	Scripted but iterative	Fully automated intersection via SQL
GRZ calculation	Iterative, parcel-by-parcel	Set-based, executed as one SQL query
Reuse on new dataset	Partial: requires repeating steps	High: same SQL queries can be reused

The most significant distinction lies in automation capabilities. The PostGIS workflow achieves full automation through SQL-based operations, where data cleaning, geometry validation, spatial joins, and GRZ calculations are handled seamlessly within the database environment. In contrast, the QGIS workflow, while partially scriptable, requires active supervision and manual intervention at multiple stages.

Repeatability represents another crucial advantage for the PostGIS approach. Once SQL queries are defined and tested, they can be reused or adapted quickly for other datasets or study areas with minimal adjustment. The QGIS workflow, while supporting some automation through Python scripting, still requires validation of intermediate steps and manual quality control, making it more suitable for exploratory or small-scale tasks where visual control is advantageous.

Ease of use and debugging varied between approaches, with each offering distinct advantages. QGIS provided a more intuitive environment for troubleshooting, with immediate visual feedback that facilitated issue detection and resolution through map-based inspection. However, this approach became increasingly labor-intensive as dataset size increased. PostGIS required more technical skills for setup and debugging, typically involving query logs and schema checks, but enabled faster and more precise error identification once the system was understood.

These empirical findings raise important questions about the practical application, limitations, and broader implications of automated urban parameter calculations. In the following chapter, these results will be interpreted in light of the research questions posed in Chapter 1 and situated within the broader literature on urban morphology, spatial analysis methods, and digital planning tools.

5. Discussion

The previous chapter established that the both Workflows produce highly consistent GRZ values across Hamburg's parcel dataset, despite using different technical approaches. This chapter builds on those results by interpreting the methodological differences, discussing their relevance for planning practice, and identifying limitations to guide future enhancements.

5.1. Interpretation of Findings

Both approaches differ in practical implementation and alignment with planning workflows. These differences provide valuable insights into the evolution of digital tools in urban morphological analysis. To structure this reflection, we begin by revisiting the research questions that guided the study and evaluating how effectively each method addressed them.

5.1.1. Addressing Research Questions

The first research question (on comparing GIS workflows to spatial SQL methods for large-scale urban calculations) is addressed through the empirical comparison conducted on the Hamburg dataset. The PostGIS workflow demonstrates superior performance for large-scale applications, successfully processing over 250.000 parcels in limited time with minimal user intervention after initial setup. In contrast, the QGIS workflow, requires significant manual oversight at each separate processing stage.

The second research question (on the comparative strengths and limitations of each method in terms of result agreement, efficiency, and scalability) reveals a set of trade-offs. The GIS workflow proves valuable for visual exploration, initial data validation, and examining spatial relationships. Its intuitive interface allows for hands-on interaction with the dataset, offering clear visual feedback on anomalies and distribution patterns. However, its reliance on manual steps reduces repeatability and increases the potential for user error; aligning more closely with traditional, exploratory planning practices.

In contrast, the Spatial Query method emerges as a fully automated approach that produces consistent outputs across Hamburg's extensive dataset. The method ensures reproducibility by encapsulating the full workflow in structured SQL queries. This level of methodological consistency enables the processing of updated or new datasets with minimal adjustments, making it especially advantageous in institutional planning contexts.

Overall, both workflows produced nearly identical GRZ results (differences on the order of 10^{-3}), confirming their consistency aside from a few edge cases (e.g. very small or overlapping parcels)

5.1.2. Methodological Significance

Beyond the immediate comparison of workflows, the study offers broader insights into the methodological implications of automating urban parameter calculations. The successful implementation of both approaches using the standardised ALKIS dataset highlights the strength of Germany's spatial data infrastructure in supporting detailed-resolution, automated urban analysis. The availability of geometries and rich attribute information allows for sophisticated spatial computations that would be difficult to achieve using less comprehensive datasets.

A particularly important structural consideration in GRZ calculation is the distinction between main and ancillary buildings. As discussed in Sections 2.2 (legal context) and 3.3.2 (data-level structure), both workflows approach this issue through attribute-based classification. Although not legally definitive, this method offers a practical way to approximate planning categories in a consistent, automated manner.

5.2. Limitations of the Study

Beyond the methodological considerations outlined in Chapter 3, this study faces several conceptual and interpretive limitations that affect the generalizability and practical application of its findings.

Dimensional Constraints: The exclusive focus on 2D spatial analysis fundamentally limits the study's contribution to comprehensive urban intensity assessment. By concentrating

solely on GRZ calculations, the research provides only a partial view of urban density patterns. This limitation is particularly significant given that contemporary urban planning increasingly emphasizes three-dimensional density management, where building height and floor area ratios serve as critical regulatory tools. The absence of volumetric analysis means the findings cannot fully inform planning decisions that require understanding of both horizontal and vertical urban intensification patterns.

Regulatory Alignment Challenges: The reliance on cadastral data classification systems to approximate planning regulatory categories introduces a fundamental interpretive challenge. The mismatch between ALKIS *Building Function codes* and actual planning regulatory distinctions highlights a broader issue in automated urban analysis: the gap between data structure and planning practice. This current semantic disconnect suggests that fully automated approaches to urban parameter calculation may inherently struggle to capture the contextual details that inform planning decisions.

Validation Constraints: The absence of benchmark validation data represents a critical limitation that extends beyond technical accuracy to questions of methodological reliability. Without ground-truth comparison, the study cannot establish the degree of confidence appropriate for different planning applications. This limitation is particularly consequential for high-stakes planning decisions where small errors in density calculations could have significant regulatory or financial implications. The reliance on inter-method agreement as a proxy for accuracy, while methodologically justifiable, cannot substitute for empirical validation against established planning standards.

Implications for Planning Practice: In summary, although automated GRZ calculations greatly improve efficiency and consistency, they cannot replace the local knowledge and judgment of planners. This thesis demonstrates both the potential and the limits of automation, guiding future research and implementation to better balance computational efficiency with planning precision.

5.3. Urban Research Implications

The results of this study carry practical implications for urban planning. They particularly support data-driven decision-making and spatial policy formulation. By automating urban parameters (in this case GRZ) calculations, planners can monitor land use intensity more accurately and consistently over time and across administrative boundaries.

For instance, areas with low GRZ values can indicate potential opportunities for infill development or targeted policy interventions; especially true for those surrounded by higher-intensity development. Conversely, parcels showing unrealistically high GRZ values (greater than 1,0) can be flagged for further review. The department responsible for maintaining and updating the dataset can investigate these anomalies.

The GRZ_aux metric adds analytical depth by incorporating ancillary structures in a separate metric. However, a detailed quantification of its impact compared to GRZ_main across different parcels would strengthen its interpretive value. This distinction is particularly important for assessing open space availability and ensuring compliance with zoning regulations. Such detailed analysis supports more refined development strategies and contributes to greater transparency in planning decisions.

5.3.1. Implications within the HCU–LIG Collaboration

The findings of this thesis offer direct methodological and operational contributions to the ongoing HCU–LIG research collaboration. Thanks to its basis in official standardized data, planners and researchers can replicate the analysis for specific locations, monitor land use, and identify underutilized parcels using the same method.

One key contribution lies in the pre-processing strategies for handling ALKIS datasets, especially regarding building–parcel linkage. The challenges encountered highlight critical data management considerations. These include the absence of relational keys and the need for spatial joins. These considerations are equally relevant when the step of incorporating XPlanung data is conducted. The techniques developed here will inform how XPlanung is processed in future research work. These include spatial filtering, classification logic, and automated GRZ comparison.

Beyond the technical contributions, this thesis also documents the learning process involved in transitioning from traditional GIS workflows to database-driven spatial analysis. This knowledge transfer is valuable for the wider research team and supports capacity development within both HCU and LIG. The documentation of challenges and limitations helps establish realistic expectations.

5.4. Ethical and Societal Implications

Automating urban planning metrics, such as GRZ, raises ethical and societal questions. The workflows developed for the cadastral data promise efficiency and consistency in spatial analysis, yet they also have the potential to reshape how cities are understood and governed. This section draws on the author's practical experience working with urban data in both Hamburg and Barcelona. It includes comparative insights grounded in familiarity with local planning practices. Following concepts from urban theory and digital urbanism, the discussion explores how data tools influence the formation of planning knowledge, the recognition of expertise, and the accountability of decision-making processes.

Key concerns include biases in data and algorithms, transparency of decision-making, and the shift from planner-led judgement to technology-driven processes. Specific examples from Hamburg and Barcelona illustrate both the opportunities and challenges of automating planning metrics.

5.4.1. Data-Driven Urbanism

The growing use of computational metrics and big data is reshaping how planning knowledge is produced. Data dashboards present the city as a set of measurable, visualised facts. This reinforces a type of instrumental rationality that interprets urban reality through numbers. While this data-driven perspective can be a powerful foundation for decision making, it also has important limitations.

As Kitchin et al. (2015) point out, many indicator and benchmarking initiatives tend to "*privilege a realist, quantitative epistemology*". They promote an instrumental approach that overlooks the political and contingent nature of these tools, as well as their technical constraints. In other words, automated metrics do not merely describe the city. They influence what is considered important, shaping how planners define problems and where they choose to focus attention.

In this research, the effort to calculate parameters such as GRZ across the entire city reflects a broader shift in how urban form is analysed. The ability to calculate citywide urban parameters at the click of a button transforms neighbourhoods into datasets. Reducing complex environments to percentages. This way of "seeing like a computer" can reveal valuable patterns and comparisons, offering new insights into urban structure. But, it also runs the risk of overlooking aspects that fall outside the scope of the data.

5.4.2. Transparency in Algorithmic Planning

As cities increasingly integrate automation into spatial analysis, the processes of urban governance and decision-making are also being reshaped. On one hand, data-driven tools offer opportunities to enhance transparency. For example, they can make both the methods and results of spatial analysis openly accessible. Hamburg is a leader in this regard. Under its open-data legislation[11], the city has developed a robust geodata infrastructure.

Following the INSPIRE directive, Hamburg has implemented a unified Geodata Infrastructure, the city plays a leading role in Germany in expanding public access to spatial data services (Lieven, 2017). This commitment to openness means that a wide range of planning datasets are freely available, allowing for independent verification of analyses.

Initiatives like DIPAS[12] further support transparency and public engagement by publishing datasets and the outcomes of planning processes. In this context, the ability for anyone to access source data and replicate GRZ calculations using tools like QGIS or PostGIS helps reduce the so-called black-box problem. This makes analytical processes more understandable and accountable.

However, transparency is not guaranteed simply by using technology. It depends on deliberate governance and oversight. One major challenge lies in the opacity of algorithms themselves. When proprietary software or complex scripts are used without sufficient explanation, both the public and policymakers may be unaware of how specific outcomes are produced.

Barcelona provides a compelling example of how this issue can be addressed. In 2021, the City Council announced the development of a *Municipal Algorithm Transparency strategy*. This includes plans for a public registry listing all algorithms used in municipal services that affect residents (Barcelona City Council, consulted June 2025). This registry will allow citizens to access

---

11. Since 2012, Hamburg has maintained an open-data and transparency framework under the Hamburgisches Transparenzgesetz (HmbTG), a pioneering legislation that requires public authorities to proactively publish a wide range of official information, including geodata, contracts, and building permits.

12. Digital Participation System, is an open-source digital participation platform launched in 2017 by the city of Hamburg, co-developed with HCU and LGV, enabling precise, georefenced citizen feedback.

information about any algorithm influencing city decisions. Ensuring that automated systems remain open to public scrutiny.

It is important to mention as well that automating spatial analysis does not eliminate bias. On the contrary, it can reinforce or amplify existing inequalities if not critically managed. Urban datasets are not neutral. They reflect historical and institutional decisions about what to measure, who collects the data, and how it is categorised. As Sanchez et al. (2025) argue, AI tools trained on historical urban data risk "*replicating pre-existing biases*".

Bias can also emerge from technical modelling choices. For instance, decisions about how to treat underground structures in GRZ calculations, or how to classify a building as "main" or "ancillary". While these may seem like neutral decisions, they carry significant implications. They affect the reported metrics and, by extension, planning decisions based on those metrics.

Recognising these risks, some cities have begun to adopt governance strategies that explicitly address the ethical use of digital tools in planning. Barcelona's Digital City strategy places strong emphasis on ethical AI. It embeds principles of fairness, accountability, and inclusion into the framework of urban governance (Calzada, 2019). By joining the *Cities' Coalition for Digital Rights*, the city formally committed to promoting transparency. It also ensures non-discrimination in the use of data and algorithms; and promotes participatory democracy, and inclusivity in digital practices.

In this context, this thesis argues that any deployment of automated tools for urban analysis must be carefully evaluated for potential uneven impacts.

5.5. Future Research Directions

Based on the findings of this study, several promising avenues for future research emerge. Grouped into two main domains: workflow-oriented improvements, and conceptual-driven extensions.

5.5.1. Workflow Extensions

From a technical perspective, multiple enhancements can improve both the precision and scalability of the current methodology.

One important development lies in generating building-centric clusters of parcels. Instead of calculating GRZ strictly per individual parcel, buildings that span multiple parcels can be used to define parcel groups; GRZ could then be calculated for the entire cluster. The resulting GRZ value then be uniformly assigned to each constituent parcel. This leads to a more realistic representation of building coverage. Particularly true in dense or irregular areas where legal parcel divisions do not align with actual use of the land.

This clustering approach would address several methodological challenges identified in the current study. For instance, the *Holsten-Quartier* case (discussed in Section 4.1) demonstrates how a single building spanning 31 parcels creates misleading GRZ values when calculated per parcel. Under the proposed clustering method, this building would be treated as a single analytical unit. The total building footprint would be divided by the combined area of all 31 parcels, yielding a more representative coverage ratio.

Implementation would require developing spatial algorithms to identify connected building footprints and their associated parcel networks. A buffer-based approach can detect buildings within a specified distance threshold. Meanwhile, topological analysis could group parcels that share building coverage. The clustering logic would need to handle edge cases, including buildings that partially overlap parcel boundaries or configurations where a single parcel cluster contains multiple buildings.

The method would be particularly valuable for analysing large-scale developments, industrial complexes, and historical districts. In these areas, original parcel divisions do not always allign with current building configurations. In Hamburg's context, this woul provide a more accurate assessments of density and improve comparative analysis between districts. GRZ values would better reflect actual development intensity rather than administrative fragmentation.

A significant parallel direction involves incorporating “vertical dimension” urban parameters, such as FAR or total building volume. These metrics add dimensionality to the analysis, capturing the intensity of development in terms of both footprint and height. The use of 3D spatial data would make this possible (including LiDAR or the City of Hamburg's 3D City Model). In combination with ALKIS attributes such as *floor count* or *object height*, this would enable a more comprehensive assessments of density. Given the performance of the current 2D pipeline, a similar 3D implementation using PostGIS would be computationally feasible at the citywide level.

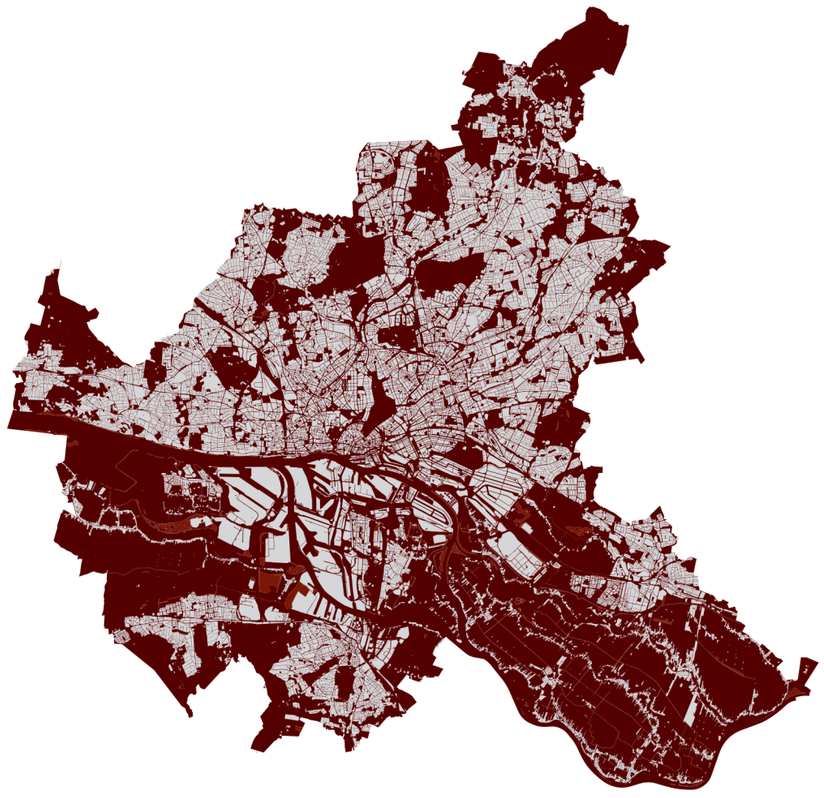

Figure 52. Map of building eligible land use categories in Hamburg. Parcels shown in light represent areas where buildings are allowed based on land use classification. (See Table 21 for classification) (author, 2025)

A third valuable extension would be the integration of land use information. This adds a crucial regulatory layer to the analysis. Land use classification is available within ALKIS dataset as a separate layer, it defines the legally designated use of land parcels. Examples include *Wohnbauflaeche*, *FlaecheGemischterNutzung*, *Fliessgewaesser*, *Hafenbecken*, and *Landwirtschaft* (see full list in Table 19 in Appendix D). While the current workflow quantifies how intensively a parcel is built, it does not yet account for whether construction is permitted on that concrete parcel.

By linking each parcel to its respective land use category, the workflow could distinguish between buildable and non-buildable areas, improving the precision and policy relevance of densification assessments.

The integration process would require spatially intersecting each parcel with the land use polygon geometry to determine its assigned category. A foreseeable challenge lies in handling parcels that intersect multiple land use zones. In such cases, methodological decisions will significantly influence how the data is interpreted and applied. Solutions include whether to assign the dominant land use, use the centroid location, or apply proportional weighting.

Greater automation represents another clear area for development. Future iterations could integrate tools like ogr2ogr[13] and establish real-time connections to ALKIS via APIs. This enables a dynamic processing pipeline that automatically updates calculations as new datasets are released. Supporting live monitoring.

Machine learning (ML) also presents valuable opportunities. Supervised learning models could be trained to better classify buildings between *Hauptanlagen* or *Nebenanlagen*. This could potentially surpass the current rule-based system by learning from labelled examples. ML could also support city-scale anomaly detection by identifying parcels with unusually high or low GRZ values relative to their surrounding urban context.

Temporal analysis is also a promising line of work. Access to stored urban parameters versions would enable researchers to map morphological changes over time. Allowing for the evaluation of the long-term impacts of zoning decisions. However, this requires methods to deal with issues such as geometry updates and data inconsistencies across time periods. Techniques such as change

13. ogr2ogr is a command-line tool within the GDAL (Geospatial Data Abstraction Library) suite used to convert and transform geospatial data between various formats and coordinate systems. It supports efficient automation of data import, export, and transformation tasks across multiple GIS platforms.

detection algorithms or temporal clustering could then be employed, helping to identify areas that share common development trajectories or transformation rates.

5.5.2. Conceptual Oriented Research Directions

Beyond the technical domain, future research can explore how automated urban analysis relates to planning concepts in several key ways.

A valuable step would be conducting comparative studies across multiple German cities with varied planning frameworks and morphological characteristics. This will help test the generalisability of the current workflow and reveal necessary adaptations for different contexts. Such studies can also clarify how differences in dataset structure (e.g., the completeness of ALKIS) influence analytical outcomes, ultimately guiding the development of more robust and adaptable tools for urban analysis.

In addition, integrating urban planning with BIM[14] presents a promising long-term research direction. By using the IFC[15] standard, GIS-based workflows could be connected to building-scale simulations, enabling multi-layered analyses within a unified spatial framework. Examples include life-cycle assessments and performance evaluations. Such integration would not only improve interoperability between disciplines but also expand the policy relevance of geospatial diagnostics.

Another important conceptual area relates to the institutional integration of automation. As discussed in Section 5.4 (ethical implications), automating planning metrics reshapes how decisions are made and who participates in that process. Future work can examine how automated tools interact with local governance, regulatory frameworks, and civic participation initiatives. For instance, how might periodic GRZ updates inform zoning debates or development reviews?

In summary, future research should aim to develop the current methodology into a further dynamic and context-aware system. By combining technical enhancements with conceptual inquiry, the workflow has the potential to become a powerful tool for effective land management.

---

14. Building Information Modelling.
15. Industry Foundation Classes.

6. Conclusion

What began as a focused effort to automate repetitive urban parameter calculations (specifically BCR) evolved into a broader enquiry: *How can cities be represented, interpreted, and shaped through data?* Driven by the need to move beyond labor-intensive manual workflows, the present thesis draws from traditional planning processes and complements them with new automation capabilities. It brings computational tools within institutional and legal frameworks.

The research argues that automation in urban analysis transcends mere efficiency gains. When thoughtfully integrated, computational tools enrich planning processes. They serve not only as background processors but as analytical agents capable of guiding, validating, and informing urban decisions. This becomes particularly relevant in data-rich environments where information often remains underutilised due to fragmented systems or inaccessible workflows.

In summary, the thesis compared a GIS-based workflow (which offered a user-friendly, visual analysis environment) with a database-driven workflow (that provided fully automated, scalable processing). A key innovation was development of a solution for building-to-parcel assignment. This addresses a recurring challenge in urban data modelling with precision and flexibility.

Beyond technical results, the research demonstrated how spatial automation can support more refined interpretations of urban form. By mapping the citywide results, and comparing in a urban block scale, the study revealed underutilized parcels and possible mismatches between the built form and what planning regulations allow. These insights open opportunities for evidence-based land-use policy, particularly in fast-changing areas.

The research contributes across three interconnected levels: technical, methodological, and conceptual. Technically, it delivers a fully operational pipeline for BCR calculation using official cadastral data. This bridges file-based GIS tools and relational spatial databases to support scalable and repeatable analysis.

Methodologically, the thesis advances spatial analysis by introducing intersection-based allocation and dictionary logic for handling partial building overlaps; issues often overlooked in broader urban studies. The precision required is essential for aligning calculations with legal frameworks.

Conceptually, the project reframes spatial metrics from static outputs to dynamic indicators. These are recalculable, visualisable, and adaptable to iterative design and policy processes. Challenging the conventional separation between design and regulation. It encourages more adaptive, feedback-oriented planning systems.

The research also represented a significant interdisciplinary learning journey. Trained as an architect with experience in parcel-scale urban planning, the present research required transitioning from conventional manual calculation methods to large-scale spatial computation. While familiar with metrics such as BCR and FAR, applying computational logic to urban-scale datasets using geospatial technologies and spatial databases was new territory.

Developing the PostgreSQL-based workflow provided hands-on experience with large-scale geospatial computation, deepening understanding of how automation can serve as an analytical tool. This learning path, shaped by real data and regulatory challenges, represents a meaningful step in bridging disciplinary boundaries between architecture, urban planning, and geoinformatics.

From this perspective, cities are seen as dynamic systems shaped by data, policy, spatial form, and regulatory feedback. Tools such as geospatial scripting and regulatory modelling enable new ways of interpreting and managing urban environments.

Automation operates within complex systems of values and assumptions. Data-driven tools carry embedded modelling choices that influence decision-making processes and outcomes. Cities like Hamburg demonstrate the importance of robust institutional frameworks, such as open-data legislation, standardised datasets, and collaborative planning cultures, this help ensure automation is applied responsibly.

Cities are not destined to accept opaque ‘black-box’ analytics; they can shape digital urbanism through policy and ethics. As discussed in Chapter 5, some cities are already planning algorithm registries, demonstrating how transparency and accountability can be formally embedded in planning technologies.

These examples demonstrate that technology is not the destiny. The challenge lies not in choosing between human and machine, but in designing systems where both collaborate. This supports more just, transparent, and responsive urban environments.

This thesis offers both method and mindset, one that values clarity, reproducibility, and critical reflection in pursuing intelligent urban systems. As cities continue evolving through data, the task ahead is ensuring that automation augments human insight.

7. References

AdV. (2018). ALKIS-Signaturenkatalog Teil A: Vorbemerkungen (No. Kapitel 7 ALKIS-Katalogwerke; Dokumentation Zur Modellierung Der Geoinformationen Des Amtlichen Vermessungswesens). Arbeitsgemeinschaft der Vermessungsverwaltungen der Länder der Bundesrepublik Deutschland (AdV).

AdV. (2022). Ausleitung des ALKIS-Objektartenkatalogs DLKM (Dokumentation Zur Modellierung Der Geoinformationen Des Amtlichen Vermessungswesens). Arbeitsgemeinschaft der Vermessungsverwaltungen der Länder der Bundesrepublik Deutschland (AdV).

Alfasi, N., & Portugali, J. (2007). Planning rules for a self-planned city. Planning Theory, 6, 146–163. https://doi.org/10.1177/1473095207077587

Amtliches Deutsches Vermessungswesen. (2022). Data format description of Official Land Parcel Information of Germany (p. 4). Landesamt für Digitalisierung, Breitband und Vermessung Bayern.

Arbeitsgemeinschaft der Vermessungsverwaltungen—AdV-Online. (n.d.). Retrieved 30 January 2025, from https://www.adv-online.de/GeoInfoDok/

Baeza, J. L., Sievert, J. L., Landwehr, A., Luft, J., Preuner, P., Bruns-Berentelg, J., Noyman, A., & Noennig, J. R. (2021). CityScope Platform for Real-Time Analysis and Decision-Support in Urban Design Competitions: International Journal of E-Planning Research, 10(4), 121–137. https://doi.org/10.4018/IJEPR.20211001.oa8

Bartoszewski, D., Piórkowski, A., & Lupa, M. (2019). The Comparison of Processing Efficiency of Spatial Data for PostGIS and MongoDB Databases (pp. 291–302). https://doi.org/10.1007/978-3-030-19093-4_22

Berghauser Pont, M., & Haupt, P. (2021). Spacematrix—Space, Density and Urban Form.

Biljecki, F., Ledoux, H., Stoter, J., & Vosselman, G. (2016). The variants of an LOD of a 3D building model and their influence on spatial analyses. ISPRS Journal of Photogrammetry and Remote Sensing, 116, 42–54. https://doi.org/10.1016/j.isprsjprs.2016.03.003

Biljecki, F., Stoter, J., Ledoux, H., Zlatanova, S., & Çöltekin, A. (2015). Applications of 3D City Models: State of the Art Review. ISPRS International Journal of Geo-Information, 4(4), Article 4. https://doi.org/10.3390/ijgi4042842

Bruns-Berentelg, J. (2014). Die Hafencity Hamburg – Identität, Nachhaltigkeit und Urbanität. HafenCity Hamburg GmbH.

Calzada, I. (2019). Barcelona's Grassroots-led Urban Experimentation: Deciphering the 'Data Commons' Policy Scheme. SSRN Electronic Journal. https://doi.org/10.2139/ssrn.3359268

Casali, Y., Aydin, N. Y., & Comes, T. (2022). Machine learning for spatial analyses in urban areas: A scoping review. Sustainable Cities and Society, 85, 104050. https://doi.org/10.1016/j.scs.2022.104050

Chen, C., Guo, Z., & Judge, J. (2024). A QGIS Plugin for GIS-based Multicriteria Decision Analysis: An Application of Developing Alternative Future Land-Use Scenarios in Ghana. Applied Spatial Analysis and Policy, 17(2), 779–797. https://doi.org/10.1007/s12061-024-09566-x

Creuzer, P. (2012, October). Cadastre in Germany—The ALKIS Approach. Landesamt für Geoinformation und Landentwicklung Niedersachsen.

Creuzer, P. (2022). Availability and Accessibility of Official Geospatial Reference Data in Germany.

Dale, M., & Alejandra, M. (2022). Impact of Digital Planning Tools on the enhancement of the Urban Microclimate: Case study: Grasbrook New District, Hamburg [Thesis, Hafencity Universität Hamburg]. Retrieved 28 January 2025, from https://repos.hcu-hamburg.de/handle/hcu/649

Darmanto, N. S., Varquez, A. C. G., & Kanda, M. (2017). Urban roughness parameters estimation from globally available datasets for mesoscale modeling in megacities. Urban Climate, 21, 243–261. https://doi.org/10.1016/j.uclim.2017.07.001

Dovey, K., & Pafka, E. (2016). The science of urban design? URBAN DESIGN International, 21, 1–10. https://doi.org/10.1057/udi.2015.28

Eicker, U., Schumacher, J., Coors, V., Zirak-Nora Bartke, M., & Nouvel, R. (2015). An Automated Method for Urban Energy Simulation Based on 3D City Models. 14, 2477–2482. https://doi.org/10.26868/25222708.2015.2938

Esposito, A., Grulois, M., Pappaccogli, G., Palusci, O., Donateo, A., Salizzoni, P., Santiago, J. L., Martilli, A., Maffeis, G., & Buccolieri, R. (2023). On the Calculation of Urban Morphological Parameters Using GIS: An Application to Italian Cities. Atmosphere, 14(2), Article 2. https://doi.org/10.3390/atmos14020329

Ferreira, D. G., Diniz, C. B., & Assis, E. S. de. (2021). Methods to calculate urban surface parameters and their relation to the LCZ classification. Urban Climate, 36, 100788. https://doi.org/10.1016/j.uclim.2021.100788

Girindran, R., Boyd, D. S., Rosser, J., Vijayan, D., Long, G., & Robinson, D. (2020). On the Reliable Generation of 3D City Models from Open Data. Urban Science, 4(4), Article 4. https://doi.org/10.3390/urbansci4040047

Goodchild, M. (2010). Twenty years of progress: GIScience in 2010. Journal of Spatial Information Science, 1. https://doi.org/10.5311/JOSIS.2010.1.2

Guo, H., Du, B., Zhang, L., & Su, X. (2022). A coarse-to-fine boundary refinement network for building footprint extraction from remote sensing imagery. ISPRS Journal of Photogrammetry and Remote Sensing, 183, 240–252. https://doi.org/10.1016/j.isprsjprs.2021.11.005

Holub-Moorman, G. (n.d.). Ethics of AI-Enhanced Planning. American Planning Association. Retrieved 4 June 2025, from https://www.planning.org/blog/9306489/ethics-of-ai-enhanced-planning/

Jovanović, D. (2022). From QGIS to Python: Comparison of Free and Open Tools for Statistical Analysis of Cultural Heritage and Data Representation. The International Archives of the Photogrammetry, Remote Sensing and Spatial Information Sciences, XLVIII-4-W1-2022, 229–236. ISPRS WG IV/4, III/10, IV/7, V/1 & ICWG IV/III, Free and Open Source Software for Geospatial (FOSS4G) 2022 – Academic Track, 22–28 August 2022, Florence, Italy. https://doi.org/10.5194/isprs-archives-XLVIII-4-W1-2022-229-2022

Kent, C. W., Grimmond, S., Gatey, D., & Hirano, K. (2019). Urban morphology parameters from global digital elevation models: Implications for aerodynamic roughness and for wind-speed estimation. Remote Sensing of Environment, 221, 316–339. https://doi.org/10.1016/j.rse.2018.09.024

Kitchin, R., Lauriault, T., & McArdle, G. (2015). Knowing and governing cities through urban indicators, city benchmarking and real-time dashboards. Regional Studies, Regional Science, 2, 6–28. https://doi.org/10.1080/21681376.2014.983149

Klokan Technologies. (n.d.). ETRS89 / UTM zone 32N - EPSG:25832. Retrieved 9 February 2025, from https://epsg.io

Le, Q. H., Shin, H., Kwon, N., Ho, J., & Ahn, Y. (2022). Deep Learning Based Urban Building Coverage Ratio Estimation Focusing on Rapid Urbanization Areas. Applied Sciences, 12(22), Article 22. https://doi.org/10.3390/app122211428

Lieven, C. (2017). DIPAS – Towards an integrated GIS-based system for civic participation. Procedia Computer Science, 112, 2473–2485. https://doi.org/10.1016/j.procs.2017.08.182

Lindberg, F., Grimmond, C. S. B., Gabey, A., Huang, B., Kent, C. W., Sun, T., Theeuwes, N. E., Järvi, L., Ward, H. C., Capel-Timms, I., Chang, Y., Jonsson, P., Krave, N., Liu, D., Meyer, D., Olofson, K. F. G., Tan, J., Wästberg, D., Xue, L., & Zhang, Z. (2018). Urban Multi-scale Environmental Predictor (UMEP): An integrated tool for city-based climate services. Environmental Modelling & Software, 99, 70–87. https://doi.org/10.1016/j.envsoft.2017.09.020

Majic, I., & Pafka, E. (2019). AwaP-IC—An Open-Source GIS Tool for Measuring Walkable Access. Urban Science, 3(2), 48. https://doi.org/10.3390/urbansci3020048

Mutani, G., Carozza, M., Todeschi, V., & Rolando, A. (2020). Urban-Scale Energy Models: Relationship between urban form and energy performance (p. 000190). https://doi.org/10.1109/CANDO-EPE51100.2020.9337760

Mwanja, I. (2023). An Introduction to Geospatial Mapping: QGIS. Research Guides: An Introduction to Geospatial Mapping: QGIS. Retrieved 02 February 2025, from https://guides.lib.vt.edu/c.php?g=1375762&p=10194090

Neteler, M., Bowman, M. H., Landa, M., & Metz, M. (2012). GRASS GIS: A multi-purpose open source GIS. Environmental Modelling & Software, 31, 124–130. https://doi.org/10.1016/j.envsoft.2011.11.014

Nguyen, M. S. H., & Quarg, J. K. (2024). Expandable Urban Knowledge Graphs: A Use Case in CityGML with OpenStreetMap Data.

Obe, R. O. (2015). PostGIS in action (Second edition). Manning.

Okabe, A., & Sugihara, K. (2012). Spatial Analysis Along Networks: Statistical and Computational Methods. John Wiley & Sons.

Ostadabbas, H., Weippert, H., & Behr, F.-J. (2020). Using the synergy of QField for on-site data collection and QGIS for interactive map creation through ALKIS® data extraction and PostgreSQL implementation in urban planning processes. ISPRS - International Archives of the Photogrammetry, Remote Sensing and Spatial Information Sciences, XLIII-B4-2020, 679–683. https://doi.org/10.5194/isprs-archives-XLIII-B4-2020-679-2020

Pan, X.-Z., Zhao, Q.-G., Chen, J., Liang, Y., & Sun, B. (2008). Analyzing the Variation of Building Density Using High Spatial Resolution Satellite Images: The Example of Shanghai City. Sensors, 8, 2541–2550. https://doi.org/10.3390/s8042541

petersen pörksen partner. (2012). Potenziale der Innenentwicklung Altona. Fachamt Stadt- und Landschaftsplanung (Bezirksamt Altona).

PostGIS 3.5.3dev Manual. (2025).

Roberts, D. (2019, April 8). Barcelona's remarkable history of rebirth and transformation. Vox. Retrieved 11 April 2025, from https://www.vox.com/energy-and-environment/2019/4/8/18266760/barcelona-spain-urban-planning-history

Sanchez, T. W., Brenman ,Marc, & Ye, X. (2025). The Ethical Concerns of Artificial Intelligence in Urban Planning. Journal of the American Planning Association, 91(2), 294–307. https://doi.org/10.1080/01944363.2024.2355305

Sejati, A. W., Buchori, I., Rudiarto, I., Silver, C., & Sulistyo, K. (2020). Open-Source Web GIS Framework in Monitoring Urban Land Use Planning: Participatory Solutions for Developing Countries. Journal of Urban and Regional Analysis, 12(1). https://doi.org/10.37043/JURA.2020.12.1.2

Sherman, G. E. (2008). Desktop GIS: Mapping the planet with open source tools. Pragmatic Bookshelf.

Tang, H., & Wang, Z. (2024). Urban Building Coverage Areas Calculation and 3D Modeling Based on UAV LiDAR. IGARSS 2024 - 2024 IEEE International Geoscience and Remote Sensing Symposium, 8638–8641. https://doi.org/10.1109/IGARSS53475.2024.10642745

The Municipal Algorithms and Data Strategy for an Ethical Promotion of Artificial Intelligence | Barcelona Digital City | Barcelona City Council. (n.d.). Retrieved 4 June 2025, from https://ajuntament.barcelona.cat/digital/en/technology-accessible-everyone/ethical-use-artificial/ethical-use-artificial-intelligence/municipal

Yang, F., Zeng, G., Du, C., Tang, L., Zhou, J., & Li, Z. (2008). Spatial analyzing system for urban land-use management based on GIS and multi-criteria assessment modeling. Progress in Natural Science - PROG NAT SCI, 18, 1279–1284. https://doi.org/10.1016/j.pnsc.2008.05.007

Yin, C. (2008). Comparative research of spatial control in urban detailed planning in China and Germany [doctoral Thesis]. Retrieved 28 January 2025, from http://elib.uni-stuttgart.de/handle/11682/77

Zahid, H. (2023). Integrating Regulatory Compliance into Urban Simulations: A Framework based on CityGML and XPlanung. Retrieved 28 January 2025, from https://mediatum.ub.tum.de/node?id=1734901#!

Zahid, H., Hijazi, I., Donaubauer, A., & Kolbe, T. H. (2024). Enhancing Realism in Urban Simulations: A Mapping Framework for the German National Standard XPlanung and CityGML. In T. H. Kolbe, A. Donaubauer, & C. Beil (Eds.), Recent Advances in 3D Geoinformation Science (pp. 437–457). Springer Nature Switzerland. https://doi.org/10.1007/978-3-031-43699-4_28

Zeitner, R., Marchionini, M., Neumann, G., & Irmscher, H. (2019). Flächenmanagement in der Immobilienwirtschaft: Grundlagen und konkrete Anwendung. Springer. https://doi.org/10.1007/978-3-662-58476-7

8. Appendices

8.1. Appendix A. Data & Dataset Documentation

Table 13. Overview of ALKIS layers by geometry type and english layer name (author, 2025).

Layer Name	Layer Name (English)	Geometry Type
ALKIS__Bauwerke_Punkte	Buildings (Points)	Point
ALKIS__Bauwerke_Signaturen	Building Symbols	Point
ALKIS__Bauwerke_Texte	Building Labels	Point
ALKIS__Bes_Angaben_Punkte	Special Info (Points)	Point
ALKIS__Bes_Angaben_Signaturen	Special Info Symbols	Point
ALKIS__Bes_Angaben_Texte	Special Info Labels	Point
ALKIS__Festlegungen_Punkte	Designations (Points)	Point
ALKIS__Festlegungen_Texte	Designations (Labels)	Point
ALKIS__Flurstuecke_Grenzpunkte_Texte	Boundary Point Labels	Point
ALKIS__Flurstuecke_Grenzpunkte	Boundary Points	Point
ALKIS__Flurstuecke_Nummern	Parcel Numbers	Point
ALKIS__Gebaeude_Adressen_georef	Georeferenced Building Addresses	Point
ALKIS__Gebaeude_Signaturen	Building Symbols	Point
ALKIS__Gebaeude_Texte	Building Labels	Point
ALKIS__Lage_mit_Hausnummer	Location with House Number	Point
ALKIS__Lage_mit_Pseudonummer	Location with Pseudo Number	Point
ALKIS__Lage_ohne_Hausnummer_pkt	Location w/o House Number (Point)	Point
ALKIS__Nutzung_Signaturen	Land Use Symbols	Point
ALKIS__Nutzung_Texte	Land Use Labels	Point
ALKIS__Relief_Signaturen	Relief Symbols	Point
ALKIS__Schaetzung_Grabloecher	Valuation Excavations	Point
ALKIS__Schaetzung_LMVS_Punkte	Valuation LMVS (Points)	Point
ALKIS__Schaetzung_Signaturen	Valuation Symbols	Point
ALKIS__Schaetzung_Texte	Valuation Labels	Point
ALKIS__Bauwerke_Linien	Buildings (Lines)	MultiLineString
ALKIS__Bes_Angaben_Linien	Special Info (Lines)	MultiLineString
ALKIS__Flurstuecke_Zuordnungspfeile	Assignment Arrows	MultiLineString
ALKIS__Flurstuecke_bes_Grenzen	Special Boundaries	MultiLineString
ALKIS__Gebaeude_Gebaeudelinien	Building Outlines	MultiLineString
ALKIS__Relief_Gelaendekanten	Terrain Edges	MultiLineString
ALKIS__Relief_Linien	Relief Lines	MultiLineString
ALKIS__Schaetzung_Linien	Valuation (Lines)	MultiLineString
ALKIS__Bauwerke_Flaechen	Buildings (Areas)	MultiPolygon
ALKIS__Bes_Angaben_Flaechen	Special Info (Areas)	MultiPolygon
ALKIS__Festlegungen_Flaechen	Designations (Areas)	MultiPolygon
ALKIS__Flurstuecke_Flaechen	Cadastral Parcels (Areas)	MultiPolygon
ALKIS__Gebaeude_Bauteile_Flaechen	Building Parts (Areas)	MultiPolygon
ALKIS__Gebiete_Flaechen	Area Units	MultiPolygon
ALKIS__Hist_Flurstuecke_Flaechen	Historic Parcels (Areas)	MultiPolygon
ALKIS__Nutzung_Flaechen	Land Use (Areas)	MultiPolygon
ALKIS__Relief_Flaechen	Relief (Areas)	MultiPolygon
ALKIS__Schaetzung_Flaechen	Valuation (Areas)	MultiPolygon
ALKIS__Schaetzung_LMVS_Flaechen	Valuation LMVS (Areas)	MultiPolygon
ALKIS__Verwaltung_Bezirke	Administrative Districts	MultiPolygon
ALKIS__Verwaltung_DHDN_GK_1KM	DHDN GK Grid 1km	MultiPolygon
ALKIS__Verwaltung_Gemarkungen	Cadastral Districts	MultiPolygon
ALKIS__Verwaltung_Landesgrenze	State Borders	MultiPolygon
ALKIS__Verwaltung_Ortsteile	Localities	MultiPolygon
ALKIS__Verwaltung_Stadtteile	City Districts	MultiPolygon
ALKIS__Verwaltung_UTM_100M	UTM Grid 100m	MultiPolygon
ALKIS__Verwaltung_UTM_DK5_Kacheln	UTM DK5 Tiles	MultiPolygon
ALKIS__Verwaltung_UTM_Kachel_1KM	UTM Grid 1km	MultiPolygon
ALKIS__Aktualitaet	Update Status	NoGeometry
ALKIS__Fachdatenverbindungen	Specialist Data Links	NoGeometry
ALKIS__Hist_Flurstuecke_ALB	Historic Parcels (ALB)	NoGeometry
ALKIS__Hist_Flurstuecke_Nachfolger	Historic Parcels (Successors)	NoGeometry
ALKIS__Hist_Flurstuecke_Vorgaenger	Historic Parcels (Predecessors)	NoGeometry
ALKIS__Katalog_Lagebezeichnungen	Location Descriptions Catalog	NoGeometry
ALKIS__Relationen	Relations	NoGeometry
ALKIS__SDP_GID_Zuordnung	SDP GID Assignment	NoGeometry

Table 14. Overview and evaluation of attribute fields in the ALKIS **Parcel Dataset** (author, 2025).

Attribute Short Name	Attribute Name (German)	Attribute Name (English)	Data Type	Data Ava. (%)	Possible Values	Usefulness	Sample Value (HCU Parcel)
AFL	AmtlicheFlaeche	Official Area	double	100	[…] unique	usefull	9171
FSKALB	Flurstuecks/kennzALB	Parcel Identifier Alb	string	100	[…] unique	usefull	020102-000-02191/0000.00
FSK	Flurstuecks/kennzeichen	Parcel Identifier	string	100	[…] unique	usefull	020102___02191_____
FSKO	Flurstuecks/kennzOhneFolge	Parcel Identifier Without Sequence	string	100	[…] unique	usefull	020102___02191____
ZAE	Flurstuecksnr/zaehler	Parcel Number/Counter	string	100	[…] unique	usefull	2191
NAMGMK	Gemarkung/name	Cadastral District / Name	string	100	[…]	usefull	Altstadt Süd
GMK	Gemarkung/schluessel	Cadastral District / Key	string	100	[…]	usefull	102
UUID	Identifikator	Identifier	string	100	[…] unique	usefull	DEHHALKAJ0000HjR
ISTGEBUCHT	istGebuchtBuchungsstelle	Is Booked Booking Office	string	100	[…]	usefull	DEHHALKA100011nv
BEG	LZI/beginnt	Lzi Starts	date & time	100	[…]	usefull	09.11.20 08:49:29 (UTC)
OBJECTID	OBJECTID	Object Id	integer	100	[…] unique	usefull	7387
ZDEBS	ZeitpunktDerEntstehung	Time Of Creation	string	100	[…]	could be usefull	20091008
FDV	Fachdatenverbindung_vorhanden	Specialized Data Connection Available	string	100	[ja, nein]	could be usefull	ja
NAMFLN	Flur/name	Cadastral District/Name		100	[…]	could be usefull	
FLN	Flur/nummer	Cadastral District/Number		100	[…]	could be usefull	
FSF	Flurstuecksfolge	Parcel Sequence		100	[…]	could be usefull	
NEN	Flurstuecksnr/nenner	Parcel Number/Denominator		100	[…]	could be usefull	
NAMGMT	Gemeindeteil/name	Municipality Part/Name		100	[…]	could be usefull	
GMT	Gemeindeteil/schluessel	Municipality Part/Code		100	[…]	could be usefull	
NORDWERT	NordwertFlurstuecksnummer	Northern Value Parcel Number	double	100	[…]	could be usefull	5,932,843,218
HOW	ObjektkoordinateHochwert	Object Coordinate Northing	double	100	[…]	could be usefull	5932872,43
REW	ObjektkoordinateRechtswert	Object Coordinate Easting	double	100	[…]	could be usefull	566,554,572
OSTWERT	OstwertFlurstuecksnummer	Eastern Value Parcel Number	double	100	[…]	could be usefull	566,603,102
RBV	Rechtsbehelfsverfahren	Legal Remedy Procedure		100	[…]	could be usefull	
	Shape_Area	Nan	double	100	[…]	could be usefull	9,163,591,080,751,980
	Shape_Length	Nan	double	100	[…]	could be usefull	45,426,346,854,370,200
ENDE	LZI/endet	Lzi Ends	date & time	0	-	could be usefull	
NRA	NummerImAufteilungsplan	Number In Subdivision Plan		0	-	could be usefull	
BEZEICH	AAA-Beschreibung	Description		100	“AX_Flurstueck”	not usefull	
ARZ	AbweichenderRechtszustand	Divergentlegalstatus		100	[…]	not usefull	
KENN	ALKIS-Kennung	Alkis Identifier	string	100	“AX11001”	not usefull	AX11001
DPRIO	Darstellungsprioritaet	Display Priority	string	100	700	not usefull	700
DVAR	Darstellungsvariante	Display Variant	string	100	7	not usefull	7
NAMGEM	Gemeinde/name	Municipality/Name		100	“Hamburg”	not usefull	
GEM	Gemeinde/schluessel	Municipality/Code		100	0	not usefull	
GDZ	Gemeindekennzeichen	Municipality Code	string	100	200000	not usefull	2000000
STATUS	BearbeitungStatus	Processing Status	string	100	“Insert”	not usefull	Insert

Continuation Table 14.

Attribute Short Name	Attribute Name (German)	Attribute Name (English)	Data Type	Data Ava. (%)	Possible Values	Usefulness	Sample Value (HCU Parcel)
CRS	Koordinatenreferenzsystem	Coordinate Reference System		100	“ETRS89_UTM32”	not usefull	
NAMKRS	Kreis/name	County/Name		100	“Hamburg”	not usefull	
KRS	Kreis/schluessel	County/Code		100	0	not usefull	
NAMLAN	Land/name	State/Name		100	“Hamburg”	not usefull	
LAN	Land/schluessel	State/Code		100	2	not usefull	
DLAN	LandZustaendigeStelle	State Responsible Agency		100	-	not usefull	
MAT	Modellart	Model Type	string	100	“DLKM”	not usefull	DLKM
NAMRBZ	Regierungsbezirk/name	Government District/Name		100	“Hamburg”	not usefull	
RBZ	Regierungsbezirk/schluessel	Government District/Code		100	0	not usefull	
SNR	Signaturnummer	Signature Number	string	100	2028	not usefull	2028
SES	SonstigeEigenschaften_vorhanden	Other Properties Available	string	100	“nein”	not usefull	nein
STM	SonstigesModell	Other Model		100	-	not usefull	
DST	StelleZustaendigeStelle	Responsible Agency		100	-	not usefull	
STATUSDAT	ZeitpunktBearbeitungsStatus	Time Of Processing Status	date & time	100	2023-12-30T06:10:19	not usefull	30.12.23 06:10:19 (UTC)
ZFN	ZweifelhafterFlurstuecksnachweis	Questionable Parcel Proof		100	-	not usefull	
ANEN	AnteilNenner	Share Denominator		0	-	not usefull	
BUB	BeschreibungDesUmfangsDerBuchung	Description Of Booking Extent		0	-	not usefull	
BEZBAR	Buchungsart/bezeichnung	Booking Type/Designation		0	-	not usefull	
AZAE	AnteilZaehler	Share Numerator		0	-	not usefull	
BSO	BeschreibungDesSondereigentums	Description Of Separate Ownership		0	-	not usefull	
BAR	Buchungsart/schluessel	Booking Type/Code		0	-	not usefull	
BTX	Buchungstext	Booking Text		0	-	not usefull	
UUID_ZUSO	Identifikator/ZUSO	Nan		0	-	not usefull	
HHE	ObjektkoordinateHoehe	Object Coordinate Height		0	-	not usefull	
POS	Positionierungsregel	Positioning Rule		0	-	not usefull	
REGID	Regionskennung	Region Identifier		0	-	not usefull	

Table 15. Overview and evaluation of attribute fields in the ALKIS **Building Dataset** (author, 2025).

Attribute Short Name	Attribute Name (German)	Attribute Name (English)	Data Type	Data Ava. (%)	Possible Values
OBJECTID	Objectid	Object Id	integer	100	[…] unique
REGID	Regionskennung	Region Identifier		0	
UUID	Identifikator	Identifier	string	100	[…] unique
UUIDFLURST	Identifikatorflurstueck	Parcel Identifier	string	0	-
GFK	Gebaeudefunktion/Schluessel	Building Function/Code	integer	93	[…]
BEZGFK	Gebaeudefunktion/Bezeichnung	Building Function	string	93	[…]
WGF	Weiteregebaeudefunktion/Schluessel	Additional Building Function/Code	string	93	[…]
BEZWGF	Weiteregebaeudefunktion/Bezeichnung	Additional Building Function	string	93	[Aufgeständert, Bibliothek, Hotel, Kapelle, Kapelle:Tiefgarage, Kindergarten, Kindergarten:Kindergarten, Kindergarten:Museum, Kindergarten:Tiefgarage, Moschee, Museum, Parkdeck, Theater, Tiefgarage, Tiefgarage:Kindergarten]
OFL	Lagezurerdoberflaeche/Schluessel	Location Relative To Ground Surface/Code		3	
BEZOFL	Lagezurerdoberflaeche/Bezeichnung	Location Relative To Ground Surface		3	[Unter der Erdoberfläche, Aufgeständert]
DAF	Dachform/Schluessel	Roof Shape/Code	string	82	[3100, 3400, 5000, 3600, 3200, 3500, 2100, 2200, 1000, 3700, 9999, 3800, 4000, 3300, 3900]
BEZDAF	Dachform/Bezeichnung	Roof Shape	string	82	[Bogendach, Flachdach, Kegeldach, Krüppelwalmdach, Kuppeldach, Mansardendach, Mischform, Pultdach, Satteldach, Sheddach, Sonstiges, Turmdach, Versetztes Pultdach, Walmdach, Zeltdach]
AOG	Anzahlderobergeschosse	Number Of Above-Ground Floors	integer	93	[NULL, 1, 2, 3, 4, 5, 6, 7, 8, 9, 10, 11, 12, 13, 14, 15, 16, 17, 18, 19, 20, 21, 22, 23, 24, 26, 27, 29]
AUG	Anzahlderuntergeschosse	Number Of Underground Floors	integer	9	[NULL, 1, 2, 3, 4, 5]
HOH	Hochhaus	High-Rise Building		93	[NULL, false]
BJA	Baujahr	Year Of Construction	string	93	[…]
BAT	Bauart/Schluessel	Construction Type/Code		7	[…]
BEZBAT	Bauart/Bezeichnung	Construction Type	string	7	[…]
DHU	Durchfahrtshoehe	Clearance Height		0	-
NAM	Name	Name	string	93	[…] 883 different values
ANT	Anteil	Share/Portion		0	-
NTZ	Nutzung/Schluessel	Usage/Code		0	
BEZNTZ	Nutzung/Bezeichnung	Usage		0	
BAW	Bauweise/Schluessel	Construction Method/Code		55	[2100, 2200, 1100, 2500, 1200, 1300, 2400, 1500, 1400]
BEZBAW	Bauweise/Bezeichnung	Construction Method		55	[Gruppenhaus, Gebäudeblock in geschlossener Bauweise, Einzelgarage, Reihenhaus, Freistehendes Einzelgebäude, Sammelgarage, Doppelgarage, Freistehender Gebäudeblock, Doppelhaushälfte]
HHO	Objekthoehe	Object Height	double	0	
ZUS	Zustand/Schluessel	Condition/Code		0	
BEZZUS	Zustand/Bezeichnung	Condition		0	
DGA	Dachgeschossausbau/Schluessel	Attic Expansion/Code	integer	0	-
BEZDGA	Dachgeschossausbau/Bezeichnung	Attic Expansion	string	0	-
DAA	Dachart	Roof Type		0	-
URA	Umbauterraum	Enclosed Space/Volume	double	0	
GRF	Grundflaeche	Ground Area	double	93	[…]

Continuation Table 15.

Attribute Short Name	Attribute Name (German)	Attribute Name (English)	Data Type	Data Ava. (%)	Possible Values
GFL	Geschossflaeche	Floor Area	double	0	-
GKN	Gebaeudekennzeichen	Building Identifier		0	-
DES	Beschreibung/Schluessel	Description/Code		17	[1900, 1200, 1100, 1000, 2000]
BEZDES	Beschreibung/Bezeichnung	Description	string	17	[…]
FDV	Fachdatenverbindung_Vorhanden	Specialized Data Connection Available		100	[nein]
HAT	Hatlagebezeichungmitpseudonr	Has Location Designation With Pseudo Number		93	[…] 118000 different values
ZEIGTAUF	Zeigtauflagebezeichungmithausnr	Points To Location Designation With House Number	string	93	[…] 225314 different values
LAG	Strassen/Schluessel	Street/Code	string	84	
NAMLAG	Strassen/Name	Street Name	string	84	
HNR	Hausnummer	House Number	double	55	
PNR	Pseudonummer	Pseudo Number		4	
LNR	Laufendenummer	Serial Number		29	
SNR	Signaturnummer	Signature Number		100	[2032, 2507, 2508, 2512, 2513, 2514, 13012031, 13012505, 13042031, 13042505, 13092031, 13092505, OTHER]
DPRIO	Darstellungsprioritaet	Display Priority		100	[290, 310]
POS	Positionierungsregel	Positioning Rule		0	
DVAR	Darstellungsvariante	Display Variant		100	
KENN	Alkis-Kennung	Alkis Identifier	string	100	[AX31002, AX31001]
BEZEICH	Aaa-Beschreibung	Aaa Description	string	100	[AX_Gebaeude, AX_Bauteil]
BEG	Lzi/Beginnt	Nan	date & time	100	
ENDE	Lzi/Endet	Nan		0	
MAT	Modellart	Model Type		100	
STM	Sonstigesmodell	Nan		100	
CRS	Koordinatenreferenzsystem	Coordinate Reference System		100	[ETRS89_UTM32]
STATUS	Bearbeitungstatus	Processing Status		100	[Insert]
STATUSDAT	Zeitpunktbearbeitungsstatus	Processing Status Timestamp	date & time	100	

Table 16. Classification of building types by attribute, position with respect to ground, and functional category (author, 2025).

Attribute	Value	ground	M/A
BEZGFK	Allgemein bildende Schule	Above	Main
BEZGFK	Bahnhofsgebäude	Above	Main
BEZGFK	Berufsbildende Schule	Above	Main
BEZGFK	Betriebsgebäude	Above	Main
BEZGFK	Betriebsgebäude für Flugverkehr	Above	Main
BEZGFK	Betriebsgebäude für Schienenverkehr	Above	Main
BEZGFK	Betriebsgebäude für Schiffsverkehr	Above	Main
BEZGFK	Betriebsgebäude für Straßenverkehr	Above	Main
BEZGFK	Betriebsgebäude zur Schleuse	Above	Main
BEZGFK	Bibliothek, Bücherei	Above	Main
BEZGFK	Bootshaus	Above	Main
BEZGFK	Botschaft, Konsulat	Above	Main
BEZGFK	Brauerei	Above	Main
BEZGFK	Bürogebäude	Above	Main
BEZGFK	Campingplatzgebäude	Above	Main
BEZGFK	Empfangsgebäude Schifffahrt	Above	Main
BEZGFK	Fahrzeughalle	Above	Main
BEZGFK	Ferienhaus	Above	Main
BEZGFK	Feuerwehr	Above	Main
BEZGFK	Flughafengebäude	Above	Main
BEZGFK	Flugzeughalle	Above	Main
BEZGFK	Forschungsinstitut	Above	Main
BEZGFK	Freizeit- und Vergnügungsstätte	Above	Main
BEZGFK	Freizeit-, Vereinsheim, Dorfgemeinschafts-, Bürgerhaus	Above	Main
BEZGFK	Friedhofsgebäude	Above	Main
BEZGFK	Gebäude der Kläranlage	Above	Main
BEZGFK	Gebäude fuer religiöse Zwecke	Above	Main
BEZGFK	Gebäude für Bewirtung	Above	Main
BEZGFK	Gebäude für Bildung und Forschung	Above	Main
BEZGFK	Gebäude für Fernmeldewesen	Above	Main
BEZGFK	Gebäude für Forschungszwecke	Above	Main
BEZGFK	Gebäude für Gesundheitswesen	Above	Main
BEZGFK	Gebäude für Gewerbe und Industrie mit Wohnen	Above	Main
BEZGFK	Gebäude für Handel und Dienstleistung mit Wohnen	Above	Main
BEZGFK	Gebäude für Handel und Dienstleistungen	Above	Main
BEZGFK	Gebäude für kulturelle Zwecke	Above	Main
BEZGFK	Gebäude für Sicherheit und Ordnung	Above	Main
BEZGFK	Gebäude für soziale Zwecke	Above	Main
BEZGFK	Gebäude für Sportzwecke	Above	Main
BEZGFK	Gebäude für Vorratshaltung	Above	Main
BEZGFK	Gebäude im botanischen Garten	Above	Main
BEZGFK	Gebäude im Freibad	Above	Main
BEZGFK	Gebäude im Stadion	Above	Main
BEZGFK	Gebäude im Zoo	Above	Main
BEZGFK	Gebäude zum Busbahnhof	Above	Main
BEZGFK	Gebäude zum Parken	Above	Main
BEZGFK	Gebäude zum Sportplatz	Above	Main
BEZGFK	Gebäude zur Abfallbehandlung	Above	Main
BEZGFK	Gebäude zur Elektrizitätsversorgung	Above	Main
BEZGFK	Gebäude zur Gasversorgung	Above	Main
BEZGFK	Gebäude zur Müllverbrennung	Above	Main
BEZGFK	Gebäude zur Versorgung	Above	Main
BEZGFK	Gebäude zur Versorgungsanlage	Above	Main
BEZGFK	Gebäude zur Wasserversorgung	Above	Main
BEZGFK	Gemeindehaus	Above	Main
BEZGFK	Gemischt genutztes Gebäude mit Wohnen	Above	Main
BEZGFK	Gericht	Above	Main
BEZGFK	Geschäftsgebäude	Above	Main
BEZGFK	Gotteshaus	Above	Main
BEZGFK	Hallenbad	Above	Main
BEZGFK	Heizwerk	Above	Main
BEZGFK	Hochschulgebäude (Fachhochschule, Universität)	Above	Main
BEZGFK	Hotel, Motel, Pension	Above	Main
BEZGFK	Jugendfreizeitheim	Above	Main
BEZGFK	Jugendherberge	Above	Main
BEZGFK	Justizvollzugsanstalt	Above	Main
BEZGFK	Kapelle	Above	Main
BEZGFK	Kinderkrippe, Kindergarten, Kindertagesstätte	Above	Main
BEZGFK	Kirche	Above	Main
BEZGFK	Kloster	Above	Main
BEZGFK	Konzertgebäude	Above	Main
BEZGFK	Krankenhaus	Above	Main
BEZGFK	Krematorium	Above	Main
BEZGFK	Land- und forstwirtschaftliches Betriebsgebäude	Above	Main
BEZGFK	Land- und forstwirtschaftliches Wohn- und Betriebsgebäude	Above	Main
BEZGFK	Land- und forstwirtschaftliches Wohngebäude	Above	Main
BEZGFK	Markthalle	Above	Main
BEZGFK	Messehalle	Above	Main
BEZGFK	Moschee	Above	Main
BEZGFK	Museum	Above	Main
BEZGFK	Parkdeck	Above	Main
BEZGFK	Parkhaus	Above	Main
BEZGFK	Polizei	Above	Main
BEZGFK	Produktionsgebäude	Above	Main
BEZGFK	Rathaus	Above	Main
BEZGFK	Reithalle	Above	Main
BEZGFK	Rundfunk, Fernsehen	Above	Main
BEZGFK	Scheune und Stall	Above	Main
BEZGFK	Schloss	Above	Main
BEZGFK	Schöpfwerk	Above	Main
BEZGFK	Schutzbunker	Above	Main
BEZGFK	Speditionsgebäude	Above	Main
BEZGFK	Sport-, Turnhalle	Above	Main
BEZGFK	Stall	Above	Main
BEZGFK	Synagoge	Above	Main
BEZGFK	Tankstelle	Above	Main
BEZGFK	Theater, Oper	Above	Main
BEZGFK	Toilette	Above	Main
BEZGFK	Touristisches Informationszentrum	Above	Main
BEZGFK	Veranstaltungsgebäude	Above	Main
BEZGFK	Verwaltungsgebäude	Above	Main
BEZGFK	Waschstraße, Waschanlage, Waschhalle	Above	Main
BEZGFK	Werft (Halle)	Above	Main
BEZGFK	Werkstatt	Above	Main
BEZGFK	Wochenendhaus	Above	Main
BEZGFK	Wohngebäude mit Gemeinbedarf	Above	Main
BEZGFK	Wohngebäude mit Gewerbe und Industrie	Above	Main
BEZGFK	Wohngebäude mit Handel und Dienstleistungen	Above	Main
BEZGFK	Wohnhaus	Above	Main
BEZGFK	Wohnheim	Above	Main
BEZGFK	Zollamt	Above	Main
BEZGFK	Tiefgarage	Under	Anci.
BEZGFK	Garage	Above	Anci.
BEZGFK	Gartenhaus	Above	Anci.
BEZGFK	Gewächshaus, verschiebbar	Above	Anci.
BEZGFK	Kaserne	Above	Anci.
BEZGFK	Treibhaus, Gewächshaus	Above	Anci.
BEZGFK	Müllbunker	-	Anci.
BEZGFK	Gebäude an unterirdischen Leitungen	Above	-
BEZOFL	Unter der Erdoberfläche	Under	Anci.
BEZOFL	Aufgeständert	Above	-
BEZWGF	Bibliothek	Above	Main
BEZWGF	Hotel	Above	Main
BEZWGF	Jugendherberge	Above	Main
BEZWGF	Kapelle	Above	Main
BEZWGF	Kindergarten	Above	Main
BEZWGF	Kindergarten:Museum	Above	Main
BEZWGF	Moschee	Above	Main
BEZWGF	Museum	Above	Main
BEZWGF	Parkdeck	Above	Main
BEZWGF	Polizeiwache	Above	Main
BEZWGF	Theater	Above	Main
BEZWGF	Toilette	Above	Main
BEZWGF	Zoll	Above	Main
BEZWGF	Kindergarten:Tiefgarage	Under	Anci.
BEZWGF	Museum:Tiefgarage	Under	Anci.
BEZWGF	Tiefgarage	Under	Anci.
BEZWGF	Tiefgarage:Kindergarten	Under	Anci.
BEZWGF	Tiefgarage:Moschee	Under	Anci.
BEZWGF	Zoll:Tiefgarage	Under	Anci.

8.2. Appendix B. SQL and Script Listings

```
import time
from qgis.core
import (
    QgsProject, QgsVectorLayer, QgsSpatialIndex, QgsFeature, QgsField,
QgsFeatureRequest)
from PyQt5.QtCore import QVariant
# Start timing
start_time = time.time()
# Load layers
parcel_layer = QgsProject.instance().mapLayersByName("ALKIS__Flurstuecke_
Flaechen-parsed-validated")[0]
main_layer = QgsProject.instance().mapLayersByName("ALKIS__Gebaeude_Flaechen-
Main")[0]
aux_layer = QgsProject.instance().mapLayersByName("ALKIS__Gebaeude_Flaechen-
Ancillary")[0]


# Build spatial indexes
main_index = QgsSpatialIndex(main_layer.getFeatures())
aux_index = QgsSpatialIndex(aux_layer.getFeatures())

# Prepare output layer
fields = parcel_layer.fields()
fields.append(QgsField("GRZ_main", QVariant.Double))
fields.append(QgsField("GRZ_aux", QVariant.Double))

output_layer = QgsVectorLayer("MultiPolygon?crs=" + parcel_layer.crs().
authid(), "ALKIS__Flurstuecke_Flaechen-parsed-validated-GRZ", "memory")
output_layer.dataProvider().addAttributes(fields)output_layer.updateFields()

# Process all parcels
for i, parcel in enumerate(parcel_layer.getFeatures()):
    parcel_geom = parcel.geometry()
    parcel_area = parcel_geom.area()
    if parcel_area == 0:
        continue
    # Find intersecting main buildings
    main_ids = main_index.intersects(parcel_geom.boundingBox())
    main_feats = main_layer.getFeatures(
                               QgsFeatureRequest().setFilterFids(main_ids))
    main_area = sum(
        feat.geometry().intersection(parcel_geom).area()
        for feat in main_feats
        if not feat.geometry().intersection(parcel_geom).isEmpty()
        and inter. area() > 1.0
    )


    # Find intersecting ancillary buildings
    aux_ids = aux_index.intersects(parcel_geom.boundingBox())
    aux_feats = aux_layer.getFeatures(
                              QgsFeatureRequest().setFilterFids(aux_ids))
    aux_area = sum(
        feat.geometry().intersection(parcel_geom).area()
        for feat in aux_feats
        if not feat.geometry().intersection(parcel_geom).isEmpty()
        and inter. area() > 1.0
    )

    # Calculate GRZ values
    grz_main = round(main_area / parcel_area, 1)
    grz_aux = round((main_area + aux_area) / parcel_area, 1)

    # Add result to output layer
    out_feat = QgsFeature(output_layer.fields())
    out_feat.setGeometry(parcel_geom)
    out_feat.setAttributes(parcel.attributes() + [grz_main, grz_aux])
    output_layer.dataProvider().addFeature(out_feat)

# Finalize
QgsProject.instance().addMapLayer(output_layer)
print("GRZ calculation complete for all parcels.")

end_time = time.time()
elapsed = end_time - start_time
print(f"Time elapsed: {elapsed:.2f} seconds")
```

Listing 5. Python script for GRZ calculation within QGIS using spatial indexing

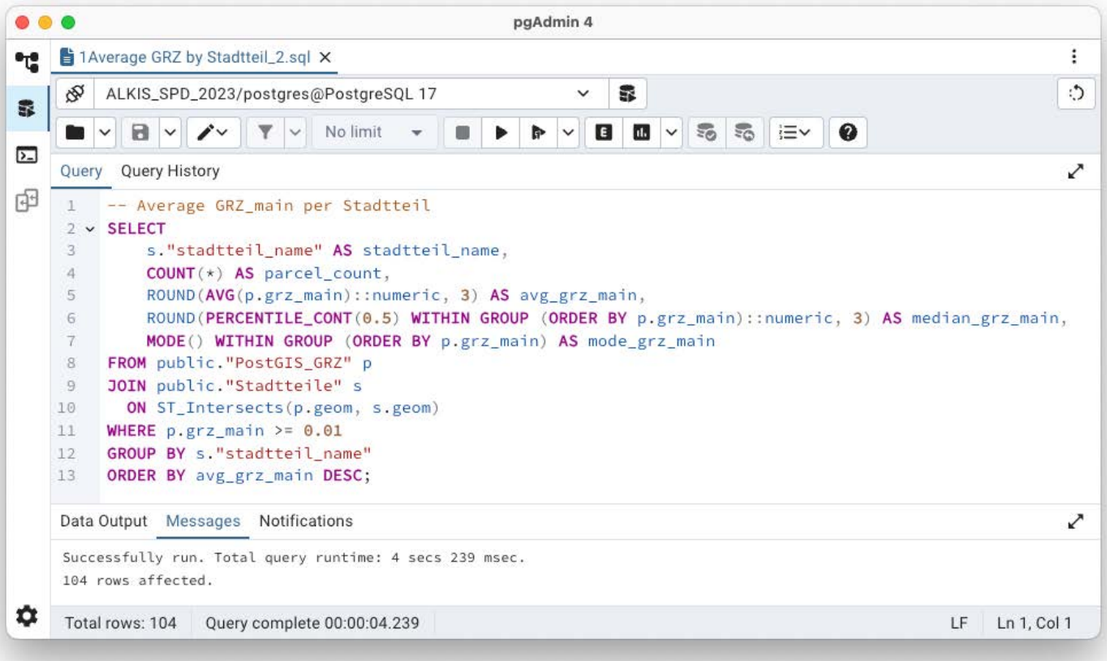

Listing 6. Screenshot of SQL Query in pgAdmin. `GRZ_main` aggregation by Stadtteil. Query completed successfully with a total runtime of 4,239 seconds, affecting 104 rows.

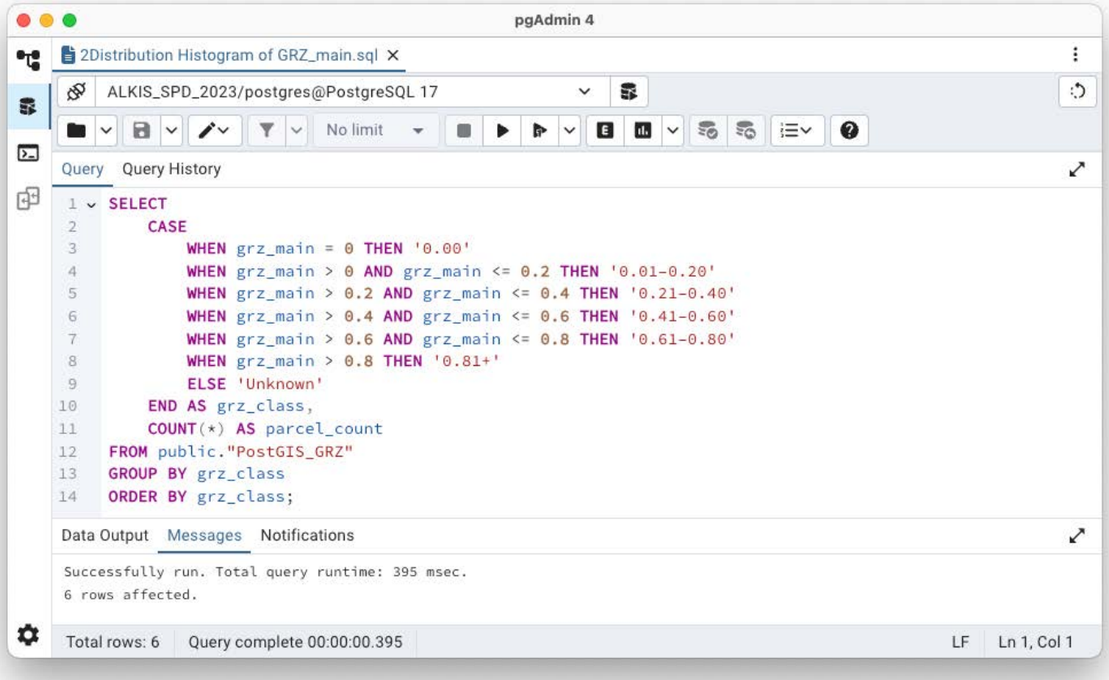

Listing 7. Screenshot of SQL Query in pgAdmin. Distribution histogram of `GRZ_main`. Query completed successfully with a total runtime of 395 milliseconds, affecting 6 rows.

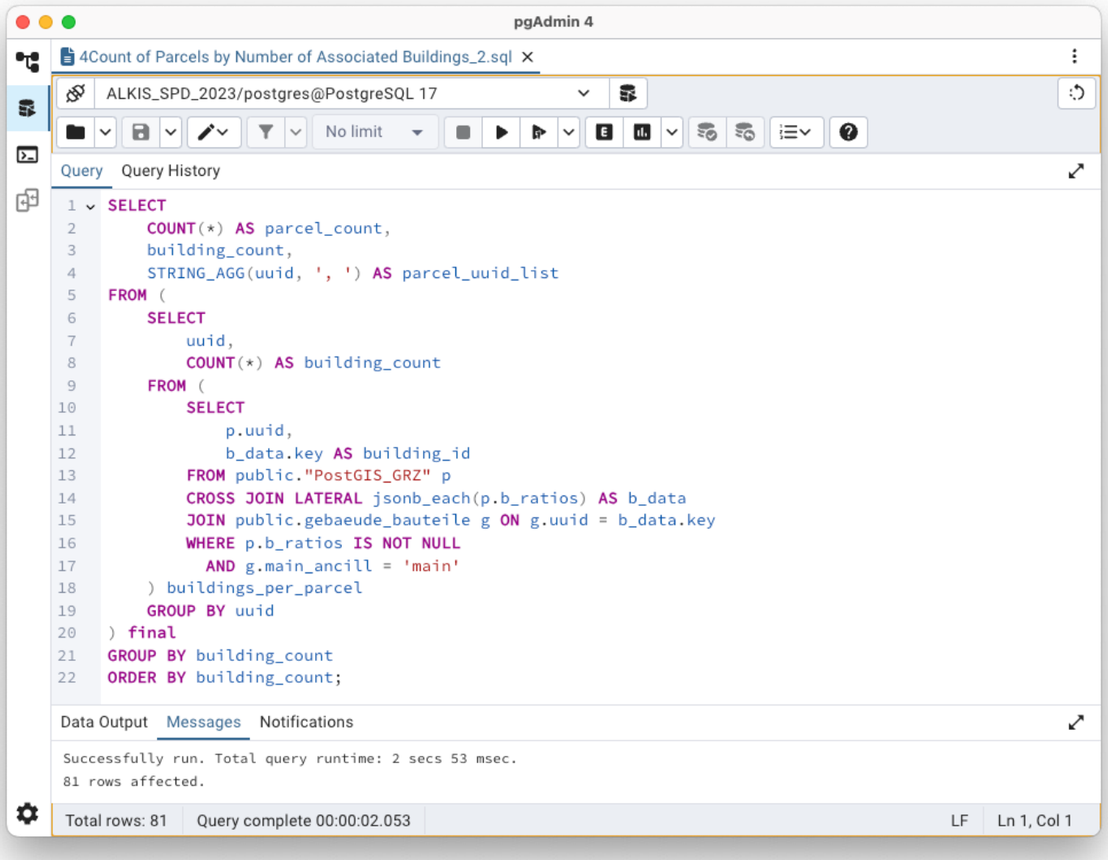

Listing 9. Screenshot of SQL Query in pgAdmin. Count of parcels by number of associated buildings. Query completed successfully with a total runtime of 2,053 seconds, affecting 81 rows.

```sql
WITH neighbors AS (
    SELECT
        p.uuid AS center_uuid,
        p.grz_main AS center_grz,
        n.uuid AS neighbor_uuid,
        n.grz_main AS neighbor_grz
    FROM public."PostGIS_GRZ" p
    JOIN public."PostGIS_GRZ" n
      ON ST_Touches(p.geom, n.geom)
    WHERE n.grz_main >= 0.5
),
comparison AS (
    SELECT
        center_uuid,
        COUNT(*) FILTER (
            WHERE neighbor_grz - center_grz >= 0.3
        ) AS higher_neighbors
    FROM neighbors
    GROUP BY center_uuid
)
SELECT p.*
FROM public."PostGIS_GRZ" p
JOIN comparison c
ON p.uuid = c.center_uuid
WHERE c.higher_neighbors > 0;
```

Listing 8. SQL query to identify geometries (center parcels) with at least one neighboring parcel whose GRZ value is higher by 0,3 or more.

```sql
-- STEP 1 : geometry validation-- for flurstuecke database
DELETE FROM public.flurstueckeWHERE geom IS NULL OR ST_IsEmpty(geom);
UPDATE public.flurstueckeSET geom = ST_MakeValid(geom)
WHERE NOT ST_IsValid(geom);
DELETE FROM public.flurstueckeWHERE NOT ST_IsValid(geom);
-- for gebaeude_bauteile database
DELETE FROM public.gebaeude_bauteileWHERE geom IS NULL OR ST_IsEmpty(geom);
UPDATE public.gebaeude_bauteileSET geom = ST_MakeValid(geom)
WHERE NOT ST_IsValid(geom);
DELETE FROM public.gebaeude_bauteileWHERE NOT ST_IsValid(geom);


-- STEP 2 : main_ancill building classification
ALTER TABLE public.gebaeude_bauteileADD COLUMN main_ancill VARCHAR;
-- classify as 'ancillary' based on GFK values
-- 2463: Garage-- 1313: Garden shed-- 2742: Mobile greenhouse
-- 2465: Underground garage-- 2740: Greenhouse
UPDATE public.gebaeude_bauteileSET main_ancill = 'ancillary'WHERE gfk IN (2465,
2463, 1313, 2742, 2740);
-- set remaining rows to 'main'
UPDATE public.gebaeude_bauteileSET main_ancill = 'main'WHERE main_ancill IS
NULL;


-- STEP 3 : parcels-builidings relation
ALTER TABLE public.flurstueckeADD COLUMN IF NOT EXISTS b_ratios JSONB;
-- filter relevant buildings and precompute their area
WITH filtered_buildings AS (    SELECT uuid, geom, ST_Area(geom) AS b_area
FROM public.gebaeude_bauteile    WHERE bezeich = 'AX_Gebaeude'),
-- compute intersection area between each building and parcel
intersections AS (
    SELECT
        p.uuid AS parcel_uuid,
        b.uuid AS building_uuid,
        ST_Area(ST_Intersection(b.geom, p.geom))
AS intersection_area,        b.b_area
    FROM public.flurstuecke p
    JOIN filtered_buildings b
      ON ST_DWithin(p.geom, b.geom, 1.0)
    WHERE ST_Intersects(p.geom, b.geom)),
-- calculate relative overlap ratios and format as a JSONB object
ratios AS (
    SELECT
        parcel_uuid,
        jsonb_object_agg(
            building_uuid,
            ROUND(CASE
                    WHEN intersection_area / NULLIF(b_area, 0) > 0.95 THEN 1.0
                    WHEN intersection_area / NULLIF(b_area, 0) < 0.05 THEN 0.0
                    ELSE intersection_area / NULLIF(b_area, 0)END::numeric,2
            ))
AS json_result    FROM intersections
    GROUP BY parcel_uuid)
UPDATE public.flurstuecke AS parcelsSET b_ratios = ratios.json_result
FROM ratiosWHERE parcels.uuid = ratios.parcel_uuid;
```

```sql
-- STEP 4 : GRZ calculation
ALTER TABLE public.flurstueckeADD COLUMN IF NOT EXISTS grz_main DOUBLE
PRECISION,ADD COLUMN IF NOT EXISTS grz_aux DOUBLE PRECISION;
-- Unnest JSONB (building_uuid -> ratio) from each parcel
WITH unnested_ratios AS (
SELECT
        f.uuid AS parcel_uuid,
        b_data.key::VARCHAR AS building_uuid,
        b_data.value::NUMERIC AS overlap_ratio,
        f.afl AS parcel_area
    FROM public.flurstuecke f,
         LATERAL jsonb_each(f.b_ratios) AS b_data
    WHERE f.b_ratios IS NOT NULL),building_data AS (
-- Join to buildings table to get area and type
    SELECT
        u.parcel_uuid,
        u.overlap_ratio,
        u.parcel_area,
        g.grf AS building_ground_area,
        g.main_ancill
    FROM unnested_ratios u
    JOIN public.gebaeude_bauteile g      ON g.uuid = u.building_uuid
    WHERE g.grf IS NOT NULL),building_contributions AS (
-- Compute adjusted area contribution per building
    SELECT
        parcel_uuid,
        main_ancill,
        overlap_ratio * building_ground_area
AS effective_area,
        parcel_area
    FROM building_data),aggregated AS (
-- Sum areas per parcel by classification
    SELECT
        parcel_uuid,
        SUM(CASE WHEN main_ancill = 'main' THEN effective_area ELSE 0 END) AS
total_main_area,
        SUM(effective_area) AS total_combined_area,
        MAX(parcel_area) AS parcel_area
-- same for each parcel_uuid
    FROM building_contributions
    GROUP BY parcel_uuid)
-- Final update of flurstuecke table
UPDATE public.flurstuecke f
SET
     grz_main = COALESCE(ROUND((aggregated.total_main_area / NULLIF(aggregated.
parcel_area, 0))::numeric, 2), 0),
    grz_aux  = COALESCE(ROUND((aggregated.total_combined_area /
NULLIF(aggregated.parcel_area, 0))::numeric, 2), 0)
FROM aggregatedWHERE f.uuid = aggregated.parcel_uuid
AND aggregated.parcel_area IS NOT NULL;
```

Listing 10. SQL script to calculate `GRZ_main` and `GRZ_aux` for each parcel. Validating geometries, classifying buildings, computing building-to-parcel overlap ratios, and aggregating effective building areas.

8.3. Appendix C. Extended Results

Table 17. `GRZ_main` statistics by Stadtteil in Hamburg. The results are based on spatial aggregation of parcel-level data and highlight variations in building coverage intensity across urban and suburban areas (author, 2025).

stadtteil_name	parcel count	avg grz_main	median	mode
"Hamburg-Altstadt"	571	0.816	0.920	1
"Neustadt"	847	0.743	0.810	1
"HafenCity"	233	0.680	0.700	1
"St. Georg"	736	0.655	0.680	1
"St. Pauli"	1129	0.645	0.650	1
"Sternschanze"	410	0.630	0.650	0.74
"Ottensen"	1782	0.537	0.540	0.65
"Altona-Altstadt"	1476	0.534	0.500	0.41
"Hammerbrook"	413	0.531	0.530	0.52
"Harburg"	1729	0.526	0.500	1
"Altona-Nord"	865	0.507	0.490	0.33
"Eimsbüttel"	2386	0.505	0.500	0.54
"Hoheluft-Ost"	452	0.501	0.500	0.55
"Hoheluft-West"	624	0.481	0.475	0.46
"Rotherbaum"	1170	0.464	0.440	0.35
"Eppendorf"	1273	0.437	0.440	0.47
"Barmbek-Süd"	1390	0.437	0.400	0.36
"Hohenfelde"	600	0.431	0.400	0.33
"Winterhude"	2287	0.407	0.390	0.31
"Rothenburgsort"	457	0.404	0.380	0.27
"Barmbek-Nord"	1236	0.397	0.380	0.37
"Borgfelde"	268	0.395	0.360	0.35
"Eilbek"	1209	0.394	0.370	0.31
"Uhlenhorst"	1018	0.393	0.360	0.35
"Hamm"	1223	0.381	0.360	0.35
"Harvestehude"	1326	0.374	0.350	0.3
"Dulsberg"	329	0.364	0.370	0.37
"Billbrook"	446	0.348	0.340	0.01
"Veddel"	209	0.330	0.340	0.01
"Wandsbek"	2713	0.328	0.280	0.2
"Neuallermöhe"	1926	0.315	0.320	0.33
"Steilshoop"	542	0.293	0.270	0.23
"Bahrenfeld"	2824	0.291	0.240	0.18
"Stellingen"	2060	0.288	0.250	0.21
"Altenwerder"	17	0.287	0.210	0.01
"Heimfeld"	2050	0.283	0.240	0.15
"Horn"	1008	0.282	0.270	0.16
"Finkenwerder"	1818	0.269	0.220	0.19
"Bergedorf"	4519	0.266	0.200	0.15
"Lohbrügge"	4283	0.261	0.240	0.2
"Groß Borstel"	1087	0.259	0.230	0.17
"Wilstorf"	1627	0.258	0.220	0.18
"Lokstedt"	2324	0.256	0.230	0.2
"Kleiner Grasbrook"	37	0.251	0.180	0.01
"Wilhelmsburg"	3899	0.244	0.190	0.16
"Sülldorf"	1453	0.242	0.220	0.15
"Osdorf"	2997	0.241	0.210	0.19
"Alsterdorf"	1336	0.241	0.210	0.19
"Blankenese"	3229	0.238	0.210	0.14
"Bramfeld"	5923	0.236	0.210	0.2
"Jenfeld"	1958	0.235	0.190	0.2
"Hummelsbüttel"	2397	0.235	0.200	0.17
"Marienthal"	1772	0.234	0.210	0.16
"Ohlsdorf"	1242	0.233	0.210	0.2
"Langenbek"	1155	0.230	0.220	0.17
"Niendorf"	6145	0.229	0.210	0.2
"Langenhorn"	6171	0.225	0.200	0.16
"Rahlstedt"	10399	0.224	0.190	0.15
"Groß Flottbek"	2164	0.221	0.200	0.16
"Eidelstedt"	3367	0.221	0.200	0.2
"Billstedt"	5118	0.221	0.200	0.18
"Marmstorf"	1877	0.220	0.190	0.16
"Fuhlsbüttel"	1559	0.220	0.200	0.16
"Othmarschen"	2304	0.219	0.190	0.13
"Tonndorf"	1788	0.219	0.190	0.17
"Allermöhe"	582	0.218	0.150	0.13
"Lurup"	3245	0.214	0.190	0.19
"Neugraben-Fischbek"	4639	0.213	0.200	0.19
"Iserbrook"	1847	0.213	0.190	0.16
"Poppenbüttel"	4752	0.212	0.200	0.2
"Schnelsen"	3957	0.211	0.190	0.2
"Neuland"	566	0.210	0.180	0.2
"Steinwerder"	40	0.208	0.150	0.01
"Sinstorf"	729	0.206	0.190	0.14
"Nienstedten"	1520	0.206	0.180	0.15
"Eißendorf"	2984	0.202	0.180	0.19
"Hausbruch"	1988	0.198	0.180	0.17
"Neuenfelde"	807	0.197	0.170	0.16
"Cranz"	162	0.195	0.180	0.13
"Moorburg"	277	0.194	0.150	0.01
"Rönneburg"	611	0.194	0.180	0.15
"Rissen"	2899	0.190	0.170	0.15
"Farmsen-Berne"	3373	0.190	0.170	0.19
"Moorfleet"	404	0.189	0.150	0.15
"Sasel"	5747	0.186	0.180	0.2
"Francop"	218	0.185	0.160	0.01
"Volksdorf"	4674	0.183	0.160	0.13
"Bergstedt"	2121	0.183	0.170	0.18
"Wellingsbüttel"	2576	0.175	0.170	0.16
"Lemsahl-Mellingstedt"	2026	0.170	0.170	0.15
"Kirchwerder"	3010	0.166	0.150	0.14
"Duvenstedt"	1508	0.164	0.160	0.14
"Curslack"	913	0.150	0.140	0.2
"Billwerder"	337	0.147	0.130	0.1
"Neuwerk"	38	0.143	0.125	0.1
"Wohldorf-Ohlstedt"	1340	0.141	0.130	0.13
"Ochsenwerder"	870	0.141	0.130	0.14
"Altengamme"	656	0.138	0.130	0.17
"Neuengamme"	1149	0.137	0.120	0.11
"Spadenland"	172	0.129	0.105	0.04
"Reitbrook"	180	0.123	0.100	0.02
"Tatenberg"	186	0.115	0.105	0.02
"Waltershof"	32	0.115	0.075	0.02
"Gut Moor"	28	0.072	0.055	0.02

Table 18. Distribution of parcels by number of associated buildings (author, 2025).

Associated Buildings	Amount of Parcels	Parcel UUID
180	1	DEHHALKA1n1000Uj
162	1	DEHHALKAP0006sqo
144	1	DEHHALKAz0000fcO
126	1	DEHHALKA1ms0006A
125	1	DEHHALKAJ0000EY2
124	1	DEHHALKAP0006skq
112	1	DEHHALKA70000O8c
104	1	DEHHALKAP0006rQa
90	1	DEHHALKAP0000LQq
89	1	DEHHALKAz0000qoR
80	1	DEHHALKAP00075sF
77	1	DEHHALKAP0006sGm
76	1	DEHHALKAJ0000FG2
71	1	DEHHALKAV0000x61
70	3	DEHHALKA70000YB8 DEHHALKAJ0000FCO DEHHALKAP0000GpU
69	2	DEHHALKA60000A2r DEHHALKAJ0000Qt9
67	1	DEHHALKAP00007g4
66	3	-
65	2	-
64	2	-
63	2	-
62	2	-
60	3	-
59	1	-
57	1	-
56	1	-
55	2	-
54	2	-
53	3	-
52	4	-
51	6	-
50	4	-
49	7	-
48	8	-

Associated Buildings	Amount of Parcels	Parcel UUID
47	3	-
46	5	-
45	2	-
44	3	-
43	1	-
42	3	-
41	10	-
40	10	-
39	7	-
38	11	-
37	14	-
36	12	-
35	9	-
34	7	-
33	11	-
32	15	-
31	13	-
30	15	-
29	23	-
28	18	-
27	16	-
26	22	-
25	23	-
24	24	-
23	28	-
22	40	-
21	36	-
20	42	-
19	57	-
18	73	-
17	79	-
16	85	-
15	84	-
14	150	-
13	162	-
12	184	-

Associated Buildings	Amount of Parcels	Parcel UUID
11	249	-
10	348	-
9	490	-
8	780	-
7	1166	-
6	2340	-
5	4792	-
4	10872	-
3	42308	-
2	52839	-
1	78395	-

8.4. Appendix D. Legal Context & References

Entry 1: Original and Translated Excerpt of § 14 BauNVO. Regulations on Ancillary Facilities and Renewable Energy Installations. Source: www.gesetze-im-internet.de/baunvo, consulted in May 2025.

§ 14 Nebenanlagen; Anlagen zur Nutzung solarer Strahlungsenergie und Kraft-Wärme-Kopplungsanlagen	**§ 14 Ancillary Facilities; Installations for the Use of Solar Radiation Energy and Combined Heat and Power Plants**
(1) Außer den in den §§ 2 bis 13 genannten Anlagen sind auch untergeordnete Nebenanlagen und Einrichtungen zulässig, die dem Nutzungszweck der in dem Baugebiet gelegenen Grundstücke oder des Baugebiets selbst dienen und die seiner Eigenart nicht widersprechen. Soweit nicht bereits in den Baugebieten nach dieser Verordnung Einrichtungen und Anlagen für die Tierhaltung, einschließlich der Kleintiererhaltungszucht, zulässig sind, gehören zu den untergeordneten Nebenanlagen und Einrichtungen im Sinne des Satzes 1 auch solche für die Kleintierhaltung. Zu den untergeordneten Nebenanlagen und Einrichtungen im Sinne des Satzes 1 gehören auch Anlagen zur Erzeugung von Strom oder Wärme aus erneuerbaren Energien. Im Bebauungsplan kann die Zulässigkeit der Nebenanlagen und Einrichtungen eingeschränkt oder ausgeschlossen werden.	(1) In addition to the installations listed in §§ 2 to 13, subordinate ancillary facilities and installations are also permissible, provided they serve the purpose of use of the properties located within the building area or of the building area itself, and do not conflict with its character. If facilities and installations for animal husbandry, including small animal breeding, are not already permitted within the building areas according to this regulation, then such installations for small animal keeping are also considered subordinate ancillary facilities under sentence 1. Installations for the generation of electricity or heat from renewable energies are also considered subordinate ancillary facilities within the meaning of sentence 1. The permissibility of such ancillary facilities and installations may be restricted or excluded in the development plan.
(1a) In den Baugebieten nach den §§ 2 bis 11 sind Nebenanlagen, die der öffentlichen Versorgung mit Telekommunikationsdienstleistungen dienen, zulässig; Absatz 1 Satz 4 gilt entsprechend.	(1a) In building areas as defined in §§ 2 to 11, ancillary facilities used for public telecommunications services are permissible; sentence 4 of paragraph 1 applies accordingly.
(2) Die der Versorgung der Baugebiete mit Elektrizität, Gas, Wärme und Wasser sowie zur Ableitung von Abwasser dienenden Nebenanlagen können in den Baugebieten als Ausnahme zugelassen werden, auch soweit für sie im Bebauungsplan keine besonderen Flächen festgesetzt sind. Dies gilt auch für fernmeldetechnische Nebenanlagen sowie für Anlagen für erneuerbare Energien, soweit nicht Absatz 1 Satz 1 oder Absatz 1a Anwendung findet.	(2) Ancillary facilities used to supply the building areas with electricity, gas, heat, and water, as well as to dispose of wastewater, may be permitted as exceptions in the building areas even if no special areas are designated for them in the development plan. This also applies to telecommunications infrastructure as well as to installations for renewable energies, insofar as paragraph 1 sentence 1 or paragraph 1a do not already apply..
(3) Soweit baulich untergeordnete Anlagen zur Nutzung solarer Strahlungsenergie in, an oder auf Dach- und Außenwandflächen oder Kraft-Wärme-Kopplungsanlagen innerhalb von Gebäuden nicht bereits nach den §§ 2 bis 13 zulässig sind, gelten sie auch dann als Anlagen im Sinne des Absatzes 1 Satz 1, wenn die erzeugte Energie vollständig oder überwiegend in das öffentliche Netz eingespeist wird. In Gewerbe-, Industrie- und sonstigen Sondergebieten gilt Satz 1 auch für sonstige baulich untergeordnete Anlagen zur Nutzung solarer Strahlungsenergie.	(3) To the extent that structurally subordinate installations for the use of solar radiation energy on, in, or attached to roof and outer wall surfaces or combined heat and power plants within buildings are not already permissible under §§ 2 to 13, they shall still be considered installations under paragraph 1 sentence 1, even if the energy produced is fed entirely or predominantly into the public grid. In commercial, industrial, and other special-use areas, this also applies to other structurally subordinate solar energy installations.
(4) In einem Gebiet nach § 11 Absatz 2 für Anlagen, die der Nutzung solarer Strahlungsenergie dienen, sind Anlagen zur Herstellung oder Speicherung von Wasserstoff zulässig, wenn die Voraussetzungen entsprechend § 249a Absatz 4 gegeben sind. In Gewerbe- und Industriegebieten gilt Satz 1 entsprechend, wenn dort eine Anlage, die der Nutzung solarer Strahlungsenergie dient und die keine Nebenanlage im Sinne dieser Vorschrift ist, tatsächlich vorhanden ist. Absatz 1 Satz 4 gilt entsprechend.	(4) In an area under § 11(2) designated for the use of solar radiation energy, installations for the production or storage of hydrogen are permissible if the conditions of § 249a(4) are met. In commercial and industrial areas, sentence 1 applies accordingly, provided that a solar radiation energy installation, though not considered an ancillary facility under this provision, is actually present. Sentence 4 of paragraph 1 applies accordingly.

Entry 2: Original and Translated Excerpt of § 19 BauNVO. Building Coverage Ratio (GRZ) and Permissible Building Area . Source: www.gesetze-im-internet.de/baunvo, consulted in May 2025.

§ 19 Grundflächenzahl, zulässige Grundfläche

(1) Die Grundflächenzahl gibt an, wieviel Quadratmeter Grundfläche je Quadratmeter Grundstücksfläche im Sinne des Absatzes 3 zulässig sind.

(2) Zulässige Grundfläche ist der nach Absatz 1 errechnete Anteil des Baugrundstücks, der von baulichen Anlagen überdeckt werden darf.

(3) Für die Ermittlung der zulässigen Grundfläche ist die Fläche des Baugrundstücks maßgebend, die im Bauland und hinter der im Bebauungsplan festgesetzten Straßenbegrenzungslinie liegt. Ist eine Straßenbegrenzungslinie nicht festgesetzt, so ist die Fläche des Baugrundstücks maßgebend, die hinter der tatsächlichen Straßengrenze liegt oder die im Bebauungsplan als maßgebend für die Ermittlung der zulässigen Grundfläche festgesetzt ist.

(4) Bei der Ermittlung der Grundfläche sind die Grundflächen von
1. Garagen und Stellplätzen mit ihren Zufahrten,
2. Nebenanlagen im Sinne des § 14,
3. baulichen Anlagen unterhalb der Geländeoberfläche, durch die das Baugrundstück lediglich unterbaut wird,

mitzurechnen. Die zulässige Grundfläche darf durch die Grundflächen der in Satz 1 bezeichneten Anlagen bis zu 50 vom Hundert überschritten werden, höchstens jedoch bis zu einer Grundflächenzahl von 0,8; weitere Überschreitungen in geringfügigem Ausmaß können zugelassen werden. Im Bebauungsplan können von Satz 2 abweichende Bestimmungen getroffen werden. Soweit der Bebauungsplan nichts anderes festsetzt, kann im Einzelfall von der Einhaltung der sich aus Satz 2 ergebenden Grenzen abgesehen werden
1. bei Überschreitungen mit geringfügigen Auswirkungen auf die natürlichen Funktionen des Bodens oder
2. wenn die Einhaltung der Grenzen zu einer wesentlichen Erschwerung der zweckentsprechenden Grundstücksnutzung führen würde.

(5) Soweit der Bebauungsplan nichts anderes festsetzt, darf die zulässige Grundfläche in Gewerbe-, Industrie- und sonstigen Sondergebieten durch die Grundflächen von Anlagen zur Erzeugung von Strom und Wärme aus solarer Strahlungsenergie und Windenergie überschritten werden.

§ 19 Building Coverage Ratio, Permissible Floor Area

(1) The Building Coverage Ratio indicates how many square meters of floor area are permitted per square meter of plot area, as defined in paragraph 3.

(2)The permissible floor area is the portion of the building plot, calculated according to paragraph 1, that may be covered by structures.

(3) To determine the permissible floor area, the relevant area of the building plot is that which lies within the building land and behind the street boundary line specified in the development plan. If no such boundary line is specified, the relevant area is that behind the actual street boundary or that which is designated in the development plan as relevant for calculating the permissible floor area.

(4) In calculating the floor area, the following must also be included:
1. the floor areas of garages and parking spaces, including their driveways,
2. ancillary facilities as defined in § 14,
3. structural installations beneath the surface of the terrain that only underbuild the building plot.

The permissible floor area may be exceeded by up to 50 percent through the inclusion of the floor areas of the installations mentioned in sentence 1, but not beyond a total floor area ratio of 0.8. Further minor exceedances may be permitted. The development plan may stipulate deviations from sentence 2. Where the development plan contains no contrary provisions, deviations from the limits defined in sentence 2 may be permitted in individual cases if:
1. the exceedance has only minor effects on the natural functions of the soil, or
2. adherence to the limits would significantly hinder the appropriate use of the property.

(5) Where the development plan does not provide otherwise, in commercial, industrial, and other special-use areas, the permissible floor area may be exceeded by the floor areas of facilities used to generate electricity and heat from solar radiation and wind energy.

Entry 3: Translated Excerpt from Flächenmanagement in der Immobilienwirtschaft by Zeitner et al. (2019). GRZ and the Differentiation Between Main and Ancillary Structures

Definition of GRZ: The GRZ specifies how many square meters of floor area are allowed per square meter of plot area (e.g., GRZ 0.4 means 40% of the land can be built on).

Permissible Floor Area: This is the part of the building plot that may be covered by buildings and related structures.

Relevant Plot Area: Only the part of the property within designated building zones and behind street boundary lines (either actual or defined in the development plan) counts toward GRZ calculations.

Hauptanlagen (§ 19(2) BauNVO). "Main Structures"

These are primary buildings and their essential components. They form the core of what is allowed within the basic GRZ value set by the Bebauungsplan (e.g., GRZ 0.3).

Definition: "Permissible floor area is the portion of the building plot that may be covered by structures."

Included in Hauptanlagen:

1. Residential or commercial buildings
2. Balconies
3. Loggias
4. Terraces (if elevated/constructed)
5. Canopies (if attached)
6. Staircases (if attached)
7. Extensions to the main building

Determination Criteria:

1. Must be above ground
2. Must seal the soil surface (i.e., impervious)
3. Must be part of the main use of the building plot
4. Calculated using horizontal projection of the outermost dimensions (including insulation and cladding)

Nebenanlagen im weiteren Sinne (§ 19(4)). "Ancillary Structures in the Broad Sense"

These do not fall under the base GRZ but may extend it by up to 50%, capped at a total GRZ of 0.8, unless exceptions apply.

BauNVO explicitly lists three types of areas in § 19 (4):

1. Garages and Stellplätze - Garages and driveways
2. Nebenanlagen - Ancillary facilities (like sheds, small greenhouses)
3. Underground Structures:
   These count if they seal the ground above, but not if >1 m topsoil is provided above (can then be excluded with approval).

Up to 50% of the original allowed area can be added, but not exceeding GRZ 0.8, unless negligible environmental impact or hardship in use is proven.

Important Terms:

1. "Permanently sealed": Surfaces that block natural ground functions.
2. Vertical projection: Calculations are based on horizontal area, not sloped surfaces.
3. Outer dimensions: Including insulation, cladding, etc.
4. Some elements (balconies, stairs) count toward GRZ; others (e.g., small steps, gutters) do not.

Bagatelle Clause - Minor GRZ overruns may be tolerated, especially when:

1. Ground remains permeable (e.g., porous pavements)
2. Necessary use of the property would otherwise be unreasonably limited
3. Capping Rule (Kappungsgrenze): Even with § 19 (4) expansions, the GRZ must stay under 0.8 unless exceptions apply.

Entry 4: Object Class Definitions for `AX_Gebaeude` and `AX_Bauteil` in the ALKIS Object Catalogue (DLKM). excerpt from the GeoInfoDok (Version 7.1.2, dated 01.11.2022)

15.2 AX_Gebaeude

Objektart: AX_Gebaeude	Kennung: 31001
Definition:	
[A] 'Gebäude' ist ein dauerhaft errichtetes Bauwerk, dessen Nachweis wegen seiner Bedeutung als Liegenschaft erforderlich ist sowie dem Zweck der Basisinformation des Liegenschaftskatasters dient.	
Abgeleitet aus:	
AX_Gebaeude_Kerndaten AG_Objekt	
Objekttyp:	
REO	
Modellarten:	
DLKM	
Grunddatenbestand:	
DLKM	
Bildungsregeln DLKM:	
Objektbildende Eigenschaften sind länderspezifisch im Erhebungsprozess zu berücksichtigen. Differenzierungen innerhalb eines Gebäudes (z. B. bei Gebäuden mit vertikaler Gliederung) sind als 'Bauteile' modelliert. Unterirdische Bauteile gehören nicht zur Gebäudegrundfläche. Gebäude können aus polyhedralen Flächen (PolyhedralSurface), zusammengesetzten Flächen (CompositeSurface) oder mehreren Flächen (MultiSurface) bestehen. Eine Teilfläche besteht dabei aus einem Polygon, dessen Linien orientiert sind und einen Ring bilden. Als Interpolationsmethode sind 'cubicSplines' nicht zugelasssen. Die Flächen der Gebäude können durch äußere und innere Umringe begrenzt sein. Baulich zusammengehörende Gebäude mit gleichrangiger Bedeutung können mit Hilfe der Relation 'gehoertZu' verbunden werden.	
Relationsart:	
Bezeichnung:	zeigtAufOhne
Kennung:	31001-12001
Definition:	'Gebäude' zeigt auf 'Lagebezeichnung ohne Hausnummer'
Modellarten:	DLKM
Multiplizität:	0..1
Zielobjektart:	AX_LagebezeichnungOhneHausnummer
Inverse Relationsart:	gehoertZuOhne
Attributart:	
Bezeichnung:	gebaeudefunktion

15.3 AX_Bauteil

Objektart: AX_Bauteil	Kennung: 31002
Definition:	
[E] 'Bauteil' ist ein charakteristisches Merkmal eines Gebäudes mit gegenüber dem jeweiligen Objekt 'Gebäude' abweichenden bzw. besonderen Eigenschaften.	
Abgeleitet aus:	
AX_Gebaeude_Kerndaten AG_Flaechenobjekt	
Objekttyp:	
REO	
Modellarten:	
DLKM	
Bildungsregeln:	
Die Attributart 'Bauart' ist objektbildend. Bauteile können aus polyedrischen Flächen (PolyhedralSurface), zusammengesetzten Flächen (CompositeSurface) oder mehreren Flächen (MultiSurface) bestehen. Eine Teilfläche besteht dabei aus einem Polygon, dessen Linien orientiert sind und einen Ring bilden. Als Interpolationsmethode sind 'cubicSplines' nicht zugelasssen. Die Flächen der Bauteile können durch äußere und innere Umringe begrenzt sein.	
Konsistenzbedingungen:	
Der 'Bauteil' als Teil eines Gebäudes liegt immer innerhalb des Gebäudeumrisses, sofern er nicht unterhalb der Erdoberfläche liegt. Die Werteart 1200 'Unter der Erdoberfläche' der Attributart 'Lage zur Erdoberfläche' darf nur in Verbindung mit 'Keller' oder 'Tiefgarage' vorkommen.	
Attributart:	
Bezeichnung:	bauart
Kennung:	BAT
Definition:	'Bauart' ist die Angabe der abweichenden baulichen Eigenschaften.
Modellarten:	DLKM
Multiplizität:	1
Datentyp:	AX_Bauart_Bauteil
Wertearten:	Bezeichnung — Wert
	Geringergeschossiger Gebäudeteil — 1100
	Ein 'geringergeschossiger Gebäudeteil' hat eine niedrigere Geschosshöhe als der größte Teil des Gebäudes.
	Höhergeschossiger Gebäudeteil (nicht Hochhaus) — 1200
	Ein 'höhergeschossiger Gebäudeteil' hat eine höhere Geschosshöhe als der größte Teil des Gebäudes.

Table 19. Assessment of building permissibility by land use type based on ALKIS classifications. Source: Modellierung der Geoinformationen des amtlichen Vermessungswesens (GeoInfoDok), Kapitel 7. ALKIS-Katalogwerke (author, 2025).

Object Type	Building Allowed	Explanation (Short)
Wohnbauflaeche	Yes	Area for residential use; buildings explicitly defined.
IndustrieUndGewerbeflaeche	Yes	Defined for industrial, commercial, and service buildings.
FlaecheGemischterNutzung	Yes	Mixed-use with residential buildings included.
FlaecheBesonderer-FunktionalerPraegung	Yes	Public/historical buildings and facilities are part of the definition.
Bahnverkehr	Possibly	Railway buildings and related structures included.
Flugverkehr	Possibly	Airport-related buildings and facilities included.
Friedhof	Possibly	Chapel, crematorium, and other burial structures allowed.
Platz	Possibly	Includes rest stops, stations, and parking areas with structures.
Schiffsverkehr	Possibly	Land-based port facilities, locks, and transport structures included.
SportFreizeit-UndErholungsflaeche	Possibly	Facilities like sports halls, climbing areas, and leisure structures included.
UnlandVegetationsloseFlaeche	No	No general allowance, but structures like waterworks can be present.
TagebauGrubeSteinbruch	No	Operational buildings may exist, but the core is resource extraction.
Strassenverkehr	No	Defined as areas necessary for the road structure
Fliessgewaesser	No	Defined as flowing water; only specific utility structures are possible.
StehendesGewaesser	No	Defined as standing water; no mention of buildings.
Weg	No	Paths for light traffic; buildings not included.
Hafenbecken	No	Water body; land-based facilities are defined elsewhere.
Landwirtschaft	No	Defined by agricultural use; no general building allowance stated.
Meer	No	Natural marine area; buildings not applicable.
Moor	No	Natural wetland; no building described.
Sumpf	No	Marshland; not associated with building activity.
Wald	No	Forest area; building not part of core definition.
Heide	No	Heathland; no building use mentioned.
Halde	No	Mining dump; building not mentioned.
Gehoelz	No	Shrubland or tree stands; no structures described.

Entry 5: Bebauungsplan-Entwurf (Preliminary Zoning Plan) "Altona-Nord 28". Source: www.hamburg.de/politik-und-verwaltung/bezirke/altona, consulted in June 2025.

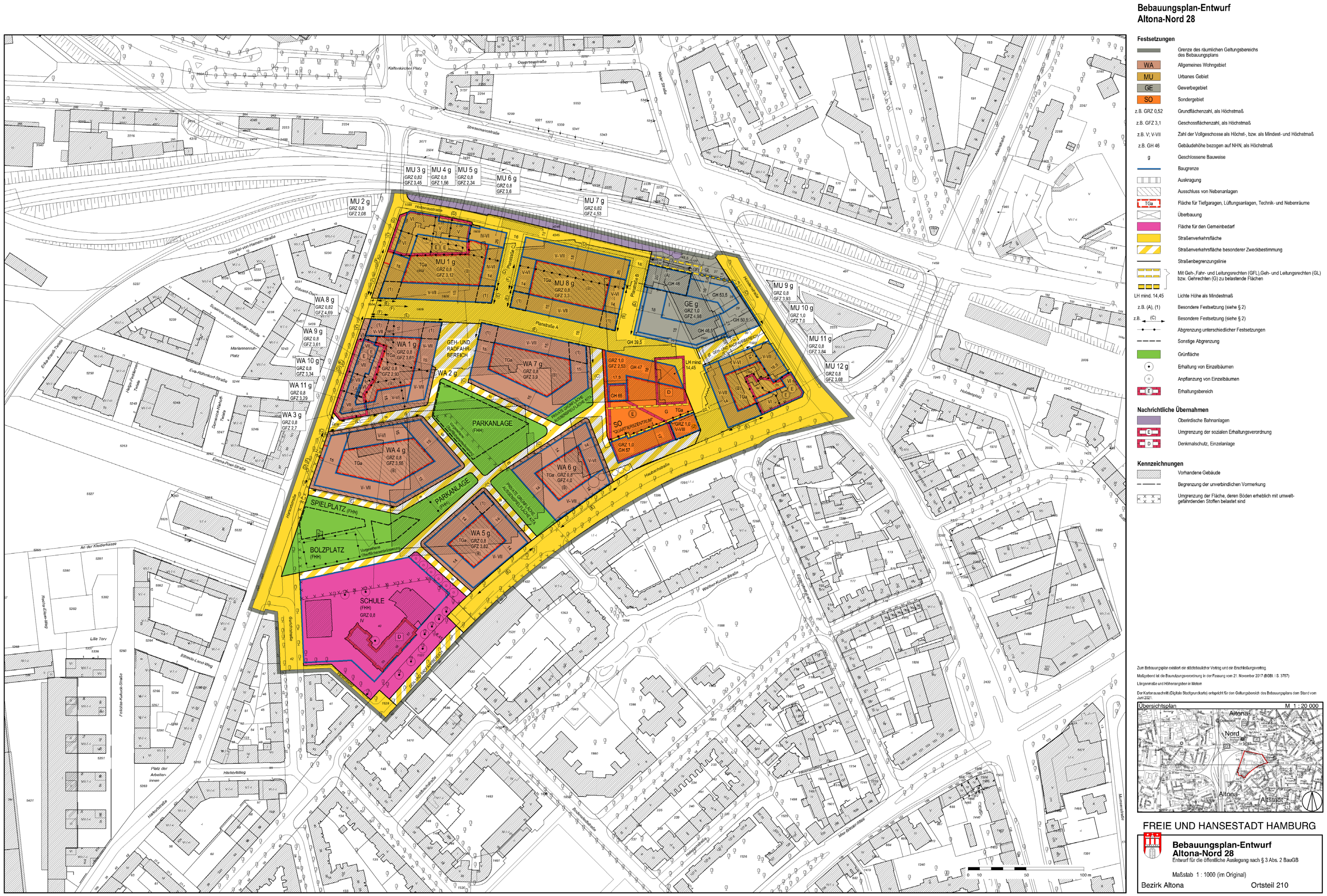

Entry 6: Baustufenplan Farmsen. Source: www.daten-hamburg.de/infrastruktur_bauen_wohnen, consulted in June 2025.

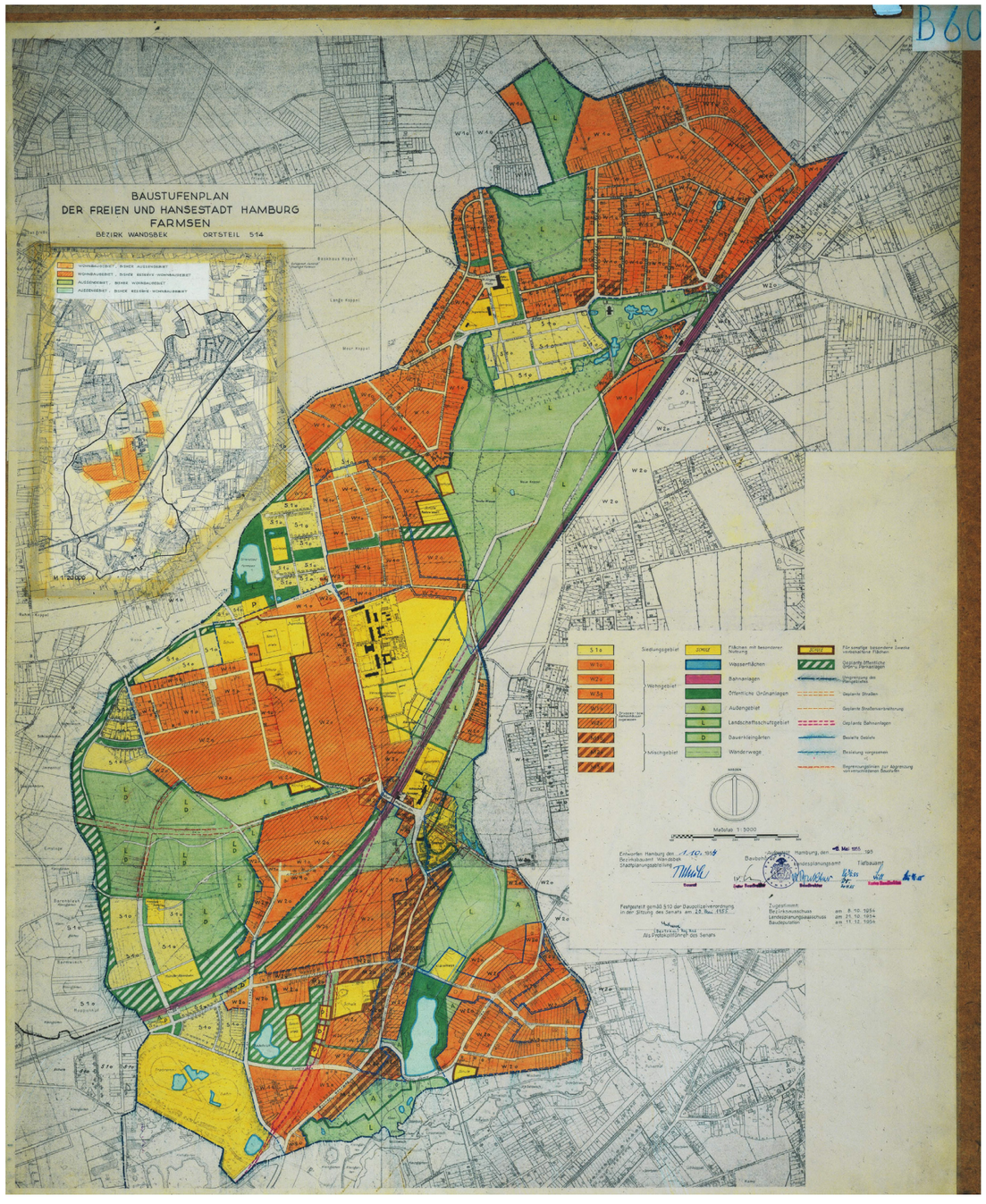

Entry 7: Bebauunsplan Welligsbüttel 16. Source: www.daten-hamburg.de/infrastruktur_bauen_wohnen, consulted in June 2025.

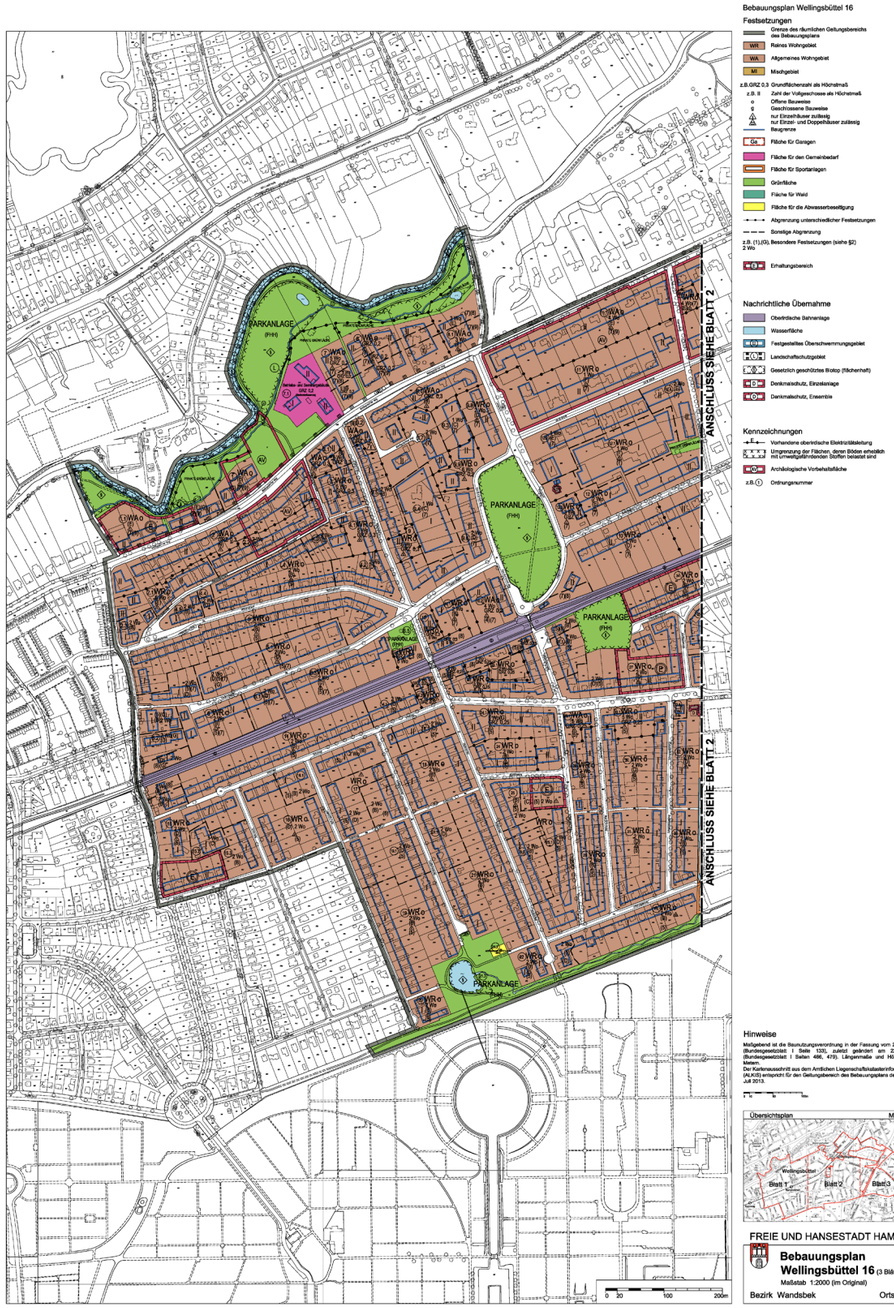

Bebauungsplan Wellingsbüttel 16

Festsetzungen

- Grenze des räumlichen Geltungsbereichs des Bebauungsplans
- WR Reines Wohngebiet
- WA Allgemeines Wohngebiet
- MI Mischgebiet
- z.B. GRZ 0,3 Grundflächenzahl als Höchstmaß
- z.B. II Zahl der Vollgeschosse als Höchstmaß
- o Offene Bauweise
- g Geschlossene Bauweise
- E nur Einzelhäuser zulässig
- ED nur Einzel- und Doppelhäuser zulässig
- Baugrenze
- Ga Fläche für Garagen
- Fläche für den Gemeinbedarf
- Fläche für Sportanlagen
- Grünfläche
- Fläche für Wald
- Fläche für die Abwasserbeseitigung
- Abgrenzung unterschiedlicher Festsetzungen
- Sonstige Abgrenzung
- z.B. (1),(G), 2 Wo Besondere Festsetzungen (siehe §2)
- Einwirkungsbereich

Nachrichtliche Übernahme

- Oberirdische Bahnanlage
- Wasserfläche
- Festgestelltes Überschwemmungsgebiet
- Landschaftsschutzgebiet
- Gesetzlich geschütztes Biotop (flächenhaft)
- Denkmalschutz, Einzelanlage
- Denkmalschutz, Ensemble

Kennzeichnungen

- Vorhandene oberirdische Elektrizitätsleitung
- Umgrenzung der Flächen, deren Böden erheblich mit umweltgefährdenden Stoffen belastet sind
- Archäologische Vorbehaltsfläche
- z.B. 1 Ordnungsnummer

Hinweise

Maßgebend ist die Baunutzungsverordnung in der Fassung vom 23. Januar 1990 (Bundesgesetzblatt I Seite 133), zuletzt geändert am 22. April 1993 (Bundesgesetzblatt I Seiten 466, 479). Längenmaße und Höhenangaben in Metern.

Der Kartenausschnitt aus dem Amtlichen Liegenschaftskatasterinformationssystem (ALKIS) entspricht für den Geltungsbereich des Bebauungsplans dem Stand vom Juli 2013.

Übersichtsplan M 1: 25 000

FREIE UND HANSESTADT HAMBURG

Bebauungsplan Wellingsbüttel 16 (3 Blätter) Blatt 1

Maßstab 1:2000 (im Original)

Bezirk Wandsbek Ortsteil 517

8.5. Appendix E. Research Data Management Strategy

This thesis relies on extensive geospatial data analysis, primarily using official cadastral datasets (ALKIS) provided by the Landesbetrieb Immobilienmanagement und Grundvermögen (LIG). To ensure the transparency, reproducibility, and long-term integrity of the research, a structured data management strategy was followed throughout the project, in line with Open Science principles.

Definition of Research Data. The data used in this thesis include:

1. Raw geospatial vector datasets (parcels and building footprints)
2. Derived spatial layers (e.g. cleaned parcels, classified buildings)
3. Intermediate and final analysis outputs (e.g. GRZ_main, GRZ_aux)
4. Python and SQL scripts used for automation and spatial querying
5. Visualisations and statistical summaries

All datasets are stored in digital form and were processed using QGIS and PostgreSQL/PostGIS environments.

Data Organisation and Storage. Data and scripts were organised according to the following structure:

`/data/raw`	original ALKIS files (.gdb)
`/data/processed`	cleaned shapefiles, PostGIS exports (.csv)
`/scripts/python`	QGIS preprocessing and validation
`/scripts/sql`	PostGIS workflows and GRZ calculation
`/output/maps`	GRZ visualisations
`/output/charts`	analytical figures and diagrams
`/docs`	README, data dictionaries

All files were backed up locally and stored on a university provided cloud service to prevent data loss.

Data Reuse and Acquisition. This research created new data from official datasets made available through institutional collaboration with LIG. The primary dataset, ALKIS_SDP_2023.gdb, contains authoritative parcel and building geometries for the city of Hamburg. Supplementary metadata was reviewed to validate geometric and attribute integrity.

Metadata and Documentation. Each dataset and script is accompanied by metadata (README.txt or comments within scripts) documenting:

1. File origin and date
2. Projection system used (EPSG:25832)
3. Purpose and data usage
4. Processing steps

This documentation aligns with the FAIR principles, making data Findable, Accessible, Interoperable, and Reusable.

Data Sharing and Licensing. The ALKIS datasets used in this project are publicly available through official sources such as Geoportal Hamburg. This thesis shares the specific version of the data used during the research period to support reproducibility. In addition, derived data products and scripts developed during this project, such as selected SQL queries, Python scripts, and example workflows, are available through a public GitHub repository (github.com/JH-hcu/BCR-calc-postgis-qgis). These are accompanied by documentation and released under open licenses (MIT for scripts and CC-BY 4.0 for figures).

8.6. Appendix F. AI Tools and Assistance Disclosure

In the preparation of this thesis, AI-based tools were used in as supportive capacity for specific tasks:

1. ChatGPT (by OpenAI) was used during the initial planning stages to brainstorm phrasing for methodological descriptions, and comparative framing. All interpretations and results were independently developed and validated by the author. It was also used in optimising selected code snippets and SQL queries, primarily to improve performance, or syntactic correctness. All suggestions provided were critically reviewed, tested, and, where necessary, modified by the author to ensure accuracy and suitability for the specific spatial workflows

2. Grammarly (https://www.grammarly.com) was employed for final grammar, spelling, and stylistic refinement. Suggestions were reviewed and selectively implemented by the author, without affecting the substantive content or analysis.

These tools served as auxiliary aids. The thesis reflects the author's original research, critical thinking, and academic work, including all data analysis, writing decisions, and methodological implementation.

Automating Urban Parameter Calculations -
A Comparative Study of GIS Workflows and Spatial Query Methods
for Large-Scale Urban Analysis.

"Indicator and dashboard initiatives have much to offer city managers and citizens, but they need to make fully clear what is on offer"
—Kitchin, Lauriault & McArdle (2015, p.24)